technische universität dortmund

2016

SCIENTIFIC HIGHLIGHTS
Annual Report

a)

emulsion stable for years

b)

organic phase

aqueous phase

cell pellet

phase separation within minutes

coordinator/management

λ^k

λ^*

$\sum_{i=1}^{n} R_i = 0$

R_1^k

R_3^k

R_n^k

plant 1

plant 3

plant n

plant 2

R_2^k

R_i^k

plant i

based on raw temperature data

$k_{t,s}$ [W m^{-2} K^{-1}]

$k_{t,s}$ [W m^{-2} K^{-1}]

[W m^{-2} K^{-1}]

60

40

20

0

50

30

20

10

15

REPROCESS

SMASH

90 mm

air

3295 mm

2 mm

w_{water} [m/s]

0,067

-0,068

Fakultät Bio- und Chemieingenieurwesen

Content

Content

Department of BCI

Preface

Dear Reader,

I am proud to present the best of research of the Faculty Biochemical and Chemical Engineering of the year 2016. In this collection of brief research highlights you will recognize the broad spectrum of basic to applied research, which is typical for BCI due to the fact that we are a mixed faculty of natural scientists and engineers. The presented work is also testament of the broad experimental and theoretical skills taught to our excellent bachelor, master and PhD students, which come from all over the world. In 2016 we were happy to welcome our new faculty members Prof. Nett and Prof. Luetz. Since we have limited space and cannot present all research activities, a list of the recent publications will be attached to the Scientific Highlights of every group from this year on. I hope as every year that these highlights will be of interest to our students, collaborators, and colleagues from academia and industry. Maybe some topics can be seeds for new scientific or industrial collaborations.

Enjoy the reading,

Joerg C. Tiller
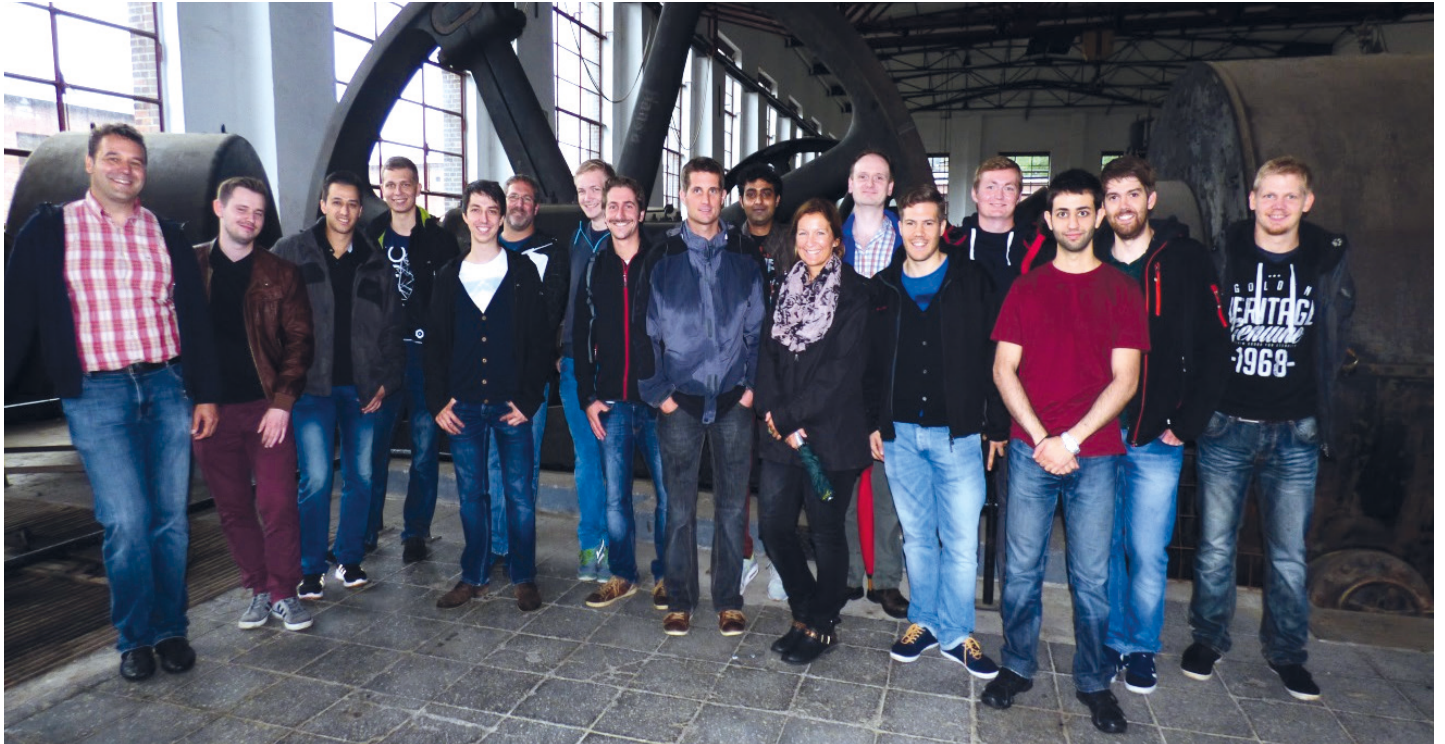
Equipment Design (AD)

Characterization of a Lab-scale Coiled Tubular Cooling Crystallizer

Lukas Hohmann, Norbert Kockmann

Development of continuous processes for specialty products requires well-characterized lab-scale equipment in order to validate and optimize the process concept early in a project with low materials consumption and limited demands concerning experimental cost and safety. A tubular cooling crystallizer was designed as a coiled flow inverter (CFI) and was experimentally characterized according to heat transfer and particle handling.

A coiled tubular crystallizer was designed in order to transfer batch cooling crystallization processes to continuous operation on lab-scale (Figure 1).
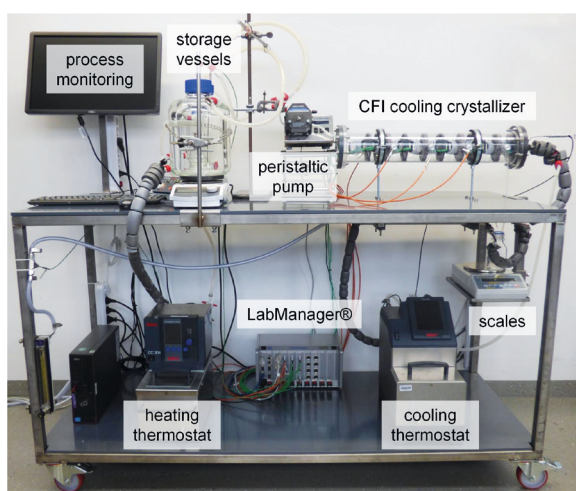
Figure 1: Lab-scale experimental setup.

The coiled flow inverter (CFI) design of the crystallizer (d_i = 4 mm, L = 6.8 m, $\dot{m}$ = 10 – 40 g min^{-1}) provides a narrow residence time distribution of the liquid phase due to the Dean vortices forming in the laminar flow through the coiled tubes. 90° directional changes of the helical coils enhance this effect. For cooling crystallization applications of the system, a cold gas flows in counter-current mode on the shell-side of the CFI. The axial temperature profile along the crystallizer can be adjusted with a single cooling thermostat for precooling the gas stream. The heat transfer from tube to shell and the heat losses from the shell pipe to environment were characterized by experimentally measured axial temperature profiles of the product and the cooling agent.

A heat transfer model was used to estimate the overall heat transfer coefficients (Figure 2) from the experimental data and an empirical heat transfer correlation was derived. This allows for model prediction of temperature profiles and suitable process parameters for designing experimental campaigns.

Beside temperature profiles and mean residence time, a successful continuous cooling crystallization process requires adequate flow conditions for robust particle transport through the process tubes.

Figure 2: Estimated overall heat transfer coefficients. Tube/shell (left), Shell/environment (right).

Generally, Dean vortices enhance the particle transport in the tubes and aid suspending settled particles. Nevertheless, if the flow velocity is too slow or crystals are too large, the particle transport can no longer be achieved and particle settling or even clogging of the tubes can occur. By means of isothermal experiments with the L-alanine/water system, the impact of mass flow rate, tube diameter, crystal size, density difference, and viscosity were analyzed. Three different suspension flow regimes were identified (Figure 3). A flow map based on dimensionless numbers defines the operational range of the tubular crystallizer.
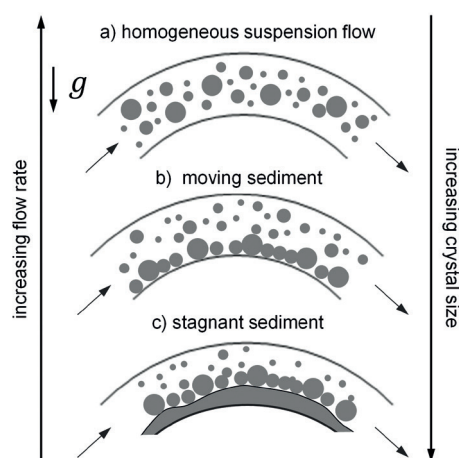
Figure 3: Suspension flow regimes in horizontal helical coils.

Contact:
lukas.hohmann@udo.edu
norbert.kockmann@udo.edu

Reactive Particle Precipitation in a Modular Coiled Flow Inverter

The Influence of Secondary Flow Profiles along with their Alternating Inversions on the Precipitation of Uniform Particles in a Multiphase Reaction System

Safa Kutup Kurt, Norbert Kockmann

Process intensification via miniaturization has become an attractive research field for industry and academia especially for the production of fine chemicals and pharmaceuticals. Additionally, small-scale equipment enables rapid process development in the lab with consistent scale-up capability. Tubular devices with dedicated arrangement are cost-efficient, reliable, and can serve for different purposes. In this work, the modular design of a tubular device, i.e., Coiled Flow Inverter (CFI) is introduced for the continuous operation of multiphase reaction systems by taking the scale-up strategies into account at the early stage of the process development. The performance of the modular CFI is tested in a reactive precipitation process and the results are elucidated by benchmarking against the performance of a batch reactor.

CFI is a helical tube, which includes 90° bends rotating the secondary flow (Dean vortices) that are induced due to the centrifugal force (F_C). This results in moving the stagnant zones on the tube cross section into the central stream of the Dean vortex pair (Figure 1), and thus, enhances the mixing in gas-liquid (G-L) slug flow patterns [1].
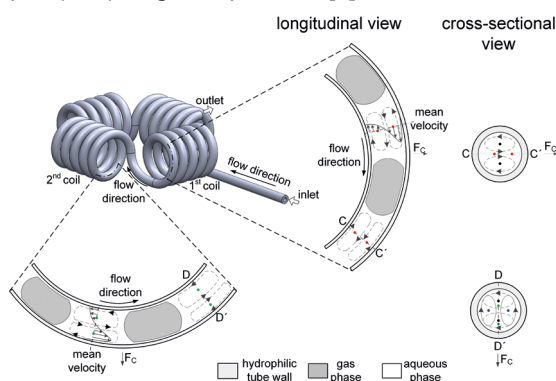
Figure 1: G-L slug flow mixing behavior in a coiled flow inverter.

In this work, a modular CFI reactor is investigated in the continuous production of the precipitated calcium carbonate (PCC) with G-L slug flow patterns in comparison to conventional batch reactors. Slug flow profile is generated by using a Y-mixer. CO_2/synthetic air mixture and the saturated calcium hydroxide solution at ambient conditions are introduced to the CFI via Y mixer. The modular design of a CFI is constructed in terms of variable residence time. PCC process is investigated for the lab scale applications. The effects of the variation in the residence time on the particle size distribution (PSD), the particle morphology, and the conversion are investigated with the modular CFI reactor. The PSD and morphology of PCC particles, which are produced with the modular CFI, are compared with the results of a batch reactor that provides the similar conversion values ($\cong$88 %) under identical process conditions. The design of the modular CFI reactor and the continuous precipitation of calcium carbonate are illustrated in Figure 2.
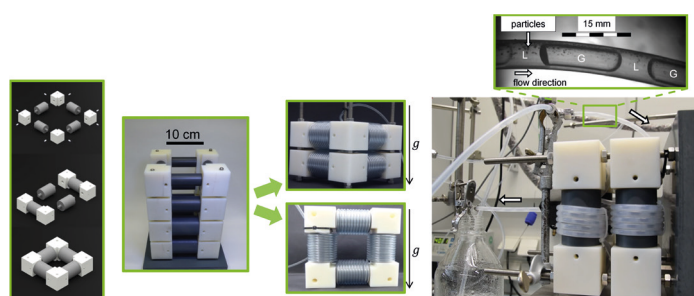
Figure 2: Modular design of CFI and its application for continuous production of PCC particles with G-L slug flow pattern.

In CFI, the enhanced radial mixing inside the liquid slugs allows controlling the nucleation and particle growth with respect to the uniform bubble size distribution. Thus, CFI provides narrower PSD with median particle diameters around 28 µm, more uniform shape (rhombohedral calcite), and larger production amounts per time in comparison to a batch reactor (Figure 3) [2].
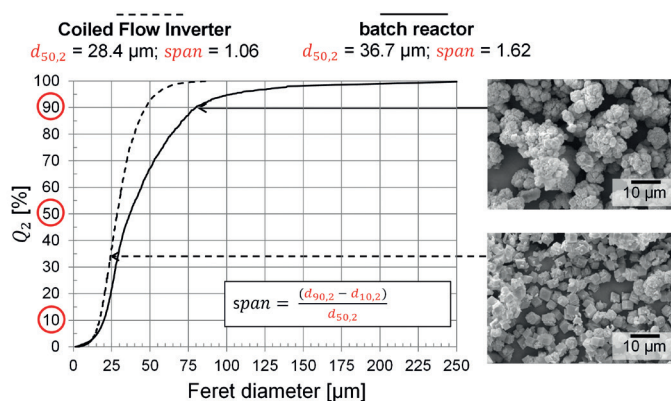
Figure 3: PSD analyses of the PCC particles and SEM pictures.

The design of a modular CFI with a robust and simple fabrication is proposed in the content of this work for the multiphase reaction systems. In future work, the modular CFI will be further investigated to achieve the production of uniform particles with larger throughputs.

Publications:
[1] S.K. Kurt, I. Vural Gürsel, V. Hessel, K.D.P. Nigam, N. Kockmann, Chem. Eng. J., 284, 2016.
[2] S.K. Kurt, M. Akhtar, K.D.P. Nigam, N. Kockmann, ASME-ICNMM, 2016, DOI: 10.1115/ICNMM2016-8004.

Contact:
kutup.kurt@udo.edu
norbert.kockmann@udo.edu

Gas-Liquid Dispersion in Micronozzles for High Interfacial Area

Microreactor Design for Intensified Gas-Liquid Reactions

Felix Reichmann, Norbert Kockmann

A multiphase microreactor has been designed with bubble generation and redispersion nozzle. Experimental analysis of primary phase contacting via T-mixer, bubble breakup mechanisms and resulting gas-liquid dispersions was carried out. The refinement of bubbly flow was characterized by means of Sauter diameter.

Multiphase flow is frequently investigated in microreactor research, but mainly focused on well-described Taylor-bubble flow. Yet, dispersed flow with small bubbles results in higher specific surface-to-volume ratio and more stable flow in microchannels, leading to intensified mass transfer and reactions. Especially, the combination of microstructured elements and millichannels allows for fine dispersions and monodisperse particle size distribution due to turbulent flow in macroscopic systems. The microreactor is designed in a way that various micronozzle geometries can be tested and easily exchanged (Figure 1). The influence of geometrical parameters such as the hydraulic diameter d_0 and the length of the smallest cross section l_0 were observed via high speed camera at up to 30.000 fps. Additionally, a 90° elbow (Figure 1b) was introduced in the smallest cross section to increase energy dissipation rate. The impact of process parameters, here, total flow rate and gas content, on redispersion was observed.
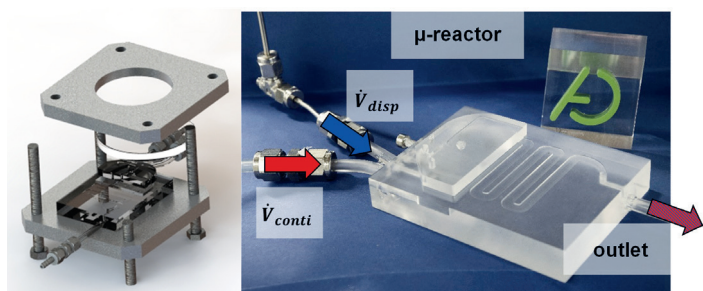
Figure 1: a) Model of multiscale reactor concept. b) Reaction plate with exchangeable inlet element.

Various bubble breakup mechanisms were examined downstream of the micronozzle. Laminar and turbulent breakup could be distinguished, see Figure 2.
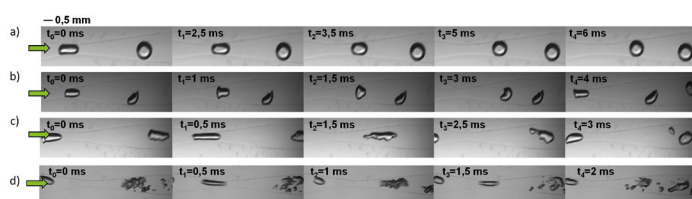
Figure 2: Bubble breakup mechanisms in micronozzle. a) no breakup/no deformation; b) no breakup/deformation; c) laminar breakup; d) transition to turbulent breakup. Gas content: 10 vol%.

Bubbles regained their previous spherical form (Figure 2a) once the channel width exceeded the bubble diameter for low Reynolds numbers (Re = 233). Increased volume flow rate resulted in bubble deformation and no breakup (Fig. 2b, Re = 827). Further increase in Reynolds number leads to laminar breakup (Figure 2c, Re = 1523); and finally, turbulent breakup featuring numerous small bubbles (Figure 2d, Re = 3460).

With increased volumetric flow rate and, hence, higher energy dissipation rates smaller Sauter diameters were obtained (Figure 3). Structures featuring smaller hydraulic diameter (d_0 = 0.25 mm) showed smallest values (Figure 3, A - diamonds). For constant nozzle diameter d_0 = 0.5 mm increased nozzle length leads to smaller Sauter diameters (Figure 3, C - triangles). Introducing an elbow (Fig. 3, D - bars) did not increase Sauter diameter compared to straight nozzle geometry (Figure 3, B - squares). Therefore, straight nozzle geometry is preferable.
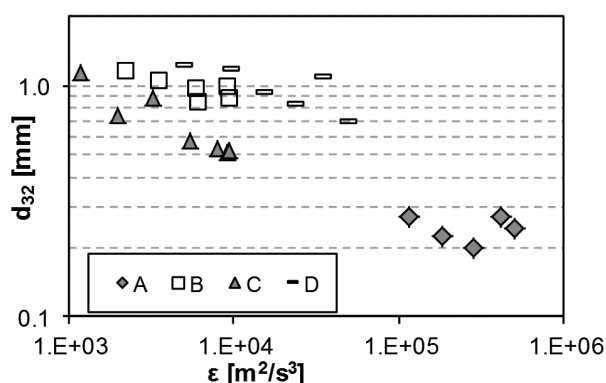
Figure 3: Sauter diameter in dependence of energy dissipation rate.

Future work will concentrate on increasing the understanding of described phenomena regarding turbulent regions and bubble breakup mechanism with related mass transfer.

Contact:
felix.reichmann@udo.edu
norbert.kockmann@udo.edu

Separation Units and Equipment for Lab-Scale Process Development

Sebastian Soboll, Norbert Kockmann

Miniaturized unit operations for phase and component separation are important for entire process development on laboratory scale. Liquid–liquid extraction is often performed in columns, which were miniaturized for higher separation efficiency and to be suitable for flow rates in flow chemistry processes. Two-phase mass transfer processes in capillaries benefit from rapid final phase separation, which can be performed in an in-line phase splitter based on different surface wetting behavior. Crystallization is often a final purification step, which is performed in a continuously operated helical tube setup with narrow residence time distribution. These unit operations are continuously developed and improved in our laboratory. Distillation will be the next separation technique to be implemented in a miniaturized device.

While the development of microreactors has advanced quite far, there is still a huge demand for lab-scale, continuous separation devices, which are well-characterized and widely applicable. In the following, three miniaturized separation devices are introduced.

Microchannels have been widely used for contacting of liquid-liquid systems. Here, the instantaneous and continuous phase splitting is crucial for certain applications, such as reactive extractions. The splitting process can be performed based on the different wetting characteristics by using a T-junction with a hydrophilic outlet made of stainless steel and a lipophilic outlet made of polymers. The splitting efficiency is further enhanced by placing a stainless steel sieve at the hydrophilic outlet.

The application of lab-scale equipment for continuous crystallization processes is challenging due to solid formation and handling. Thus, an efficient particle fluidization is important for robust operation. The coiled flow inverter (CFI), which consists of segments of helically coiled tubes oriented perpendicular to each other, provides enhanced particle fluidization through the formation of Dean vortices and a residence time distribution close to ideal plug flow behavior. Combined with a jacket pipe, this type of apparatus is used for continuous cooling crystallizations. A prototype with an inner tube diameter of 4 mm works with mass flow rates in the range of 10 g min^{-1} and provides a nearly linear axial temperature profile through air cooling in counter-current flow.

For implementation of counter-current liquid-liquid (LL) extraction processes on lab-scale, miniaturized extraction columns are used. The prototype of a stirred-pulsed extraction column with 15 mm (DN15) inner diameter can be operated at flow rates in the range of 1 – 20 ml min^{-1}, which is suitable for lab-scale applications (Figure 1). The column has already been used for several studies, such as the investigation of enantioselective LL extraction of various substances, extraction of sugars from aqueous solution and separation of castor oil methyl esters.

Recently, the counter-current extraction of 5-hydroxymethylfurfural (HMF) from aqueous solution was studied. HMF is considered to be a potential bio-based platform chemical, which can be used as a feedstock for furan-based polymers. In situ extraction of HMF during its synthesis can enhance reaction yield, since consecutive reactions are prevented. Operating parameters were investigated for the HMF extraction using methyl isobutyl ketone as solvent. In a DN15 stirred-pulsed column with 1.1 m active extraction height, extraction yields of >99 % were achieved for an initial HMF weight fraction of 10 % in the feed. The axial concentration profile in the aqueous phase is shown in Figure 2.
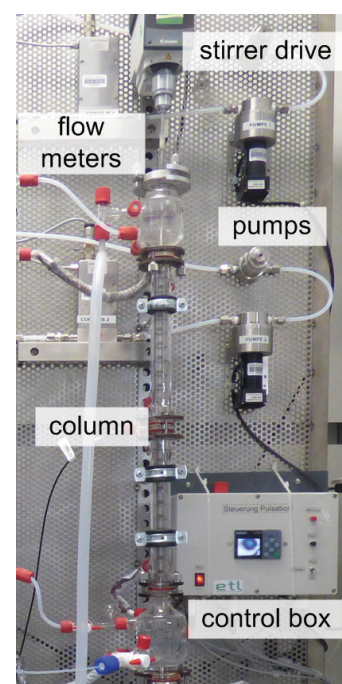
Figure 1: DN15 stirred pulsed extraction column.
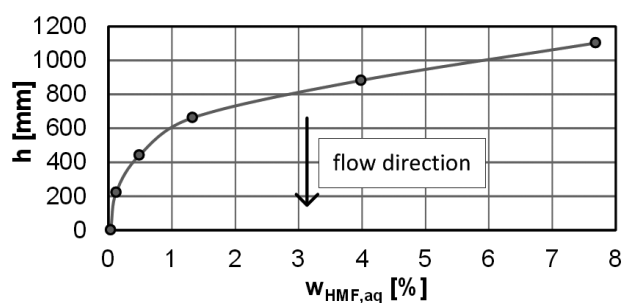
Figure 2: Concentration profile for HMF extraction in DN15 column.

Contact:
sebastian.soboll@udo.edu
norbert.kockmann@udo.edu

Publications 2016 - 2014
Peer reviewed journal papers

2016

- L. Hohmann, K. Kössl, N. Kockmann, G. Schembecker, C. Bramsiepe
  Modules in Process Industry - A life cycle definition
  Chemical Engineering & Processing: PI, DOI: 10.1016/j cep.2016.09.017, (2016)

- F. Reichmann, A. Tollkötter, S. Körner, N. Kockmann
  Gas-Liquid Dispersion in Micronozzles and Microreactor Design for High Interfacial Area
  Chemical Engineering Science, DOI: 10.1016/j.ces.2016.10.028, (2016)

- F. Braun, S. Schwolow, J. Seltenreich, N. Kockmann, T. Röder, N. Gretz, M. Rädle
  Highly sensitive Raman spectroscopy with low laser power for fast in-line reaction and multiphase flow monitoring
  Analytical Chemistry, 88 (19), 9368-9374 (2016)

- L. Hohmann, S.K. Kurt, S. Soboll, N. Kockmann
  Separation Units and Equipment for Lab-Scale Process Development
  J. Flow Chemistry, 6 (3), 181-190 (2016)

- S. Schwolow, A. Neumüller, L. Abahmane, N. Kockmann, T. Röder
  Design and application of a millistructured heat exchanger reactor for an energy-efficient process
  Chemical Engineering & Processing: PI, 108, 109-116 (2016)

- L. Hohmann, R. Gorny, O. Klaas, J. Ahlert, K. Wohlgemuth, N. Kockmann
  Design of a Continuous Tubular Cooling Crystallizer for Process Development on Lab-scale
  Chemical Engineering & Technology, 39(7), 1268-1280 (2016)

- N. Kockmann
  Modular Equipment for Chemical Process Development and Small-scale Production in Multipurpose Plants
  ChemBioEng Reviews, 3 (1), 5-15 (2016)

- R. Trostorf, N. Kockmann
  Methodik zur einfachen Standardisierung von Probenahmesystemen auf Basis der beteiligten Fluidphasen
  Chemie - Ingenieur - Technik, 88 (1-2), 128-138 (2016)

- A. Tollkötter, F. Reichmann, J. Wesholowski, F. Schirmbeck, N. Kockmann
  Gas-Liquid Flow Dispersion in Micro Offices and Bubble Coalescence with High Flow Rates
  J. Electronics Packaging, 138(1):011013-011013-8, EP-15-1105 (2016)

- S. Schwolow, J.Y. Ko, N. Kockmann, T. Röder
  Enhanced heat transfer by exothermic reactions in laminar flow capillary reactors
  Chemical Engineering Science141, 356-362 (2016)

- N. Kockmann, P. Lutze, A Górak
  Grand Challenges and Chemical Engineering Curriculum-Developments at TU Dortmund University
  Universal Journal of Educational Research 4 (1), 200-204 (2016)

- E.C. Sindermann, A. Holbach, A. de Haan, N. Kockmann
  Single stage and countercurrent extraction of 5-hydroxymethylfurfural from aqueous phase systems
  Chemical Engineering Journal, 283 (1), 251-259 (2016)

- S.K. Kurt, I. Vural-Gürsel, V. Hessel, K.D.P. Nigam, N. Kockmann
  Liquid-Liquid Extraction System with Microstructured Coiled Flow Inverter and Other Capillary Setups for Single-Stage Extraction Applications
  Chemical Engineering Journal, 283 (1), 764-777 (2016)

- I. Vural-Gürsel, S.K. Kurt, Q. Wang, T. Noël, K.D.P. Nigam, N. Kockmann, V. Hessel
  Utilization of Milli-scale Coiled Flow Inverter in Combination with Phase Separator for Continuous Flow Liquid-Liquid Extraction Processes
  Chemical Engineering Journal, 283 (1), 855-868 (2016)

2015

- S. Goicoechea, E. Kraleva, S. Sokolov, M.-M. Pohl, N. Kockmann, H. Ehrich
  Support effect on structure and performance of Co and Ni catalysts for steam reforming of acetic acid
  Appl. Cat. A, 514, 182-191 (2015)

- S. Liao, J. Sackmann, A. Tollkötter, M. Pasterny, N. Kockmann, W.K. Schomburg
  Ultrasonic fabrication of PVDF micro nozzles for generating and characterizing liquid/liquid- and gas/liquid-dispersions
  Microsystems Technology, DOI: 10.1007/s00542-015-2708-z (2016)

- M. Rieks, R. Bellinghausen, N. Kockmann, L. Mleczko
  Experimental study of methane dry reforming in an electrically heated reactor
  Int. J. Hydrogen Energy, 40 (46), 15940-15951 (2015)

- S. Schwolow, F. Braun, M. Rädle, N. Kockmann, T. Röder
  Fast and efficient acquisition of kinetic data in microreactors using in-line Raman analysis
  Org. Proc. R&D, 19 (9), 1286-1292 (2015)

- A. Holbach, S. Soboll, B. Schuur, N. Kockmann
  Chiral Separation of 3,5-Dinitrobenzoyl-(R,S)-Leucine in Process Intensified Extraction Columns
  Ind. & Eng. Chem. Res., 54 (33), 8266-8276 (2015)

- C. Fleischer, J. Wittmann, N. Kockmann, T. Bieringer, C. Bramsiepe
  Sicherheitstechnische Aspekte bei der Planung und Bau modularer Produktionsanlagen
  Chemie - Ingenieur - Technik, 87 (9), 1258-1269 (2015)

- N. Kockmann
  Modulare chemische Reaktoren für die Prozessentwicklung und Produktion in kontinuierlichen Mehrzweckanlagen
  Chemie - Ingenieur - Technik, 87 (9), 1173-1184 (2015)

- A. Tollkötter, J. Sackmann, T. Baldhoff, W.K. Schomburg, N. Kockmann
  Ultrasonic hot embossed polymer micro reactors for the optical measurement of chemical reactions
  Chemical Engineering & Technology, 38 (7), 1113-1121 (2015)

- S.K. Kurt, M.G. Gelhausen, N. Kockmann
  Axial Dispersion and Heat Transfer in a Milli / Microstructured Coiled Flow Inverter for Narrow Residence Time Distribution at Laminar Flow
  Chemical Engineering & Technology, 38 (7), 1122-1130 (2015)

- M.G. Gelhausen, S.K. Kurt, N. Kockmann
  Parametrische Empfindlichkeit einer stark exothermen Reaktion im Kapillarwendelreaktor
  Chemie - Ingenieur - Technik, 87 (6), 781-790 (2015)

- A. Tollkötter, J. Sackmann, T. Baldhoff, W.K. Schomburg, N. Kockmann
  Modulares Mikroreaktorsystem aus ultraschallheißgeprägten Polymerfolien
  Chemie - Ingenieur - Technik, 87 (6), 823-829 (2015)

- S. Klutz, S.K. Kurt, M. Lobedann, N. Kockmann
  Narrow residence time distribution in tubular reactor concept for Reynolds number range of 10-100
  Chem. Eng. R&D, 95, 22-33 (2015)

- S. Goicoechea, H. Ehrich, P.L. Arias, N. Kockmann
  Thermodynamic analysis of acetic acid steam reforming for hydrogen production
  J. Power Sources, 279, 312-322 (2015)

- A. Holbach, J. Godde, R. Mahendrarajah, N. Kockmann
  Enantioseparation of Chiral Aromatic Acids in Process Intensified Liquid-Liquid Extraction Columns
  AIChE J., 61 (1), 266-276 (2015)

- N. Kockmann, P. Lutze, A. Górak
  Chemical engineering curricula and challenges resulting from global megatrends, World Congress on Engineering Education 2014
  QScience Proceedings: Vol. (2015)

2014

- J. Singh, N. Kockmann, K.D.P. Nigam
  Novel three-dimensional microfluidic device for process intensification
  Chemical Engineering & Processing: PI, 86, 78-89 (2014)

- S. Schwolow, B. Heikenwälder, L. Abahmane, N. Kockmann, T. Röder
  Kinetic and scale-up investigations of a Michael addition in microreactors
  Org. Proc. R&D, 18 (11), 1535-1544 (2014)

- D. Jaritsch, A. Holbach, N. Kockmann
  Counter-current Extraction in Microchannel Flow: Current Status and Perspectives
  Trans. ASME J. Fluids Eng. 136, 091211 (2014)

- C. Bramsiepe, N. Krasberg, C. Fleischer, L. Hohmann, N. Kockmann, G. Schembecker
  Information technologies for innovative process and plant design
  Chemie - Ingenieur - Technik, 86 (7), 966-981 (2014)

- A. Holbach, E. Caliskan, H.S. Lee, N. Kockmann
  Process Intensification in Small Scale Extraction Columns for Counter-Current Operations
  Chemical Engineering & Processing: PI, 80, 21-28 (2014)

- A. Holbach, D. Jaritsch, J. Godde, N. Kockmann
  Prozessentwicklung der Enantioselektiven Extraktion in miniaturisierten Laborkolonnen
  Chemie - Ingenieur - Technik, 86 (5), 621-629 (2014)

- N. Krasberg, L. Hohmann, Th. Bieringer, C. Bramsiepe, N. Kockmann
  Selection of technical reactor equipment for modular, continuous small scale plants
  MPDI Processes, 2, 265-292 (2014)

- A. Tollkötter, N. Kockmann
  Absorption and Chemisorption of a Small Levitated, Single Bubbles in Aqueous Solutions
  MPDI Processes, 2, 200-215 (2014)

- N. Kockmann
  200 Years in Innovation of Continuous Distillation
  ChemBioEng Reviews, 1, 40-49 (2014)

Peer-reviewed conference papers

2016

- L. Hohmann, S.K. Kurt, N. Pouya Far, D. Vieth, N. Kockmann
  Micro-/Milli-Fluidic Heat-Exchanger Characterization by Non-Invasive Temperature Sensors
  Proc. ASME 2016 14th Intl. Conf. Nanochannels, Microchannels and Minichannels ICNMM2016-8008, Washington, DC, July 10-14 (2016)

- F. Reichmann, A. Tollkötter, N. Kockmann
  Investigation of Bubble Break-up in Microchannel Orifices
  Proc. ASME 2016 14th Intl. Conf. Nanochannels, Microchannels and Minichannels, ICNMM2016-8048, Washington, DC, July 10-14 (2016)

- S.K. Kurt, M. Akhtar, K.D.P. Nigam, N. Kockmann
  Modular Concept of a Smart Scale Helically Coiled Tubular Reactor for Continuous Operation of Multiphase Reaction Systems
  Proc. ASME 2016 14th Intl. Conf. Nanochannels, Microchannels and Minichannels ICNMM2016-8004, Washington, DC, July 10-14 (2016)

2015

- A. Tollkötter, J. Wesholowski, F. Schirmbeck, N. Kockmann
  High flow rate micro orifice dispersion of gas-liquid flow
  Proc. ASME 2015 13th Intl. Conf. Nanochannels, Microchannels and Minichannels, ICNMM2015-48221, San Francisco, July 6-9 (2015)

- S.K. Kurt, K.D.P. Nigam, N. Kockmann
  Two-Phase Flow and Mass Transfer in Helical Capillary Flow Reactors with Alternating Bends
  Proc. ASME 2015 13th Intl. Conf. Nanochannels, Microchannels and Minichannels, ICNMM2015-48416, San Francisco, July 6-9 (2015)

2014

- M.G. Gelhausen, N. Kockmann
  Mixing and Heat Transfer in Helical Capillary Flow Reactors with Alternating Bends
  Proc. ASME 2014 12th Intl. Conf. Nanochannels, Microchannels and Minichannels, ICNMM2014-21779, Chicago, August 3-7 (2014)

- A. Tollkötter, N. Kockmann
A modular microfluidic system for high flow rate re-dispersion of gas-liquid flow
Proc. ASME 2014 12th Intl. Conf. Nanochannels, Microchannels and Minichannels, ICNMM2014-22048, Chicago, August 3-7 (2014)

Plant and Process Design (APT)

Efficient Conversion of Pretreated Brewer's Spent Grain and Wheat Bran by Submerged Cultivation of *Hericium erinaceus*

N. Wolters, C. Schabronath, J. Merz, G. Schembecker

Brewer's spent grain and wheat bran are industrial byproducts that accumulate in millions of tons per year. The approach developed here consisted of utilizing these byproducts for biomass production of the medicinal fungus H. erinaceus *through submerged cultivation. To increase the efficiency of the bioconversion, acidic pretreatment was applied yielding a bioconversion of 38.6% for pretreated BSG and 34.8% for pretreated WB. The produced fungal biomass was applied in a second fermentation step to induce the production of the secondary metabolite* erinacine C. *Contents of 174.8 mg* erinacine C *per g cells for BSG based bioconversions could be achieved.*

Brewer's spent grain (BSG) and wheat bran (WB) are industrial byproducts that can be used as substrates for the solid state cultivation of medicinal mushrooms. However, the use of these lignocellulosic substrates for submerged cultivation is not advanced yet, although this would allow the precise control of important growth parameters such as pH value, temperature or substrate concentration. The filamentous fungus *H. erinaceus* is a suitable candidate to test the named byproducts as substrates for submerged cultivation. Growth studies were performed and the fungus' morphology was analyzed. Although *H. erinaceus* was able to metabolize BSG and WB, a pretreatment of the substrates was considered (decrease the crystallinity of cellulose and solubilize the hemicellulose) to increase the biomass production per time. Several techniques, ranging from hydrothermal and/or acidic pretreatments were investigated. In addition, different BSG and WB concentrations were applied to estimate the maximum yield of biomass after cultivation (Fig. 1). Applying pretreated BSG as substrate doubled and in case of pretreated WB even tripled the productivity compared to the cultivation on untreated byproducts. In addition, it was shown that a complete degradation of the cellulose and hemicellulose into hexose and pentose units was not needed.

In a previous study, focusing on the medium optimization for biomass production of *H. erinaceus*, cell dry weights of 19.3 g/L were obtained. In contrast to the optimized medium significantly lower substrate concentrations were applied for this study. Furthermore, the substrate composition was not optimized as the substrates represent pretreated industrial byproducts only. To compare the different media regarding the biomass production, the biological efficiency, defined as the percentage of the bioconversion of dry raw material to dry biomass, was introduced. A biological efficiency of 38.6% for 20 g/L pretreated BSG and 34.8% for 30 g/L pretreated WB was achieved, whereas the optimized medium had just a slightly higher efficiency of 42.8%. Further optimizing the ratio and the strength of the acid used, a four time reduction of the acid amount could be achieved. However, the biological efficiency of the fungal bioconversion decreased due to the mild pretreatment to 25.6% for 20 g/L BSG and 31.6% for 30 g/L WB. Although the biological efficiency decreased the secondary metabolite production of erinacine C using the biomass could be increased by the mild pretreatment and thus, increased the value of the biomass. To investigate the erinacine C production, which stimulates the nerve growth factor synthesis, suggesting its application in the treatment and prevention of neuronal diseases such as Alzheimer, the biomass was utilized to inoculate the main fermentation with optimized erinacine production media. The influence of different treated BSG and WB media were tested. To compare the results the erinacine C content, defined as the amount of produced erinacine C related to the cell dry weight after cultivation, was used, as the biomass varied with the media investigated (Fig. 1). An erinacine C content of 174.8 ± 32.4 mg erinacine C per g cell dry weight was obtained, which was just the half of the erinacine C content achieved using an optimized pre-cultivation media. Although the strategy to use submerged cultivation of *H. erinaceus* on industrial byproducts did not yield an erinacine C production process it lead to the production of edible mushrooms with functional food character, whose market is increasing steadily.
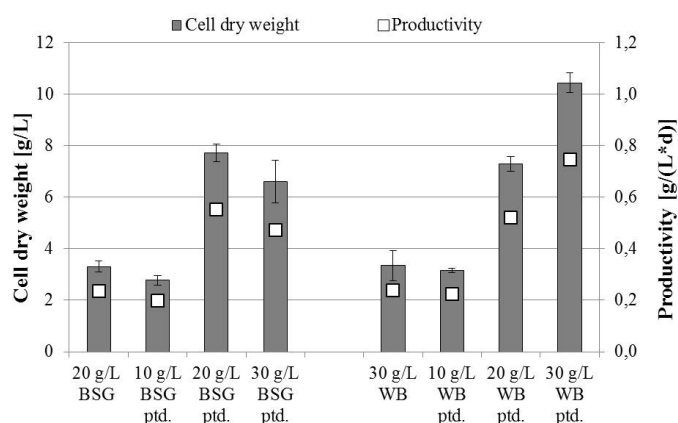

Figure 1: Cell dry weight and productivity after submerged cultivation of *H. erinaceus* with BSG and WB after 14 days at 150 rpm and 24 °C in a shaded incubation shaker. 0.2 M sulfuric acid at a liquid to solid ratio of 10:1 was used for pretreatment (ptd).

Contact:
niklas.wolters@bci.tu-dortmund.de
gerhard.schembecker@bci.tu-dortmund.de

Publications 2016 - 2014

Peer reviewed journal papers

2016

- L. Hohmann, K. Kössl, N. Kockmann, G. Schembecker, C. Bramsiepe
  Modules in process industry - A life cycle definition
  Chemical Engineering and Processing: Process Intensification (2016) DOI: 10.1016/j.cep.2016.09.017

- M. Heitmann, T. Huhn, S. Sievers, G. Schembecker, C. Bramsiepe
  Framework to decide for an expansion strategy of a small scale continuously operated modular multi-product plant
  Chemical Engineering and Processing: Process Intensification (2016) DOI: 10.1016/j.cep.2016.09.004

- T. Kleetz, F. Funke, A. Sunderhaus, G. Schembecker, K. Wohlgemuth
  Influence of Gassing Crystallization Parameters on Induction Time and Crystal Size Distribution
  Crystal Growth & Design 16, 6797-6803 (2016)

- N. Wolters, C. Schabronath, G. Schembecker, J. Merz
  Efficient conversion of pretreated brewer's spent grain and wheat bran by submerged cultivation of Hericium erinaceus
  Bioresource Technology 222, 123-129 (2016)

- M. Lochmüller, G. Schembecker
  Simultaneous optimization of scheduling, equipment dimensions and operating conditions of sequential multi-purpose batch plants
  Computers and Chemical Engineering 94, 157-179 (2016)

- S. Sievers, T. Seifert, G. Schembecker, C. Bramsiepe
  Methodology for evaluating modular production concepts
  Chemical Engineering Science 155, 153-166 (2016)

- L. Holtmann, M. Lobedann, J. Magnus, G. Schembecker
  Disposables for continuous viral clearance for the production of monoclonal antibodies
  European Pharmaceutical Review 21 (2), 22-27 (2016)

- L.-M. Terdenge, K. Wohlgemuth
  Impact of agglomeration on crystalline product quality within the crystallization process chain
  Crystal Research & Technology 51513-523 (2016)

- L. Hohmann, R. Gorny, O. Klaas, J. Ahlert, K. Wohlgemuth, N. Kockmann
  Design of a Continuous Tubular Cooling Crystallizer for Process Development on Lab-scale
  Chemical Engineering & Technology 39, 1268-1280 (2016)

- S. Klutz, L. Holtmann, M. Lobedann, G. Schembecker
  Cost evaluation of antibody production processes in different operation modes
  Chemical Engineering Science141, 63-74 (2016)

- S. Klutz, M. Lobedann, C. Bramsiepe, G. Schembecker
  Continuous viral inactivation at low pH value in antibody manufacturing
  Chemical Engineering and Processing: Process Intensification 102, 88-101 (2016)

- T. Kleetz, F. Braak, N. Wehenkel, G. Schembecker, K. Wohlgemuth
  Design of Median Crystal Diameter Using Gassing Crystallization and Different Process Concepts
  Crystal Growth & Design 161320-1328 (2016)

- C. Dowidat, M. Kalliski, G. Schembecker, C. Bramsiepe
  Synthesis of batch heat exchanger networks utilizing a match ranking matrix
  Applied Thermal Engineering 100, 78–83 (2016)

- F. Thygs, J. Merz, G. Schembecker
  Automation of Solubility Measurements on a Robotic Platform
  Journal of Chemical and Engineering Technology 39 (6), 1049-1057 (2016)

- B. Dreisewerd, J. Merz, G. Schembecker
  Modeling the Quasi-Equilibrium of Multistage Phytoextractions
  Industrial & Engineering Chemistry Research 55, 1808–1812 (2016)

- K. Brandt, G. Schembecker
  Production Rate-Dependent Key Performance Indicators for a Systematic Design of Biochemical Downstream Processes Plants
  Chemical Engineering and Technology 39, 354-364 (2016)

- S. Klutz, J. Magnus, M. Lobedann, M. Temming, G. Schembecker
  Developing the biofacility of the future based on continuous processing and single-use technology
  Source of the Document Journal of Biotechnology 213, 120-130 (2015)

2015

- C. Schwienheer, J. Merz, G. Schembecker
  Investigation, comparison and design of chambers used in centrifugal partition chromatography on the basis of flow pattern and separation experiments
  Journal of Chromatography A 1390, 39-49 (2015)

- N. Wolters, G. Schembecker, J. Merz
  Erinacine C: A Novel Approach to Produce the Secondary Metabolite by Submerged Cultivation of Hericium erinaceus
  Fungal Biology 119, 1334-1344 (2015)

- C. Schwienheer, A. Prinz, T. Zeiner, J. Merz
  Separation of active laccases from Pleurotus sapidus culturesupernatant using aqueous two-phase systems in centrifugal partition chromatography
  Journal of Chromatography B 1002, 1–7 (2015)

- T. Seifert, J.M. Elischewski, S. Sievers, F. Stenger, B. Hamers, M. Priske, M. Becker, R. Franke, G. Schembecker, C. Bramsiepe
  Multivariate risk analysis of an intensified modular hydroformylation process
  Chemical Engineering and Processing: Process Intensification 95, 124-134 (2015)

- J. Sieberz, K. Wohlgemuth, G. Schembecker
  The influence of impurity proteins on the precipitation of a monoclonal antibody with an anionic polyelectrolyte
  Separation and Purification Technology 146, 252-260 (2015)

- A. Hofmann, G. Schembecker, J. Merz
  Reply on "Comments on Role of bubble size for the performance of continuous foam fractionation in stripping mode"
  Colloids and Surfaces A: Physicochemical and Engineering Aspects 474, 105–110 (2015)

- L.-M. Terdenge, S. Heisel, G. Schembecker, K. Wohlgemuth
  Agglomeration degree distribution as quality criterion to evaluate crystalline products
  Chemical Engineering Science 133, 157-169 (2015)

- B. Dreisewerd, J. Merz, G. Schembecker
  Determining the Solute-Solid Interactions in Phytoextraction
  Chemical Engineering Science 134, 287-296 (2015)

- T. Seifert, H. Schreider, S. Sievers, G. Schembecker, C. Bramsiepe
  Real Option Framework for Equipment Wise Expansion of Modular Plants applied to the design of a continuous multiproduct plant
  Chemical Engineering Research and Design 93, 511–521 (2015)

- K. Backhaus, M. Lochmüller, M. C. Arndt, O. Riechert, G. Schembecker
  Knowledge-Based Conceptual Synthesis of Industrial-Scale Downstream Processes for Biochemical Products
  Chemical Engineering Science 38, 537–546 (2015)

- J. Krause, T. Oeldorf, G. Schembecker, J. Merz
  Enzymatic hydrolysis in an aqueous organic two-phase system using Centrifugal Partition Chromatography
  Journal of Chromatography A 1391, 72-79 (2015)

- C. Schwienheer, J. Merz, G. Schembecker
  Selection and use of poly ethylene glycol and phosphate based aqueous two-phase systems for the separation of proteins by Centrifugal Partition Chromatography
  Journal of Liquid Chromatography & Related Technologies 38, 929-941 (2015)

- C. Fleischer, J. Wittmann, N. Kockmann, T. Bieringer, C. Bramsiepe
  Safety Aspects in Planning and Construction of Modular Production Plans
  Chemie Ingenieur Technik 87, 1258 – 1269 (2015)

- C. Schwienheer, A. Prinz, T. Zeiner, J. Merz
  Separation of active laccases from Pleurotus sapidus supernatant using aqueous two-phase systems in centrifugal partition chromatography
  Journal of Chromatography B: Analytical Technologies in the Biomedical and Life Scienes 1002, 1-7 (2015)

2014

- A. Hofmann, G. Schembecker, J. Merz
  Role of bubble size for the performance of continuous foamfractionation in stripping mode
  Colloids and Surfaces A: Physicochemical and Engineering Aspects 473, 85–94 (2014)

- F.A. van Winssen, J. Merz, L. Czerwonka, G. Schembecker
  Application of the Tunable Aqueous Polymer-Phase Impregnated Resins-Technology for protein purification
  Separation and Purification Technology 136, 123-129 (2014)

- T. Seifert, P. Fakner, S. Sievers, F. Stenger, B. Hamers, M. Priske, M. Becker, R. Franke, G. Schembecker, C. Bramsiepe
  Intensified hydroformylation as an example for flexible intermediates production
  Chemical Engineering and Processing: Process Intensification 85, 1–9 (2014)

- K. Stückenschneider, J. Merz, G. Schembecker
  Molecular interaction of amino acids with acidic zeolite BEA: The effect of water
  Journal of Physical Chemistry C 118, 5810-5819 (2014)

- J. Arens, D. Bergs, M. Mewes, J. Merz, G. Schembecker, F. Schulz
  Heterologous fermentation of a diterpene from Alternaria brassisicola
  Mycology 5, 207-219 (2014)

- C. Dowidat, K. Ulonska, C. Bramsiepe, G. Schembecker
  Heat integration in batch processes including heat streams with time dependent temperature progression
  Applied Thermal Engineering 70, 321-327 (2014)

- C. Bramsiepe, N. Krasberg, C. Fleischer, L. Hohmann, N. Kockmann, G. Schembecker
  Information technologies for innovative process and plant design
  Chemie-Ingenieur-Technik 86, 966-981 (2014)

- L. Pansegrau, G. Schembecker, C. Bramsiepe
  A Model to Characterize and Predict Fugitive Emissions from Flange Joints
  Chemical Engineering and Technology 37, 1205-1210 (2014)

- N. Krasberg, L. Hohmann, T. Bieringer, C. Bramsiepe, N. Kockmann
  Selection of Technical Reactor Equipment for Modular, Continuous Small-Scale Plants
  Processes 2, 265-292 (2014)

- T. Seifert, A. Lesniak, S. Sievers, G. Schembecker, C. Bramsiepe
  Capacity Flexibility of Chemical Plants
  Chemical Engineering and Technology 37, 332-342 , (2014)

- J. Sieberz, B. Stanislawski, K. Wohlgemuth, G. Schembecker
  Identification of parameter interactions influencing the precipitation of a monoclonal antibody with anionic polyelectrolytes
  Separation and Purification Technology 127, 165–173 (2014)

- F. A. van Winssen, J. Merz, G. Schembecker
  Tunable Aqueous Polymer-Phase Impregnated Resins-Technology – a novel approach to Aqueous Two-Phase Extraction
  Journal of Chromatography A 1329, 38-44 (2014)

- J. Steimel, M. Harrmann, G. Schembecker, S. Engell
  A framework for the modeling and optimization of process superstructures under uncertainty
  Chemical Engineering Science 115, 225-237 (2014)

Biomaterials and Polymer Science (BMP)

Predictive Materials - A New Class of Smart Materials

First Example of a Predictive Material - Heating Rate Sensitive Shape Memory Polypropylene

Robin Hoeher, Thomas Raidt, Frank Katzenberg, Joerg C. Tiller

Smart materials, also named intelligent materials or more correctly responsive materials, react to environmental changes by adapting their properties to it and thus inducing not only a signal but also a mode of action, e.g. performing of mechanical work. Although such materials are sophisticated, what use might a material have that reacts to an event before it happens? We have realized the first example of such a prophetic or better predictive material, which can be considered as a new class of smart materials.

In order to predict the outcome of a certain event, the predictor has to analyze the changes in the environment. We chose the event of overheating due to thermal inertia as important problem for failure or even damage of numerous products. Systems that protect from overheating require continuous temperature monitoring to ensure detection of abnormal heating rates at an early stage and software controlled weighed reaction by e.g. closing/opening valves or limiting heating power. Alternatively, such systems can be protected by emergency shutdown at a temperature far below the maximal applicable temperature. We chose to develop a polymer that reacts differently to different heating rates. The idea for realizing a heating rate sensitive smart material was to use the kinetic of a phase transition of a semi-crystalline polymer. For this purpose we chose syndiotactic polypropylene (sPP) of low *rrrr*-pentad concentration that usually crystallizes in helical crystal modifications with melting temperatures around 120 °C. Under certain circumstances sPP can also be fully crystallized in a mesomorphic trans-planar crystal modification, e.g. by amorphous quenching from the melt and subsequent cold-drawing to large elongations. This mesomorphic *trans*-planar phase is thermodynamically metastable and melts upon heating above temperatures of 40 – 60 °C followed by recrystallization to helical (form I/II) crystals.

In order to gain a shape memory polymer that reliably responds to heating rates and actuates by recovering shape and performing mechanical work to its environment, sPP was covalently cross-linked right at the borderline between elastomer and thermoplastic. Figure 1 shows the heating-rate sensitive recovery of cold-programmed x-sPP samples triggered with heating rates ranging from 1 to 100 K/min.

All samples start recovery when heated above 40 °C but stop at different heating rate dependent intermediate shapes. Heating rates above 100 K/min result in full recovery of the permanent shape of the x-sPP sample.
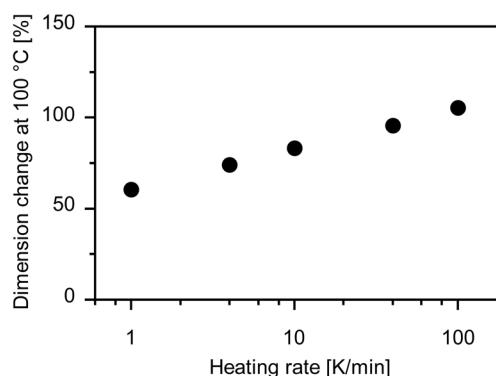
Figure 2: Recovery of cold-programmed x-sPP after heating to 100 °C using different heating rate.

Figure 2 illustrates the heating-rate sensitive response of cold programmed x-sPP when heated with different heating rates to a temperature of 100 °C. The accompanying heating rate sensitive shape change can be efficiently used for preventing overheating when cooking, e.g. water or milk.

Concluding, we could realize a novel type of smart material that is capable to specifically respond to the changing rate of an environmental signal.
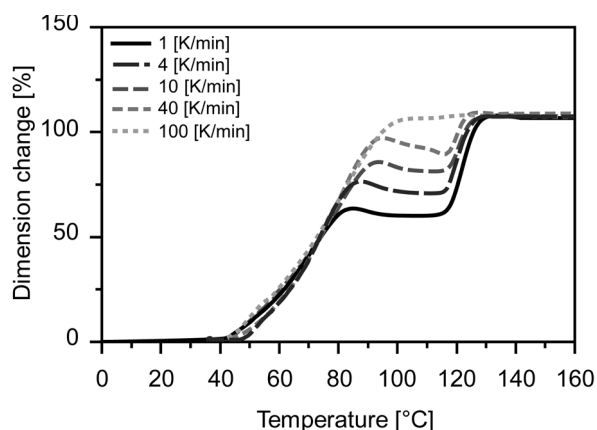

Figure 1: TMA plots of programmed x-sPP triggered with heating rates of 1, 4, 10, 40, and 100 K min^{-1}, respectively.

Contact:
frank.katzenberg@tu-dortmund.de
joerg.tiller@tu-dortmund.de

Tuning the Backbone of Biocidal Telechelic Poly(2-oxazoline)s

Evolution of Telechelic Antimicrobial Polymers

Christian Krumm, Montasser Hijazi, Sylvia Trump, Lena Richter, Joerg C. Tiller

Bacterial infections are a seemingly resolved but newly emerging threat to humankind even in industrial countries (e.g. MRSA or EHEC). The reason for the massive occurrence of diseases caused by multi drug resistant bacterial pathogens is the abusive use of antibiotics and biocides. Their dilution and permanent presence in the environment results in a selection pressure on the microorganisms leading to resistant bacterial strains. We established a biocidal polymer as alternative to common biocides that can be deactivated after its application using the satellite group effect, and will thus not cause further resistant bacterial strains in the environment. Now we raised this functional concept to the next level with respect to activity, selectivity and switchability.

The satellite group effect (SG) of telechelic antimicrobial polymers has been used to create bioswitchable biocides with controlled activity based on poly(2-methyloxazoline) and the amphiphilic biocidal dodecyltrimethylammonium group (DDA). A series of such homo- and copolymers with varying monomer mixtures of 2-methyl-2-oxazoline (MOx) and 2-ethyl-2-oxazoline (EtOx), in statistical or block-wise sequence, were prepared introducing the switchable ester SG by the initiator (OP) to obtain higher activity (Figure 1).
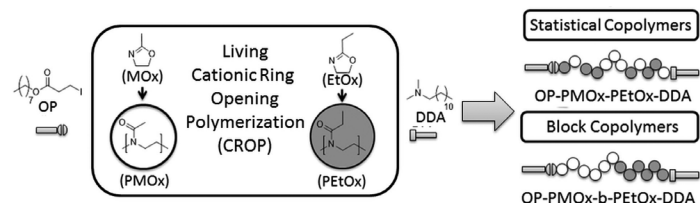
Figure 1: Schematical overview over the synthetic strategy for the preparation of the different copolymers.

The influence of the polymeric structure on the antimicrobial activity against, *S. aureus* and *E. coli*, (MIC = minimal inhibitory concentration of the polymer at which 99 % of the respective bacterial cells are inhibited in growth), their antimicrobial switching potential, and their hemocompatibility HC_{50} (concentration at which 50 % of red blood cells are lysed) was investigated.
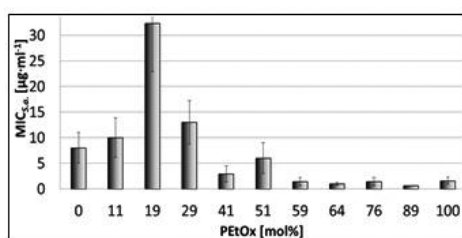
Figure 2: Minimal inhibitory concentration (MIC) of the prepared statistical copolymers based on 2-methyl-2- and 2-ethyl-2-oxazoline against the Gram-positive bacterium *S. aureus* (S.a.).

The polymers with the highest activity against *S. aureus* are PEtOx homopolymers and statistical copolymers with 64-89 mol% of EtOx. They exhibit MIC values of 1.0-1.6 µg/mL (Figure 2). Compared to previously reported antimicrobial telechelic poly(2-oxazolines) (40 µg/mL) this is an order of magnitude lower and among the most active antimicrobial polymers known to literature. Additionally, the selectivity ratios (HC_{50}/MIC) of these polymers are tremendously improved up to 1500. Further, the SG effect makes them highly selective for the Gram-positive strain *S. aureus* compared to the Gram-negative *E. coli* ($MIC_{E.c.}$/$MIC_{S.a}$ up to 750). The switching potential of these polymers allows them to lose antimicrobial activity against *S.aureus*, upon hydrolyzing the SG end group, by a factor of up to 782. This shows the excellent potential of these polymers, which means that when the single SG is exclusively and completely hydrolyzed in the environment the whole polymers lose their biocidal activity.

The study showed that, the antimicrobial activity of telechelic polymers with a satellite group effect is greatly influenced by the nature of the polymer backbone. Another difference to previous publications is the great selectivity towards Gram-positive bacteria, which is smaller for polymers without SG effect. Also the HC_{50}/MIC ratio is much higher than that of poly(2-methyloxazoline) with a DDA and a functional SG. All these data suggest that the SG effect is more complex than previously thought and the potential of these telechelic polymers as antibiotic alternative is very promising.

Contact:
christian.krumm@tu-dortmund.de
joerg.tiller@tu-dortmund.de

Biocatalytically active Nanofibers for Organic Solvents

Entrapment of Enzymes in Electrospun Polymer Nanofibers for a Biocatalytic Stirrer

Ramona Plothe, Ina Sittko, Joerg C.Tiller

Biocatalysis has become an alternative to classical organo-metal catalysis, but is often limited to aqueous media, because most enzymes show very low activities in organic solvents. A common tool to active enzymes in organic media is to immobilize them on suited carriers, but due to diffusion limitations this does not results in the highest possible activities. We have overcome this problem by electrospinning enzymes from aqueous solutions containing the polymer poly(2-ethyloxazoline), which results in highly biocatalytically active nanofibers.

The use of nanofibers for enzyme entrapment is a field of study with enormous potential. In the present work, poly(2-ethyloxazoline) (PEtOx) was used as polymer component for direct electrospinning of different enzymes in aqueous media (Figure 1). The process was optimized by varying process parameter to obtain nanofibers with few hundreds of nanometers in diameter that contain up to 10 wt% protein. It was found that not only the shape and quality of the fibers but also the activity of the enzymes in organic solvents is greatly influenced by the polymer content in the spinning solution.
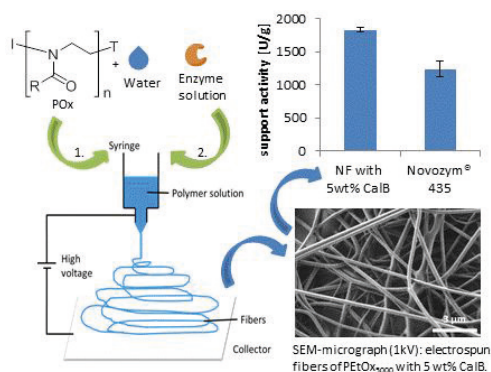
Figure 1: Electrospinning process, resulting nanofibers and carrier activities of PEtOx NF with 5wt% CaLB and Novozym® 435 in toluene.

A series of enzymes, including laccase, horseradish peroxidase, alcohol dehydrogenase, chymotrypsin, and several lipases was prepared under optimized conditions. All enzymes except alcohol dehydrogenase survived the process with only slightly diminished activity. Measuring the activity of the enzyme loaded fibers in *n*-heptane revealed that the biocatalysts are activated by up to two orders of magnitude in all cases compared to the respective enzyme powder suspended in the same solvent. The highest activation was found for proteases, which were also found to be the most stable in the spinning process. The electrospun nanofibers loaded with lipase B from *Candida antarctica* (CaLB-NF) were applied as biocatalyst systems for the esterification of 1-octanol and lauric acid in *n*-heptane and toluene, respectively.

Thereby the enzyme activity depends on the diameter of the fibers and water content of the reaction media, e.g. adding of 1 vol% water to the reaction mixture in *n*-heptane increases the carrier activity of CaLB-NF by more than 100%. However, in contrast to literature, the highest enzyme activity was found in toluene, which is due to a minor swellability of the matrixpolymer PEtOx in this solvent. Using electrospun CaLB under optimized conditions reveals a higher carrier activity than the commercial immobilized CaLB Novozym® 435 with ten times less immobilized protein (Figure 1).
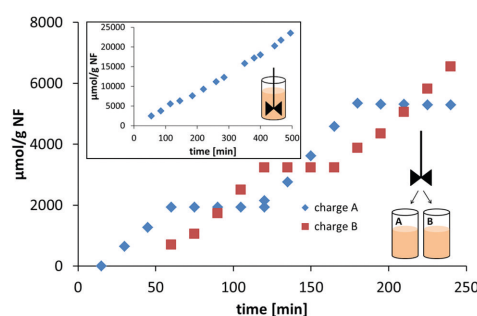
Figure 2: Biocatalytically active stirrer. Charge A and B describe two different lipase assay solutions in *n*-heptane with the same concentration of educts where the stirrer is dipped into alternately. The reaction was followed by determining the CaLB catalyzed ester formation of 1-octanol and lauric acid. The fibers were electrospun from an aqueous solution that contains 20 wt% PEtOx and 0.8 wt% CaLB, the enzyme content in the resulting fiber was 4 wt%.

Another advantage of using electrospinning is the opportunity of easily modifying various surfaces. The electrospinning of PEtOx/CaLB fibers onto a stirrer is used to realize a biocatalytic stirrer for organic solvents (Figure 2). As seen in figure 2, the fibers are highly stable on the stirrer and could repeatedly switched between two reactors without losing activity.

Contact:
ramona.plothe@tu-dortmund.de
joerg.tiller@tu-dortmund.de

Tough, Ultrastiff and Fully Transparent Hydrogels

Creating Organic/Inorganic Hybrid-Hydrogels with Glass-Like Transparency by Enzyme-Induced Calcification

Nicolas Rauner, Monika Meuris, Mirjana Zoric, Joerg C. Tiller

Hydrogels have many applications in industry and medicine. However, they break easily and are very soft. So far only nature has managed to create hydrogels with better mechanical properties such as cartilage and skin. To enhance synthetic hydrogels mechanics filling those with inorganic compounds to form composites is a promising approach, but until today this method does not lead to high stiffness. Here we show the first example for tough composite hydrogels with ultra-high stiffness and glass-like transparency by enzyme-induced mineralization.

Typically, whenever material scientist try to replicate biological tissues, nature is unattainable. In case of hydrogels, cartilage and skin are the materials to compete with. They show extraordinary mechanical properties with a high stiffness (Young's moduli up to 100 MPa) and toughness (fracture energies up to 9000 J/m^2) albeit their high water content. Usually, synthetic hydrogels have far, far lower mechanical properties (Young's modulus < 0.02 MPa, fracture energies < 50 J/m²). In an exceptional case, some pendants reach nature-like fracture energies by extreme extensibility, but exhibit low Young's moduli below 1 MPa. By filling a hydrophilic matrix with inorganic particles, composite hydrogels with a stiffness of up to 10 MPa could be obtained, which are rather brittle.

Following our previously reported approach of enzyme-induced mineralization by homogeneously embedding alkaline phosphatase inside polymer hydrogels and swelling them in calcium glycerolphosphate for 7 days, we could achieve highly water-swollen composite hydrogels with a Young's modulus up to 440 MPa that is 44-times higher than any synthetic and 4-times better than nature. Additionally the water-swollen material exhibit a still high toughness of up to 1300 J m^{-2}. It was found that the key fact is the distribution of alkaline phosphatase inside the hydrogel, which leads to the isotropic growth of inorganic, amorphous calcium phosphate structures inside the hydrogel. Although, the inorganic content is below 15 vol% the change in stiffness of the water swollen composite hydrogel is remarkable, especially because 60 vol% of the material is just water. It is proposed that at a certain amount of calcium phosphate an inorganic network is formed that increases the mechanical properties by percolation of the aggregates. Additionally, an incorporation of phosphonate group carrying monomers in the polymer matrix reduces the size of the CaP aggregates and results in optical transparent and ultrastiff water-swollen materials with high inorganic content (Figure 1).

The phosphonate groups also increase effectivity of CaP enhancement, so that stiff composite hydrogels with 56 MPa could be obtained that consist just of 4.5 vol% calcium phosphate and 90 vol% water.
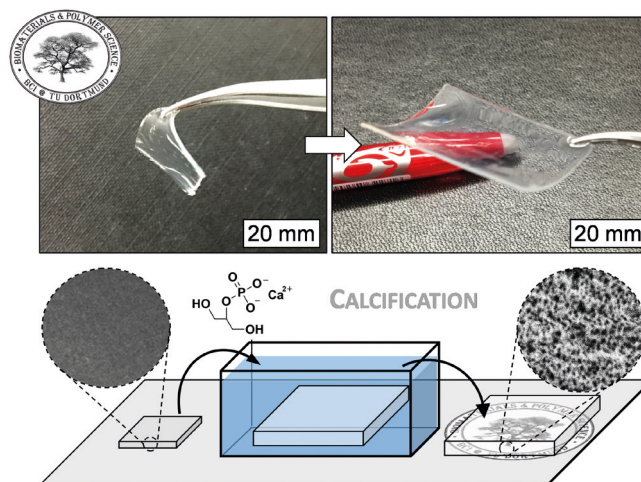
Figure 1: The images show the polymer-hydrogel with 7 wt% phosphonate group containing monomer and 0.4 wt% immobilized alkaline phosphatase before and after calcification in 0.2 M triethanol amine buffered (ph 9.8) calcium glycerolphosphate solution (11 g/l) for 7 days. The scheme illustrates the calcification process and additionally displays the cross-sections of the hydrogels examined with scanning electron microscopy (the diameter of each circles is 1.2 μm).

In future, the presented unique nanostructured material might be used in regenerative medicine as a replacement material for skin, cartilage or bone, whereby the properties and the structure of the new hydrogels can be adjusted very similar to those of the natural idols. It is also a promising candidate for pressure resistant and mechanically cleanable separation membranes or high porous electrode materials for batteries and fuel cells.

Contact:
nicolas.rauner@tu-dortmund.de
joerg.tiller@tu-dortmund.de

Ionically Cross-Linked Shape Memory Polypropylene

A Self-Healing and Thermoplastic Processable Shape Memory Polymer

Thomas Raidt, Robin Hoeher, Monika Meuris, Frank Katzenberg, Joerg C. Tiller

High performance shape memory polymers (SMPs) such as shrinking tubes offer large storable and fully recoverable strains. They are usually permanently cross-linked and can only be used in the produced shape. This greatly limits the range of applications for such polymers, because complex shapes and large bulky products are not accessible. Here we report on the first example of a thermoreversibe, ionically cross-linked SMP that is processable, fast-self healing and additionally stores large strains.

Covalently cross-linked syndiotactic polypropylene (x-sPP) is a powerful shape memory polymer, which distinguishes itself by large strain storage, cold-programmability, heating-rate sensitivity, etc.. In order to additionally make this polymer thermoprocessable with potential of self-healing, we chose to cross-link the material using ionic bonds that are stable at room temperature and cleave above the melting temperature of the shape-stabilizing polymer crystals. This way, the polymer can be heated to form a programmable elastomer and further heated to be processed as thermoplast.

We chose to cross-link sPP by grafting maleic anhydride and letting them react with ZnO. This way carboxylate zinc bridges are formed. They melt above 200 °C, which is well above the melting temperature of the sPP crystals. The ionically cross-linked syndiotactic polypropylene (ix-sPP) was optimized with respect to the degree of cross-linking to be right at the borderline between elastomer and thermoplastic to ensure large extensibility while keeping the original properties of the thermoplastic sPP as unchanged as possible.

Disregarding a smaller fully recoverable stored strain of 300% for ix-sPP instead of 550% for x-sPP, we found the same amazing shape memory properties known from x-sPP for ix-sPP.

After thermal reprocessing, we found a fast network reformation of the ix-sPP within some minutes and no significant loss of properties could be quantified even after intensive mixing in a double-screw extruder, where the ix-sPP was treated at a temperature of 230 °C for 5 min (Fig.1).
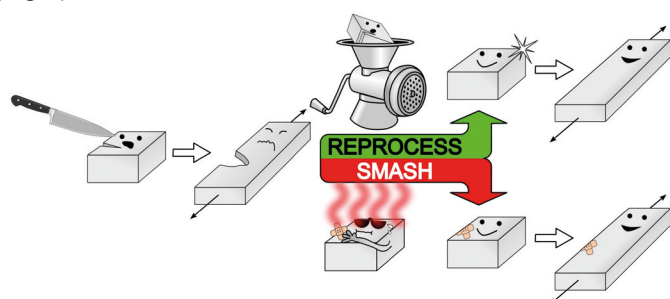
Figure 1: Ionic cross-linking offers thermal reprocessing and shape memory assisted self-healing as options for repairing/renewing a damaged sample.

Furthermore, we found that a damaged ix-sPP sample can be repaired upon applying a shape memory cycle (see Fig. 2). Here a notched sample (a) is heated to 180 °C and quenched in an ice bath. This keeps the sample amorphous for several minutes. Stretching such a sample, results in immediate formation of crystals, which stabilize the new shape (b). Heating the sample again to 180°C results in recovery of the original shape, but also affords healing of the notches (c, d). The healed sample can be programmed again showing no indication of a notch (e) and exhibiting the same mechanical properties as an unnotched sample. This effect is known as shape memory assisted self-healing (SMASH). The ix-sPP is one of a very few examples that are capable of repairing a damaged sample without significant loss of its mechanical as well as shape memory properties.
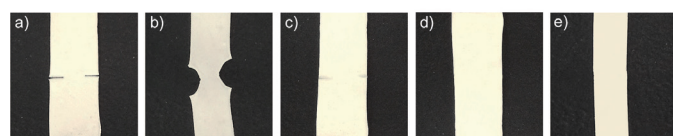
Figure 2: Shape memory assisted self-healing (S.M.A.S.H.) of an ix-sPP sample after a) notching, b) cold-programming, c) shape recovery at 180 °C, d) storing at 180 °C for 30 min, and d) renewed cold-programming.

Additionally, the ix-sPP can be shredded to pieces and reprocessed in an extruder. The resulting material has the same properties as the material before. Thus, ix-sPP is the first representative of thermally reprocessable shape memory polymers that offers fast network-reformation and self-healing while showing the same excellent shape memory properties as its covalently cross-linked analog.

Contact:
frank.katzenberg@tu-dortmund.de
joerg.tiller@tu-dortmund.de

Publications 2016 - 2014

2016

- T. Raidt, R. Hoeher, M. Meuris, F. Katzenberg, J. C. Tiller
  Ionically Cross-Linked Shape Memory Polypropylene
  Macromolecules 49 (18), 6918-6927 (2016)

- R. Plothe, I. Sittko, F. Lanfer, M. Fortmann, M. Roth, V. Kolbach, J. C. Tiller
  Poly(2-ethyloxazoline) as matrix for highly active electrospun enzymes in organic solvents
  Biotechnology and Bioengineering 114 (1), 39-45 (2016)

- R. Hoeher, T. Raidt, F. Katzenberg, J. C. Tiller
  Heating Rate Sensitive Multi-Shape Memory Polypropylene: A Predictive Material
  ACS Applied Materials & Interfaces 8, 13684-13687 (2016)

- F. Katzenberg, J. C. Tiller
  Shape Memory Natural Rubber
  Journal of Polymer Science Part B: Polymer Physics 54, 1381-1388 (2016)

- M. Leurs, P. S. Spiekermann, J. C. Tiller
  Optimization of and Mechanistic Considerations for the Enantioselective Dihydroxylation of Styrene Catalyzed by Osmate-Laccase-Poly(2-Methyloxazoline) in Organic Solvents
  ChemCatChem 8 (3), 593-599 (2016)

- N. Gushterov, F. Doghieri, D. Quitmann, E. Niesing, F. Katzenberg, J. C. Tiller, G. Sadowski
  VOC Sorption in Stretched Cross-Linked Natural Rubber
  Industrial & Engineering Chemistry Research 55 (26), 7191-7200 (2016)

- W. Tillmann, L. Hagen, F. Hoffmann, M. Dildrop, A. Wibbeke, V. Schöppner, V. Resonnek, M. Pohl, C. Krumm, J. C. Tiller, M. Paulus, C. Sternemann
  The detachment behavior of polycarbonate on thin films above the glass transition temperature
  Polymer Engineering & Science 56 (7), 786-797 (2016)

- S. Sommer, T. Raidt, B. M. Fischer, F. Katzenberg, J. C. Tiller, M. Koch
  THz-Spectroscopy on High Density Polyethylene with Different Crystallinity
  Journal of Infrared, Millimeter, and Terahertz Waves 37 (2), 189-197 (2016)

- A. Drahten, J. Reiber, C. Krumm, M. Meuris, J. C. Tiller, C. M. Niemeyer, S. Brakmann
  Genetic Engineering of Silaffin-Like Peptides for Binding and Precipitating Siliceous Materials
  Chemistry Select 1 (15), 4765-4771 (2016)

2015

- M. Schmidt, S. Harmuth, B. E. Barth, E. Wurm, R. Fobbe, A. Sickmann, C. Krumm, J. C. Tiller
  Conjugation of Ciprofloxacin with Poly(2-oxazoline)s and Polyethylene Glycol via End Groups
  Bioconjugate Chemistry 26 (9), 1950-1962 (2015)

- A. Strassburg, F. Kracke, J. Wenners, A. Jemeljanova, J. Kuepper, H. Petersen, J. C. Tiller
  Nontoxic, Hydrophilic Cationic Polymers - Identified as Class of Antimicrobial Polymers
  Macromolecular Bioscience 15 (12), 1710-1723 (2015)

- R. Hoeher, T. Raidt, N. Novak, F. Katzenberg, J.C. Tiller
  Shape Memory PVDF Exhibiting Switchable Piezoelectricity
  Molecular Rapid Communications 36 (23), 2042-2046 (2015)

- I. Sittko, K. Kremser, M. Roth, S. Kuehne, S. Stuhr, J. C. Tiller
  Amphiphilic Polymer Conetworks With Defined Nanostructure and Tailored Swelling Behavior for Exploring the Activation of an Entrapped Lipase in Organic Solvents
  Polymer 64, 122-129 (2015)

- F. Katzenberg, J.C. Tiller
  Vielmehr als nur Gummi
  Nachrichten aus der Chemie (6)623-626 (2015)

- T. Raidt, R. Hoeher, F. Katzenberg, J. C. Tiller
  Chemical Cross-linking of Polypropylenes Towards New Shape Memory Polymers
  Macromolecular Rapid Communications 36 (8), 744-749 (2015)

- D. Quitmann, F. M. Reinders, B. Heuwers, F. Katzenberg, J. C. Tiller
  Programming of Shape Memory Natural Rubber for Near-Discrete Shape Transitions
  ACS Applied Materials and Interfaces 7 (3), 1486-1490 (2015)

- S. Konieczny, M. Leurs, J. C. Tiller
  Polymer Enzyme Conjugates as Chiral Ligands for Sharpless Dihydroxylation of Alkenes in Organic Solvents
  ChemBioChem 16 (1), 83-90 (2015)

- N. Rauner, L. Buenger, S. Schuller, J. C. Tiller
  Post-Polymerization of Urease-Induced Calcified, Polymer Hydrogels
  Macromolecular Rapid Communications 36 (2), 224-230 (2015)

- D. Quitmann, M. Dibolik, F. Katzenberg, J.C. Tiller
  Altering the Trigger-Behavior of Programmed SMNR by Solvent Vapor
  Macromolecular Materials and Engineering 300 (1), 25-30 (2015)

- E. J. Kepola, L. Elena, C. S. Patrickios, L. Epameinondas, V. Chrysovalantis, S. Triantafyllos, R. Schweins, M. Gradzielski, C. Krumm, J. C. Tiller, M. Kushnir, C. Wesdemiotis
  Amphiphilic Polymer Conetworks Based on End-Linked "Core-First" Star Block Copolymers: Structure Formation with Long-Range Order
  ACS Macro Letters 4, 1163-1168 (2015)

2014

- C. Krumm, J. C. Tiller
  Antimikrobielle Oberflächen - Kontaktaktiv oder durch Biozide
  Nachrichten aus der Chemie 62 (10), 984-987 (2014)

- C. P. Fik, S. Konieczny, D. H. Pashley, C. J. Waschinski,
  R. S. Ladisch, U. Salz, T. Bock, J.C. Tiller
  **Telechelic Poly(2-oxazoline)s with a Biocidal and a Polymerizable
  Terminal as Collagenase Inhibiting Additive for Long-Term Active
  Antimicrobial Dental Materials**
  Macromolecular Bioscience 14 (11), 1569-1579 (2014)

- N. Rauner, M. Meuris, S. Dech, J. Godde, J.C. Tiller
  **Urease-induced calcification of segmented polymer hydrogels - a
  step towards artificial biomineralization**
  Acta Biomaterialia 10 (9), 3942-3951 (2014)

- S. Konieczny, C. Krumm, D. Doert, K. Neufeld, J.C. Tiller
  **Investigations on the activity of poly(2-oxazoline) enzyme conjugates
  dissolved in organic solvents**
  Journal of Biotechnology 181, 55-63 (2014)

- J. Tobis, J.C. Tiller
  **Impact of the configuration of a chiral, activating carrier on the
  enantioselectivity of entrapped lipase from Candida rugosa in
  cyclohexane**
  Biotechnology Letters 36 (8), 1661-1667 (2014)

- C. Krumm, S. Harmuth, M. Hijazi, B. Neugebauer, A.-L. Kampmann,
  H. Geltenpoth, A. Sickmann, J.C. Tiller
  **Antimicrobial Poly(2-methyloxazoline)s with Bioswitchable Activity
  through Satellite Group Modification**
  Angewandte Chemie International Edition 53 (15), 3830-3834 (2014)

- C. Krumm, S. Harmuth, M. Hijazi, B. Neugebauer, A.-L. Kampmann,
  H. Geltenpoth, A. Sickmann, J.C. Tiller
  **Biologisch schaltbare antimikrobielle Poly(2-methyloxazoline) auf
  Grundlage des Satellitengruppeneffekts**
  Angewandte Chemie 126 (15), 3908-3913 (2014)

- D. Quitmann, N. Gushterov, G. Sadowski, F. Katzenberg, J.C. Tiller
  Environmental Memory of Polymer Networks under Stress
  Advanced Materials 26 (21), 3441-3444 (2014)

- L. A. T. W. Asri, M. Crismaru, S. Roest, Y. Chen, O. Ivashenko,
  P. Rudolf, J.C. Tiller, H. C. v.d. Mei, T. J. A. Loontjens, H. J. Busscher
  **A Shape-Adaptive, Antibacterial-Coating of Immobilized Quaternary-
  Ammonium Compounds Tethered on Hyperbranched Polyurea and
  its Mechanism of Action**
  Advanced Functional Materials 24 (3), 346-355 (2014)

- M. Sellerberg, D. DiBartolo, J. Oberrecht, J.C. Tiller, P. Walzel
  Viscometric measurement of protease activities on gelatine substrate
  Applied Rheology 24 (6), 62660 (2014)

Patents

- Tiller, J.C., Katzenberg, F., Hoeher, R., Raidt, T.
  Method for producing an oriented polymer
  Eur. Pat. Appl. (2016), EP 3098059 A1 20161130

- Tiller, J.C., Mueller, C., Rauner, N.
  **Derivatized silicon dioxide nanoparticles coated with quaternary
  ammonium salts contg. a silane group and long alkyl chain exhibi-
  ting biocidal action**
  Ger. Offen. (2015), DE 102014108278 A1 20151217

- Tiller, J.C., Quitmann, D., Katzenberg, F.
  **Polymer network comprising shape memory polymers used as a
  sensor or force element**
  Eur. Pat. Appl. (2014), EP 2783834 A1 20141001

Bioprocess Engineering (BPT)

Biofilm-based Multi-step Synthesis of Perillic Acid

Christian Willrodt, Babu Halan, Lisa Karthaus, Jessica Rehdorf, Mattijs K. Julsing, Katja Buehler, Andreas Schmid

Many interesting reactants for industrially relevant biotransformations can be classified as hydrophobic solvents, which are toxic to whole-cell biocatalysts by affecting the cellular viability. This will in the end result in reduced biocatalyst efficiencies and lower reactor productivities. In order to overcome process constraints caused by solvent toxicity biologically and/or technologically inspired strategies may be applied. In nature, many microorganisms form biofilms to increase resistance against exogenous influences. Here, we developed a biofilm based process concept for the biotransformation of the monoterpene (R)-(+)-limonene in (R)-(+)-perillic acid as a strategy to overcome toxicity limitations.

Pseudomonas putida GS1 catalyzes limonene oxidation via the native p-cymene degradation pathway involving the enzymes CymA, CymB, and CymC (Fig. 1B) [1]. However, this approach suffered from process instabilities due to toxification of the biocatalyst. *P. putida* GS1 and recombinant solvent-tolerant *P. taiwanensis* VLB120 were evaluated for continuous perillic acid production. A tubular segmented-flow biofilm reactor was used in order to relieve oxygen limitations and to enable membrane mediated substrate supply as well as efficient in situ product removal (Fig. 1A) [2].
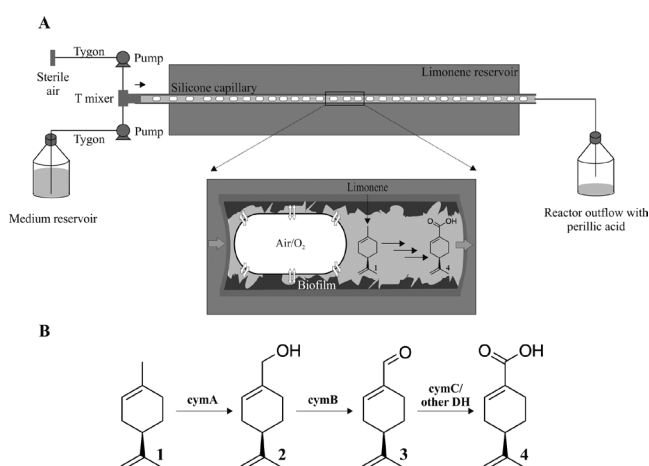
Figure 1: Schematic representation of the segmented flow biofilm reactor (A) and the reaction scheme for multi-step bioconversion of (R)-(+)-limonene to (R)-(+)-perillic acid (B).

Both, *P. putida* GS1 and *P. taiwanensis* VLB120 developed a catalytic biofilm in this system. The productivity of wild-type *P. putida* GS1 encoding the enzymes for limonene bioconversion was highly dependent on the carbon source and reached 35 g L_{tube}^{-1} day^{-1} when glycerol was supplied (Fig. 2).

Approximately 10-fold lower productivities were reached irrespective of the applied carbon source when the recombinant *P. taiwanensis* VLB120 harboring *p*-cymene monooxygenase and *p*-cumic alcohol dehydrogenase was used as biocatalyst (data not shown).
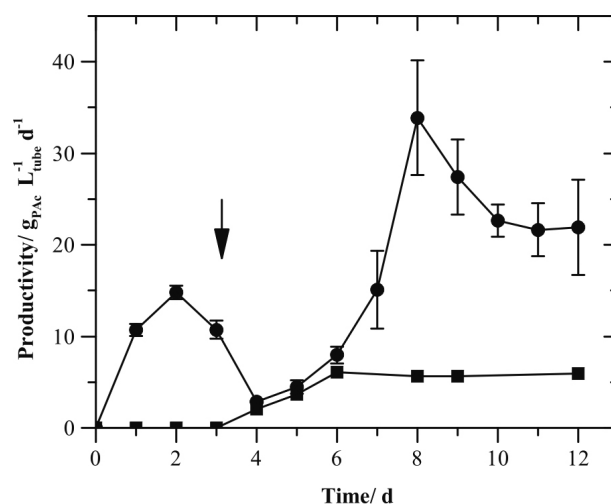
Figure 2: Synthesis of (R)-(+)-perillic acid in a segmented flow biofilm reactor with *P. putida* GS1 using either glycerol (●) or citrate (■) as carbon source. A single-phase flow of 0.1 mL min-1 was applied during the first two days after inoculation. Subsequently, the air flow was started at a flow rate of 0.4 mL min-1 (as indicated by the arrow).

The technical applicability for preparative perillic acid synthesis in the applied system was verified by purification of perillic acid from the outlet stream using an anion exchanger resin. This concept enabled the multi-step production of perillic acid, which might be transferred to other reactions involving volatile reactants and toxic end-products.

References:
[1] Mars et al. (2001) Appl. Microbiol. Biotechnol. 56: 101-107
[2] Karande et al. (2014) Biotech. Bioeng. 111: 1831-1840

Contact:
mattijs.julsing@bci.tu-dortmund.de

Publications 2016 - 2014

In peer reviewed journal (Prof. Lütz)

2016

- M. Antunes, F. Eggimann, M. Kittelmann, S. Lütz, S. P. Hanlon, B. Wirz, T. Bachler, M. Winkler
Human xanthine oxidase recombinant in *E. coli*: A whole cell catalyst for preparative drug metabolite synthesis
Journal of Biotechnology 235, 3-10 (2016)

2015

- M. Geier, T. Bachler, S. P. Hanlon, F. Eggimann, M. Kittelmann, H. Weber, S. Lütz, B. Wirz, M. Winkler
Human FMO2-based microbial whole-cell catalysts for drug metabolite synthesis
Microbial Cell Factories 14, 82 (2015)

2014

- D. Rodrigues, M. Kittelmann, F. Eggimann, T. Bachler, S. Abad, A. Camattari, A. Glieder, M. Winkler, S. Lütz
Production of Recombinant Human Aldehyde Oxidase in *Escherichia Coli* and Optimization of its Application for the Preparative Synthesis of Oxidized Drug Metabolites
ChemCatChem 6, 1028-1042 (2014)

In peer-reviewed journals (scientific coworkers)

2016

- K. Lange, A. Schmid, M.K. Julsing
Δ9-Tetrahydrocannabinolic acid synthase: the application of a plant secondary metabolite enzyme in biocatalytic chemical synthesis
Journal of Biotechnology 233, 42-48 (2016)

- C. Willrodt, A. Hoschek, B. Bühler, A. Schmid, M.K. Julsing
Decoupling production from growth by magnesium sulfate limitation boosts de novo limonene production
Biotechnology and Bioengineering 113 (6), 1305-1314 (2016)

- N. Ladkau, M. Aßmann, M. Schrewe, M.K. Julsing, A. Schmid, B. Bühler
Efficient production of the Nylon 12 monomer ω-aminododecanoic acid methyl ester from renewable dodecanoic acid methyl ester with engineered *Escherichia coli*
Metabolic Engineering, 36, 1-9 (2016)

2015

- K. Rosenthal, F. Falke, O. Frick, C. Dusny, A. Schmid
An inert continuous microreactor for the isolation and analysis of a single microbial cell
Micromachines 6 (12), 1836-1855 (2015)

- J. Volmer, A. Schmid, B. Bühler
Guiding bioprocess design by microbial ecology
Current Opinion in Microbiology 25, 25-32 (2015)

- K. Lange, A. Schmid, M.K. Julsing
Δ-9-Tetrahydrocannabinolic acid synthase production in Pichia pastoris enables chemical synthesis of cannabinoids
Journal of Biotechnology, 211, 68–76 (2015)

- K. Lange, A. Poetsch, A. Schmid, M.K Julsing
Enrichment and identification of Δ-9-tetrahydrocannabinolic acid synthase from Pichia pastoris culture supernatants
Data in Brief , 4, 68–76 (2015)

- C. Willrodt, A. Hoschek, B. Bühler, A. Schmid, M.K. Julsing
Coupling limonene formation and oxyfunctionalization by mixed-culture resting cell fermentation
Biotechnology and Bioengineering, 112(9), 1738-1750 (2015)

- C. Looße, S. Galozzi, L. Debor, M.K. Julsing, B. Bühler, A. Schmid, K. Barkovits, T. Müller, K. Marcus
Direct infusion-SIM as fast and robust method for absolute protein quantification in complex samples
EuPA Open Proteomics, 7, 20-26 (2015)

- C. Willrodt, R. Karande, A. Schmid, M.K. Julsing
Guiding efficient microbial synthesis of non-natural chemicals by physicochemical properties of reactants
Current Opinion in Biotechnology, 35, 52-62 (2015)

2014

- J. Volmer, C. Neumann, B. Bühler, A. Schmid
  Engineering of Pseudomonas taiwanensis VLB120 for constitutive solvent tolerance and increased specific styrene epoxidation activity
  Applied and Environmental Microbiology 80 (20), 6539-6548 (2014)

- C. Willrodt, C. David, S. Cornelissen, B. Bühler, M.K. Julsing, A. Schmid
  Engineering the productivity of recombinant *Escherichia coli* for limonene formation from glycerol in minimal media
  Biotechnology Journal, 9 (8), 1000-1012 (2014)

- M. Schrewe, M.K. Julsing, K. Lange, E. Czarnotta, A. Schmid, B. Bühler
  Reaction and catalyst engineering to exploit kinetically controlled whole-cell multistep biocatalysis for terminal FAME oxyfunctionalization
  Biotechnology and Bioengineering, 111 (9), 1820-1830 (2014).
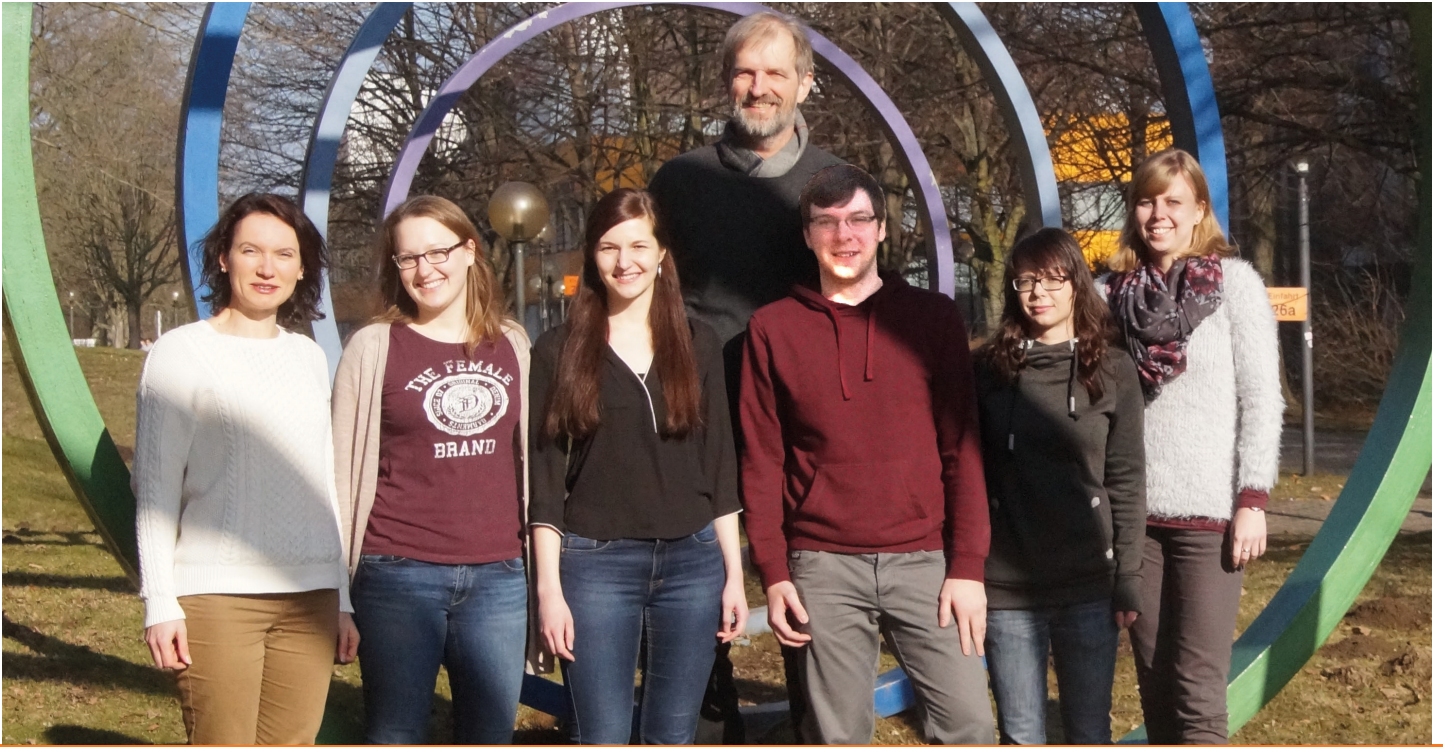
Biochemical Engineering (BVT)

Process Intensification of Fermentative Biosurfactant Production

Towards Continuous Rhamnolipid Production

Iva Anic, Arijit Nath, Pedro Franco, Rolf Wichmann

There is an increase in a market demand on biosurfactants due to the fact that the petrochemical resources for the production of surfactants are being depleted. Among biosurfactants, bacterially produced rhamnolipids have shown excellent emulsifying and antimicrobial properties, as well as an environmentally friendly nature. Their production is still not competitive to the chemical surfactants production. For this reason a strenuous research on biosurfactant production is needed. One of the mayor problems in their fermentative production is an excessive foaming due to the product concentration increase. This problem has been successfully overcome by in situ product separation with foam adsorption.

Fed-Batch cultivation of rhamnolipid producing *Pseudomonas putida* KT2440 on a hydrophilic substrate is done in a 3.1 L bioreactor. Due to the bottom aeration of the bioreactor, the produced rhamnolipids are highly concentrated in the foam phase in the upper part of the bioreactor space. Rhamnolipids are separated from the rhamnolipid-containing foam by adsorption and the rhamnolipid-free adsorption permeate is lead back into the fermentor.
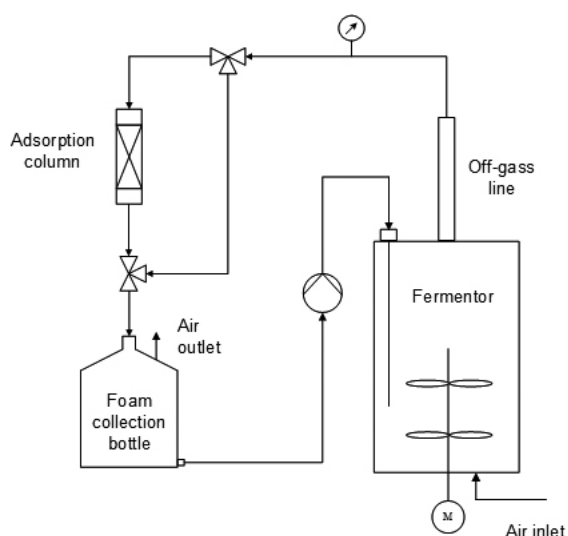
Figure 1: Schematic representation of the setup for fermentation with direct foam adsorption and foamate recycling.

Since there is no need for foam destruction or cell separation before the adsorption step, with this technology a significant downstreaming cost reduction can be achieved on a process scale. Further on, a product inhibition is avoided and the process time is reduced.

For this purpose an adsorbent was precisely chosen on the basis of its physico-chemical properties, a capacity for the rhamnolipid adsorption and the pressure drop in the adsorption column over the process time.
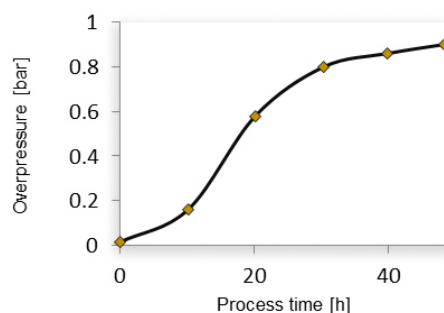
Figure 2: Pressure drop measured in the adsorption column when only one column is used for 48 hours process time.

Once the maximum adsorption capacity of the adsorbent is reached and the adsorption column is fully loaded with the product, elution of rhamnolipids with organic solvents takes place. In order to be able to operate the process continuously, at least two adsorption columns are needed.

The productivity of an in situ fed-batch process is higher than that of a similar process where only a foam recycling is done. Running a process in the continuous mode could lead to further increase in productivity. Future work is directed towards the continuous rhamnolipid fermentation and reaching high cell densities. An automation of the adsorption process step is a pre-requisite for the continuous in situ rhamnolipid separation by foam adsorption.

Contact:
iva.anic@bci.tu-dortmund.de
rolf.wichmann@bci.tu-dortmund.de

Publications 2016 - 2014

2016

- D. von der Haar, G. Gofferjé, A. Stäbler, R. Wichmann, T. Herfellner
  Kinetics of Lipase-catalyzed De-acidification of Degummed Rapeseed Oil Utilizing Monoacylglycerol as Acyl-group Acceptor
  Journal of Molecular Catalysis B-Enzymatic 127, 40-46 (2016)

- M. Kampmann, N. Riedel, Y.L. Mo, L. Beckers, R. Wichmann
  Tyrosinase Catalyzed Production of 3,4-Dihydroxyphenylacetic Acid Using Immobilized Mushroom (Agaricus bisporus) Cells and in Situ Adsorption
  Journal of Molecular Catalysis B-Enzymatic 123, 113-121 (2016)

- L.M. Halka, S. Kockelke, R. Wichmann
  In Situ Product Removal of Fermentatively Produced Fusicoccadiene Using a Two-phase System
  Chemie-Ingenieur-Technik 9, 1328 (2016)

- T. Tiso, A. Germer, B. Küpper, R. Wichmann, L.M. Blank
  Methods for Recombinant Rhamnolipid Production
  In: T.L. McGenity, K.N. Timmis, B. Nogales Fernández (Hrsg.), Hydrocarbon and Lipid Microbiology Protocols: Synthetic and Systems Biology – Applications, Springer-Verlag, Berlin Heidelberg, 65-94 (2016)

2015

- M. Kampmann, A.C. Hoffrichter, D. Stalinski, R. Wichmann
  Kinetic Characterization of Tyrosinase Containing Mushroom (Agaricus bisporus) Cells Immobilized in Silica Alginate
  Journal of Molecular Catalysis B-Enzymatic 116, 124-133 (2015)

- D. von der Haar, A. Stäbler, R. Wichmann, U. Schweiggert-Weisz
  Enzyme-assisted Process for DAG Synthesis in Edible Oils
  Food Chemistry 176, 263-270 (2015)

- S. Tomic, L. Besnard, B. Fürst, R. Reithmeier, R. Wichmann, P. Schelling, C. Hakemeyer
  Complete Clarification Solution for Processing High Density Cell Culture Harvests
  Separation and Purification Technology 141, 269-275 (2015)

- D. von der Haar, A. Stäbler, R. Wichmann, U. Schweiggert-Weisz
  Enzymatic Esterification of Free Fatty Acids in Vegetable Oils Utilizing Different Immobilized Lipases
  Biotechnology Letters 37(1), 169-174 (2015)

2014

- M. Kampmann, S. Boll, J. Kossuch, J. Bielecki, S. Uhl, B. Kleiner, R. Wichmann
  Efficient Immobilization of Mushroom Tyrosinase Utilizing Whole Cells From Agaricus bisporus and its Application for Degradation of Bisphenol A
  Water Research 57, 295-303 (2014)

Patent application

- LU No 93393, Priorität: 22.12.2016 (2016)
  In Situ Separation of Amphipathic Compound by Foam Adsorption
  I. Anic, R. Wichmann, A. Nath, P. Franco

Chemical Reaction Engineering (CVT)

BrOx Cycle: A Novel Process for CO_2-free Energy Production from Natural Gas

Jesús González-Rebordinos, David W. Agar

The research of CO_2-free energy generation from fossil fuels has led to the development of the BrOx cycle. The use of a halogen to oxidise methane and the resolution of the process in two distinct steps ensures that no CO_2 emission are produced, thus achieving a partial oxidation of methane to carbon and water. An experimental study to evaluate the methane bromination has been conducted.

Currently, the combustion of fossil fuels is the major anthropogenic source of CO_2 and the major reason for the significant increase in its atmospheric concentration over the past decades. Despite the increase in fossil fuel consumption in recent years, the available reserves have actually increased, indicating that the use of fossil fuels is limited less by their availability than by the emissions of CO_2 associated with their combustion.

Energy can be generated from methane without concomitant CO_2 emissions by means of a bromination-oxidation (BrOx) cycle. This process consists of two exothermic reaction steps with a bromine recycle, that result in an overall reaction in which energy is released with solid carbon and water as only by-products.
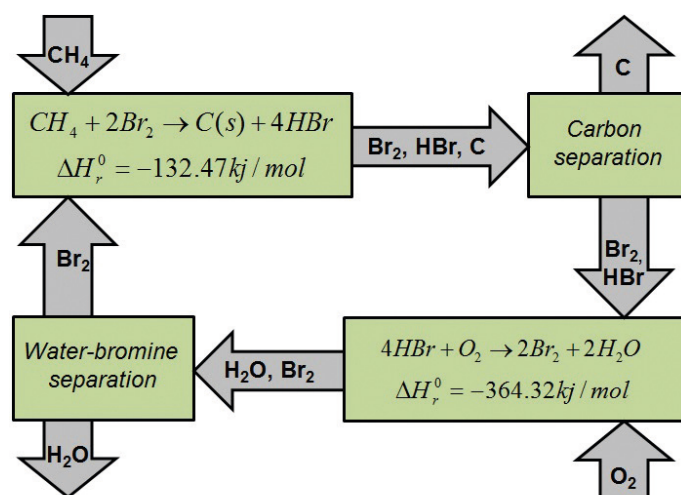
Figure 1: Schematic representation of the BrOx cycle.

An experimental study on methane bromination has been performed in a bench-scale plant. The results show that full conversion of methane is achieved at temperatures above 500°C, at which carbon formation occurs when working with substoichiometric bromine ratios. Under excess bromine conditions carbon forms at temperatures above 900°C.

Figure 2: Carbon deposition on a quartz glass reactor after methane bromination experiment.

Samples of the carbon produced have been taken from the walls of the reactor at different locations along the longitudinal axis and have been analysed with EDX showing that the bromine content greatly varies with the position. The temperature profile of the reactor shows that the bromine content (and therefore the presence of carbonaceous by-products) strongly depends on the temperature, reaching values below 2% at 1000°C. Countermeasures for further reducing the residual bromine content of the carbon and to facilitate the removal of carbon deposits from the reactor walls are being developed. Furthermore a reactor geometry has been devised, which should dramatically reduce the formation of such deposits a priori.
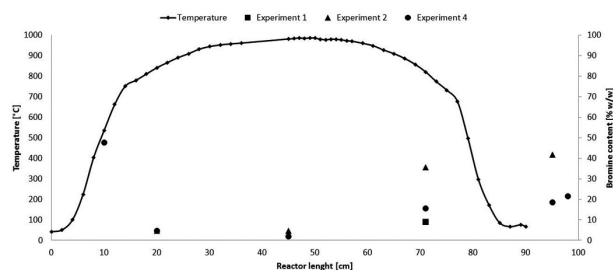
Figure 3: Relationship between bromine content in carbon samples and the temperature profile of the tubular reactor.

Contact:
jesus.gonzalez-rebordinos@bci.tu-dortmund.de
david.agar@bci.tu-dortmund.de

Publications 2016 - 2014

2016

- N. Antweiler, S. Gatberg, G. Jestel, J. Franzke, D.W. Agar
  Noninvasive Sensor for the Detection of Process Parameters for Multiphase Slug Flows in Microchannels
  ACS Sensors, (2016)

- M.G. Gelhausen, S. Yang, M. Cegla, D.W. Agar
  Cyclic mass transport phenomena in a novel reactor for gas–liquid–solid contacting
  AIChe Journal 63(1), 208-215 (2016)

- N. Antweiler, Z. Wang, D.W. Agar
  Evaluation of Ion Exchange Resins for the Esterification of Acrylic Acid with n-Butanol by Polytropic Kinetic Measurement
  Chemie Ingenieur Technik 88 (8), 1095-1101 (2016)

- L. Arsenjuk, F. Kaske, J. Franzke, D.W. Agar
  Experimental investigation of wall film renewal in liquid–liquid slug flow
  International Journal of Multiphase Flow 85, 117-185 (2016)

- J.F. Horstmeier, A. Gomez Lopez, D.W. Agar
  Performance improvement of vacuum swing adsorption processes for CO$_2$ removal with integrated phase change material
  International Journal of Greenhouse Gas Control 47, 364-375 (2016)

- F. Kaske, S. Dick, S. Aref Pajoohi, D.W. Agar
  The influence of operating conditions on the mass transfer performance of a micro capillary contactor with liquid–liquid slug flow
  Chemical Engineering and Processing: Process Intensification 108, 10-16 (2016)

- A.A. Munera Parra, F. Platte, D.W. Agar
  Multiplicity Regions in a Moving-Bed Reactor: Bifurcation Analysis, Model Extension, and Application for the High-Temperature Pyrolysis of Methane
  Chemie Ingenieur Technik 88(11), 1703-17 (2016)

- A.A. Munera Parra, D.W. Agar
  Molten Metal Capillary Reactor for the High Temperature Pyrolysis of Methane
  International Journal of Hydrogen Energy, (2016)

2015

- N. Antweiler, S. Gatberg, J. Franzke, D.W. Agar
  Neue kosteneffektive Mess- und Regeltechnik für das Numbering-up von reaktiven Pfropfenströmungen in Mikrokanälen
  Chemie Ingenieur Technik 87(9), 1221-1229 (2015)

- A.K. Liedtke, F. Scheiff, F. Bornette, R. Philippe, D.W. Agar, C. de Bellefon
  Liquid-solid mass transfer for microchannel suspension catalysis in gas-liquid and liquid-liquid segmented flow
  Industrial & Engineering Chemistry Researc 54(17), 4699-4708 (2015)

- I. Schulz, D.W. Agar
  Decarbonisation of fossil energy via methane pyrolysis using two reactor concepts: Fluid wall flow reactor and molten metal capillary reactor
  International Journal of Hydrogen Energy 40(35), 11422-11427 (2015)

2014

- J.F. Horstmeier, S. Heib, D.W. Agar
  Simulation der prozessinternen Rückgewinnung von Adsorptionswärmen durch Latentwärmespeicher
  Chemie Ingenieur Technik 86(1-2), 97-105 (2014)

- A.A. Munera Parra, N. Antweiler, R. Nagpal, D.W. Agar
  Stability Analysis of Reactive Multiphase Slug Flows in Microchannels
  Processes 2(2), 371-391 (2014)

- F. Scheiff, D.W. Agar
  Solid Particle Handling in Microreaction Technology: Practical Challenges and Application of Microfluid Segments for Particle-Based Processes
  Micro-Segmented Flow. Springer Berlin Heidelberg, 103-148 (2014)

- F. Scheiff, F. Neeman, S.J. Tomasiak, D.W. Agar
  Suspensionskatalyse im Pfropfenströmungs-Mikroreaktor – experimentelle und numerische Stofftransportbewertung
  Chemie Ingenieur Technik 86(4), 504-518 (2014)

Conference proceedings

2016

- M. Hussainy, D.W. Agar
  Structural and Operational Optimality of Adsorptive Reactors
  Chemical Engineering & Technology 39(11), 2135-2141 (2016)
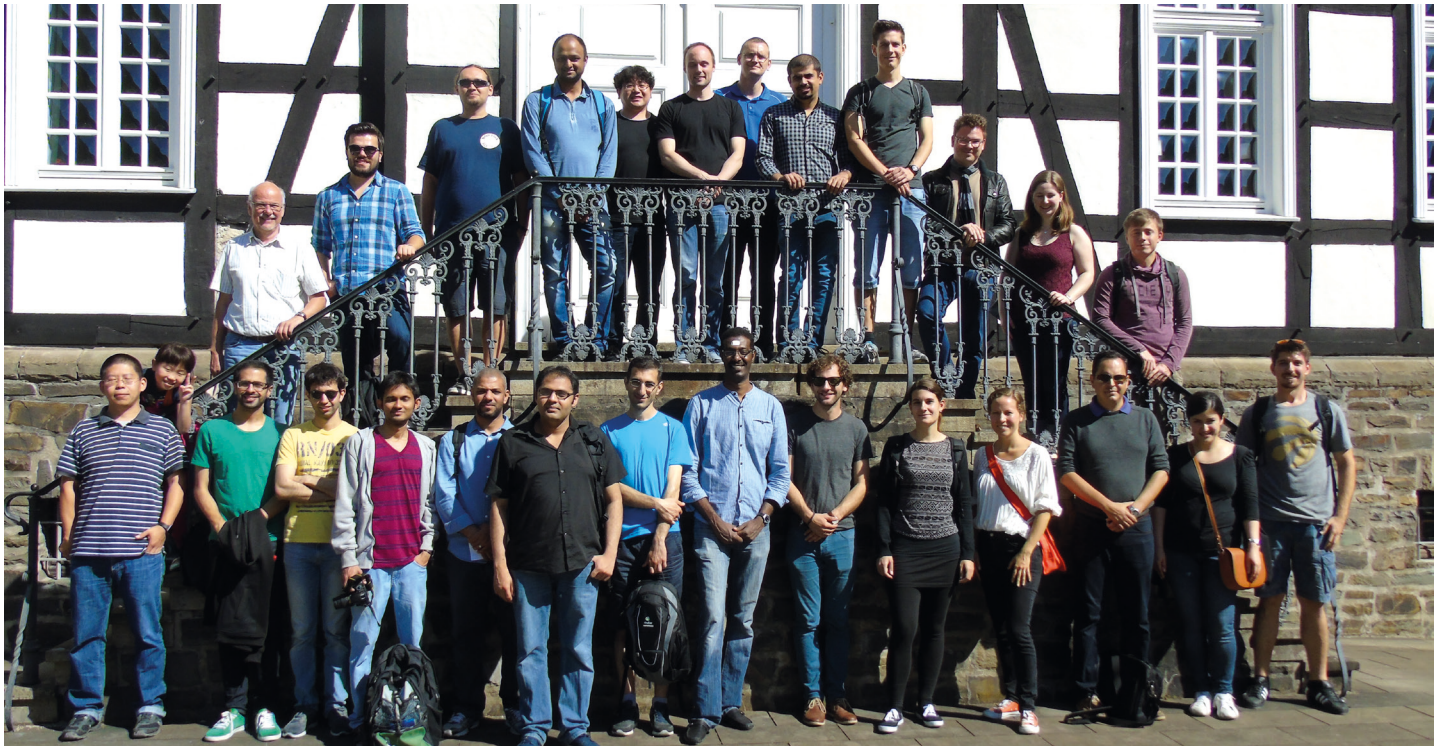
Process Dynamics and Operations (DYN)

Online Optimization of an Evaporator Network in the Viscose Fiber Production

Resource Efficient Operation of Energy Intensive Production Processes

Marc Kalliski[1], Bernhard Voglauer[2], Gerhard Seyfriedsberger[2], Christian Jasch[2], Thomas Röder[2], Sebastian Engell[1]

[1]TU Dortmund University, Dortmund, Germany / [2]Lenzing AG, Lenzing, Austria

The production of viscose fibers for textile and nonwoven applications is performed by spinning dissolved cellulose xanthogenate into an acidic spinbath to regenerate the cellulose to viscose fibers. During the production process water accumulates and dilutes the spinbath. Therefore water has to be removed continuously to ensure stable reaction conditions to produce viscose fibers within the specifications. This task is accomplished using a large evaporator network that consists of several spin bath cycles and of more than 20 evaporators. In the context of the EU project MORE, we developed an online optimization scheme for the operation of the evaporator network. It is based on a data-driven approach to the modelling of the individual evaporators.

During daily operations the operators must decide which evaporators to use in order to achieve the required evaporation capacity per spin bath cycle (see Fig.1). Each evaporator can be operated in one of the different cycles (combinatorial decision problem) and at a variable capacity (continuous decision problem). To support the operators and to ensure the most energy efficient operation, a model-based decision support system was developed.
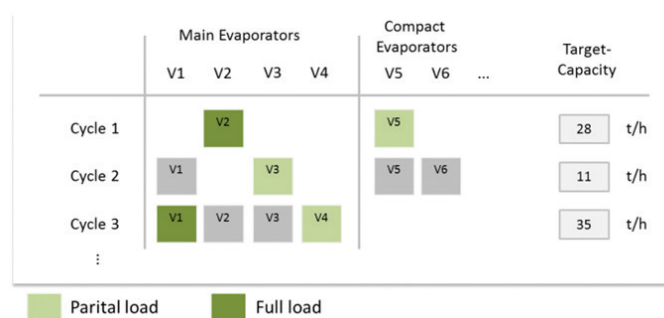
Figure 1: Subset of the evaporator network including larger and more efficient main evaporators and less efficient compact evaporators.

The efficiency of the evaporation is mainly affected by four factors:

- **Evaporator type:** The different types of evaporators have different efficiencies.

- **External influences:** The ambient temperature and humidity are affecting the evaporation via the cooling towers.

- **Fouling state:** Fouling processes in the heat exchangers lead to an increasing energy demand between cleaning cycles.

- **Operating point:** The same evaporation capacity can be obtained for different choices of the controlled variables.
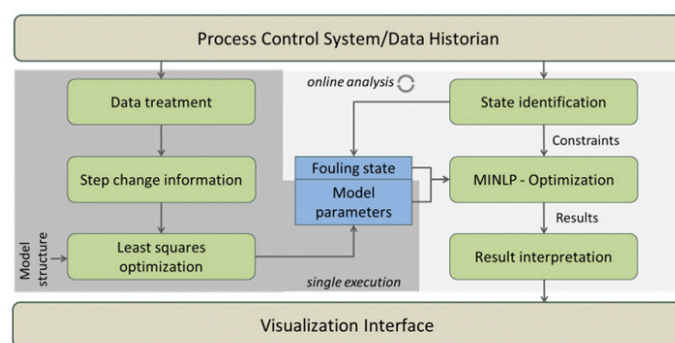
Figure 2: Online optimization scheme with modelling (dark grey) and optimization (light grey).

Preliminary experiments indicated that linear data-based models are sufficient to describe the specific steam consumption and evaporation capacity of an evaporator as a function of the controlled variables, fouling state, and external influences. Figure 2 gives an overview of the structure of the decision support system. The modeling step (dark grey) is performed once for every evaporator and includes a least squares fit of the model parameters to historical data that was automatically obtained from the data historian and reconciled for fouling effects.

The fouling state and the production constraints are dynamically changing and need to be updated before each call of the optimizer. The light grey area in figure 2 highlights the optimization procedure of the operational conditions and evaporator allocations. The evaporator model, the fouling state, and production constraints are integrated into a mixed integer non-linear program (MINLP) that rquires a large computational effort. An efficient meta-heuristic approach that decomposes the optimization problem was developed to reduce the response time to acceptable values.

The optimization results are then presented in a dashboard to provide decision support to the operators for evaporator allocation and load distribution.

Contact:
marc.kalliski@bci.tu-dortmund.de
sebastian.engell@bci.tu-dortmund.de

Publications:
M. Kalliski, B. Voglauer, G. Seyfriedsberger, T. Röder, S. Engell, Chemie Ingenieur Technik 88, 1379 (2016).
M. Kalliski, B. Voglauer, G. Seyfriedsberger, T. Röder, S. Engell, Computer Aided Chemical Engineering (2017), accepted.

Employing Surrogate Models in Chemical Process Design

Application of Artificial Neural Networks as Surrogate Models for Thermodynamic Calculations in Process Optimization

Corina Nentwich and Sebastian Engell

The quality of a process design that is provided by optimization-based design approaches depends on the quality of the process models that are used in the optimization. Kinetic models and predictions of phase equilibria are particularly important. However advanced models of phase equilibria are often too complex for a direct implementation into the optimization model. Replacing the original thermodynamic model calculations by a surrogate model is a way to overcome this problem. In this contribution, artificial neural networks are employed as surrogate models. We show that the use of such models drastically reduces the computation times of the optimization and leads to almost exactly the same results.

In the field of computer-aided optimization and design of chemical processes, the reaction kinetics and the phase equilibria of the components that are present in the process must be described as precisely as possible. Advanced thermodynamic models, as e.g. the Perturbed-Chain Statistical Associating Fluid Theory (PC-SAFT) model can provide accurate and reliable predictions of the behavior of the mixtures in the plant. However, such models are complex and often contain implicit equations that are solved iteratively in specialized software so that it is difficult to embed them in an equation-based optimization of the plant structure and operating parameters. Surrogate models are black-box models that can approximate arbitrary multivariate relationships to any desired accuracy and can easily be evaluated and integrated into equation-based models. In our work, feed forward neural networks are applied to calculate the gas solubilities and the liquid-liquid phase separation of a hydroformylation process in a thermomorphic solvent system (TMS). The process flowsheet is shown in Fig. 1..
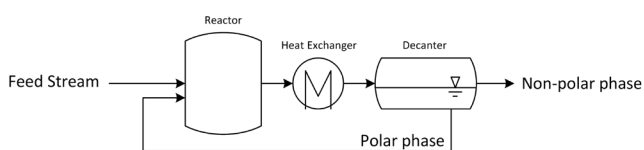
Figure 1: Process flowsheet of the hydroformylation process.

Specifically, the hydroformylation of 1-dodecene to n-tridecanal is considered here. The reaction network considers isomerisation and hydration side reactions and consists of 6 reactions. The TMS system consists of dimethylformamide (DMF) and decane. The reactor is operated at an elevated temperature so that the reaction mixture consists of one single homogeneous liquid phase. The output of the reactor is cooled down and separates into two liquid phases. The polar phase contains DMF and the catalyst and is recycled to the reactor. The non-polar phase mainly contains n-tridecanal and decane and can be further purified.

The feedforward neural networks were trained with sampled data sets that were calculated by complex thermodynamic models. The PC-SAFT model was applied to compute the gas solubilities of hydrogen and carbon monoxide in the reaction mixture.
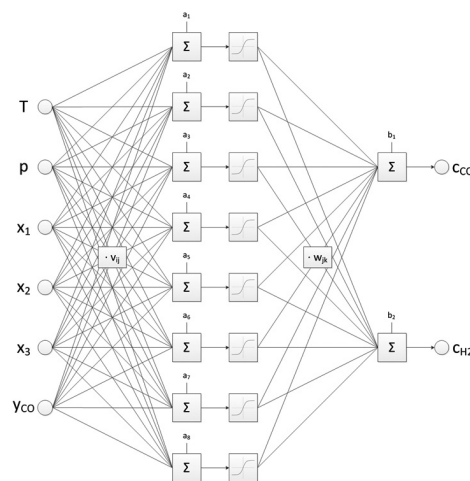
Figure 2: Structure of the neural network for the calculation of the concentrations of the dissolved gases.

The liquid-liquid-separation in the decanter is modeled by the Soave Redlich Kwong equation of state with the modified second order Huron-Viral mixing rule (SRK-MHV2). One of the neural networks is shown in Fig. 2. The surrogate models were tested with validation data sets from PC-SAFT and SRK-MHV2 that were not included in the training set. The validation showed relative deviations of 0.07 % and 0,15 % for gas concentrations, and of at most 0.25 % for the distribution coefficients of DMF, 1-dodecene, n-tridecanal, and decane.

An optimization of the operating parameters (1-dodecene feedrate, reactor and decanter temperatures) with the goal to maximize the process yield was performed using the surrogate models. Applying the optimization result to a model with the original thermodynamic calculations led to a relative deviation of less than 0.1 % of the objective function. The optimization using the surrogate models required 4 CPU seconds, which is less than required for one single call of the PC-SAFT model. The results prove that surrogate models can be successfully employed in process optimization, leading to reliable results with a drastically reduced computational effort.

Publications:
C. Nentwich, S. Engell,
Application of surrogate models for the optimization and design of chemical processes, 2016 International Joint Conference on Neural Networks (IJCNN), Vancouver, BC, 2016, pp. 1291-1296.

Contact:
corina.nentwich@bci.tu-dortmund.de
sebastian.engell@bci.tu-dortmund.de

Optimal Shared Resource Allocation in Chemical Production Sites

A Market-based Distributed Coordination Approach for Cyber-Physical Systems of Systems

Simon Wenzel[1], Radoslav Paulen[1], Benedikt Beisheim[1,2], Stefan Krämer[2], Sebastian Engell[1]
[1]Process Dynamics and Operations Group (DYN), [2]INEOS Köln GmbH

In large scale chemical and petrochemical production sites the individual processing plants exchange streams of mass and energy via shared resource networks. In order to achieve a site-wide energy and resource efficient operating point, these strong physical couplings have to be taken into account when performing an optimization. In practice, distributed optimization schemes are often favored, because they allow for an improvement of the operation without the necessity to share detailed information across the borders of the individual plants. One possibility is to employ a distributed coordination strategy at a production site that uses market-based algorithms, which iteratively change the prices for the shared resources to steer the individual plants towards optimal operation.

Large scale integrated chemical and petrochemical production sites consisting of many individual processing plants that are optimized by local computer systems and that are physically linked by streams of mass and energy can be considered as cyber-physical systems of systems. An open challenge is the optimization and control of such systems in the presence of managerial conflicts, which arise, for instance, from a division of the production sites into different business units or in the situation where different companies share one common grid of utilities at a production site.

This situation is depicted in Fig. 1, in which different plants are connected via various networks. The individual plants have a certain degree of autonomy to adjust their operating conditions according to economic measures valid for the plant on a local level. For an individual plant a balanced overall network is not the primary goal, since it behaves selfish and strives to optimize its own profit. However, from an overall site point of view, it is crucial to balance the networks of shared resources. This is because unbalanced networks lead to decreased resource efficiency on one hand and, on the other hand, this situation leads to technical infeasibilities, which have to be solved by, for example, venting excess steam to the environment.
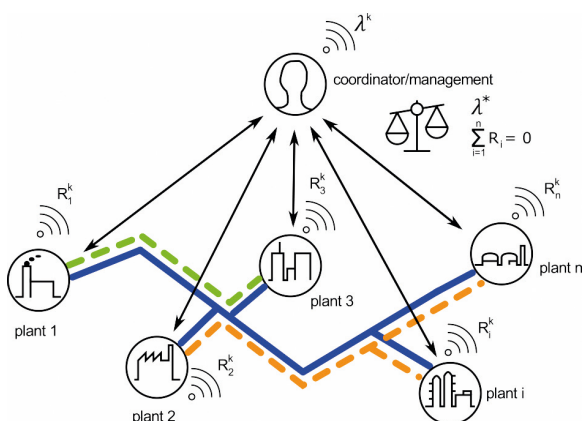
Figure 1: Schematic topology of a system of physically connected production plants that are linked by different shared resource networks and that communicate via a central market-based coordinator (adapted from [3]). λ^k are the price vectors for the shared resources and R_i^k the shared resource vectors of the plants.

Contact:
simon.wenzel@bci.tu-dortmund.de
sebastian.engell@bci.tu-dortmund.de
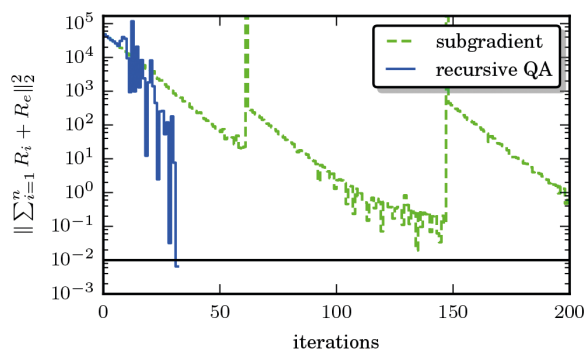
Figure 2: Evolution of the network imbalance against the number of iterations. The dashed lines show subgradient price-updates and the solid lines shows the improved price-update based on recursive quadratic approximation (originally published in [1]).

Market-based distributed coordination takes into account the shared resource network balances and can be used if privacy has to be respected with respect to the cost structures of the maket participants. A coordinator (see Fig. 1) iteratively adjusts the prices of the shared resources until an equilibrium price is found. The price update strategies are key to a successful application of the methodology [1,2,3]. At the equilibrium price the networks are balanced (see Fig. 2, which shows the overall network balance vs. price-adjustment rounds) and no plant will further increase or decrease its utilization of shared resources. The advantage of this technique is that only the information about the shared resources and their prices is shared between the coordinator and the plants and no further plant details are disclosed over the managerial boundaries of the systems.

Publications:
[1] S. Wenzel, R. Paulen, S. Krämer, B. Beisheim, S. Engell, Shared Resource Allocation in an Integrated Petrochemical Site by Price-based Coordination Using Quadratic Approximation, in Proceedings of ECC, 2016, pp. 1045–1050.

[2] S. Wenzel, R. Paulen, G. Stojanovski, S. Krämer, B. Beisheim, S. Engell, Optimal resource allocation in industrial complexes by distributed optimization and dynamic pricing, at-Automatisierungs-technik, vol. 64, no. 6, pp. 428–442, Jan. 2016.

[3] S. Wenzel, R. Paulen, S. Engell, Quadratic Approximation in Price-based Coordination of Constrained Systems-of-Systems, in Proceedings of FOCAPO/CPC, 2017.

Dual and Adaptive Control Using Output Feedback Multi-Stage NMPC

Design of a Controller that Handles Estimation Errors in Addition to Plant-Model Mismatch while Improving the Performance by Reducing the Bounds on the Uncertain Parameters

Sankaranarayanan Subramanian, Sergio Lucia, Sebastian Engell

Multi-stage NMPC is a non-conservative strategy to achieve robust constraint satisfaction in the presence of plant-model mismatch. The scheme is extended here to handle the errors of the state estimation in addition to plant-model mismatch. The performance of the controller is further improved by designing the optimizer to choose inputs that implicitly reduce the bounds of the uncertainty in order to improve the objective function (dual control). This results in an improvement of 60% in the objective function for a prototypical CSTR control problem. In addition, we also show the effectiveness of the approach for time varying uncertainties.

Economics-based Nonlinear Model Predictive Control (NMPC) can improve economic objectives for nonlinear systems while satisfying the process constraints over the prediction horizon. If the model is uncertain, there is a need for robust control which is not overly conservative. Multi-stage NMPC is a non-conservative real-time implementable robust scheme which can achieve constraint satisfaction for nonlinear systems under uncertainty. The evolution of the uncertainty is modeled by a scenario tree. The important aspect of the approach is that it considers explicitly that measurement information will become available at every new sampling instance and that the decisions that will be taken at every future stage can be adjusted accordingly and thus can act as recourse to counteract the effects of the uncertainties. This improves the performance and reduces the conservativeness compared to the traditional robust NMPC schemes.

In practice, not all state variables are measured but only noisy measurements of some states are available. This additional uncertainty about the current state as well as inexact information about the future states must be taken into account in the control algorithm. The samples of the innovations are modeled as new scenarios in the scenario tree in addition to the parametric uncertainties, and estimation techniques such as the EKF/UKF are used to predict the evolution of the future state estimates. The proposed approach is robust to plant-model mismatches and to estimation errors.

The measurement feedback from the plant can also be used to estimate uncertain parameters. Hence instead of having a global bound on the uncertain parameters, a less conservative local estimate on the bound of the parameters can be obtained online. This information is considered by formulating a dual controller which takes into account that
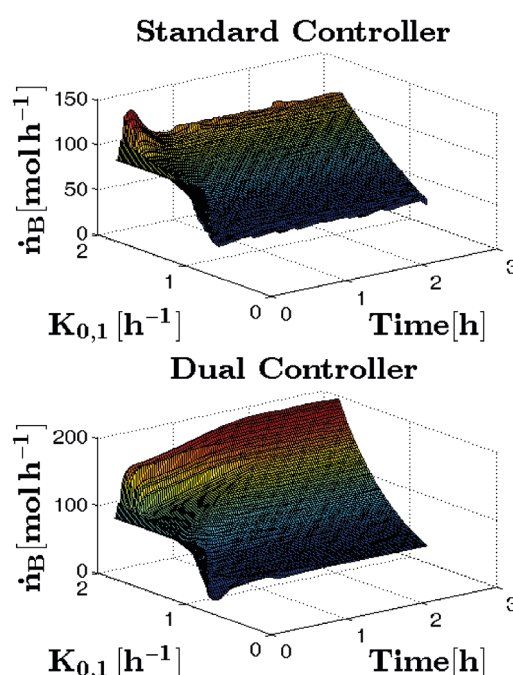
Figure 1: Comparison of Standard multi-stage controller and Dual controller. The improvement in the objective $\dot{n}_b$ by 60% for certain realization of the uncertainty $k_{0,1}$ can be seen.

depending on the available measurements, the bounds on the parameters can be reduced and it chooses a control policy that can implicitly reduce the uncertainty if this helps to improve the control objective because the distance to the constraints can be reduced. The designed dual controller was applied to a CSTR to maximize number of moles produced per hour of the product B ($\dot{n}_b$). The pre-exponential co-efficient of the reaction rate $k_{0,1}$ is uncertain by ±40%. When compared to a standard controller, the dual controller yields an improvement of 60% in the objective for certain realizations of the uncertainty and the results are shown in Figure 1.

Contact:
sankaranaraynan.subramanian@bci.tu-dortmund.de
sebastian.engell@bci.tu-dortmund.de

Publications 2016 - 2014

2016

- D. Ackerschott, B. Beisheim, S. Engell
  Decision support for optimised cooling tower operation using weather forecasts
  Chemical Engineering Transactions 52, AIDIC, 1009-1014 (2016)

- C. Dowidat, M. Kalliski, G. Schembecker, C. Bramsiepe
  Synthesis of batch heat exchanger networks utilizing a match ranking matrix
  Applied Thermal Engineering 100, 78-83 (2016)

- W. Gao, S. Engell
  Using Transient Measurements in Iterative Steady-State Optimizing Control
  Computer Aided Chemical Engineering 38511-516 (2016)

- T. Goerke, D. Kohlmann, S. Engell
  Transfer of Semibatch Processes to Continuous Processes with Side Injections - Opportunities and Limitations, Macromolecular Reaction Engineering
  Special Issue: Batch to Conti Transfer of Polymer Production Processes 10 (4), 364–388 (2016)

- A. Gottu Mukkula, R. Paulen
  Optimal dynamic experiment design for guaranteed parameter estimation
  Computer Aided Chemical Engineering 38, 757-762 (2016)

- W. Gao, S. Wenzel, S. Engell
  A reliable modifier-adaptation strategy for real-time optimization
  Computers & Chemical Engineering 91, 318-328(2016)

- R. Hashemi, D. Kohlmann, S. Engell
  Optimizing Control and State Estimation of a Continuous Polymerization Process in a Tubular Reactor with Multiple Side-streams
  Macromolecular Reaction Engineering 10 (4), Special Issue: Batch to Conti Transfer of Polymer Production Processes, 415-434 (2016)

- H. Hadera, R. Labrik, S. Engell, I. Harjunkoski
  An Improved Energy-awareness Formulation for General Precedence Continuous-time Scheduling Models
  Industrial and Engineering Chemistry Research 55, 1336-1346 (2016)

- M. Kalliski, S. Engell
  Real-Time Resource Efficiency Indicators for Monitoring and Optimization of Batch-Processing Plants
  Canadian Journal of Chemical Engineering 95 (2), 265-280 (2016)

- M. Kalliski, B. Beisheim, D. Krahé, U. Enste, S. Krämer, S. Engell
  Real-time Resource Efficiency Indicators
  atp edition - Automatisierungstechnische Praxis 1-2, 64-71 (2016)

- D. Kohlmann, M.C. Chevrel, S. Hoppe, D. Meimaroglou , D. Chapron, P. Bourson, C. Schwede, W. Loth, S. Engell, F. Durand
  Modular, Flexible, and Continuous Plant for Radical Polymerization in Aqueous Solution
  Macromolecular Reaction Engineering, Special Issue: Batch to Conti Transfer of Polymer Production Processes 10 (4), 339-353 (2016)

- R. Paulen, M. Fikar
  Optimal Operation of Batch Membrane Processes
  Springer, ISBN 978-3-319-20475-8, (2016)

- C. Schoppmeyer, H. Vermue, S. Subbiah, D. Kohlmann, P. Ferlin, S. Engell
  Operation of Flexible Multiproduct Modular Continuous Polymerization Plants
  Macromolecular Reaction Engineering 10 (4), Special Issue: Batch to Conti Transfer of Polymer Production Processes, 435-457 (2016)

- S. Wenzel, R. Paulen, G. Stojanovski, S. Krämer, B. Beisheim, S. Engell
  Optimal resource allocation in industrial complexes by distributed optimization and dynamic pricing
  at – Automatisierungstechnik 64, 428-442 (2016)

- R. Hernándes, S. Engell
  Modelling and iterative Real-time Optimization of a homogeneously catalyzed hydroformylation process
  Computer Aided Chemical Engineering 38, Elsevier, 1-6 (2016)

- H. Hadera, R. Labrik, J. Mäntysaari, G. Sand, I. Harjunkoski, S. Engell
  Integration of Energy-cost Optimization and Production Scheduling Using Multiparametric Programming
  Computer Aided Chemical Engineering 38, Elsevier, 559-564 (2016)

- F. Shamim, R. Hernández, R. Paulen, S. Engell
  A hierarchical coordination approach to the optimal operation of a sugar crystallization process
  Computer Aided Chemical Engineering 38, Elsevier, 703-708 (2016)

- L. Maxeiner, S. Engell
  Distributed minimum batch time optimization for batch reactors with shared resources
  Computer Aided Chemical Engineering 38, Elsevier, 1593-1598 (2016)

- J. Steimel, S. Engell
  Optimization-based support for process design under uncertainty: A case study
  AIChE Journal 62(9), 3404-3419 (2016)

- M. Urselmann, T. Janus, C. Foussette, S. Tlatlik, A. Gottschalk, M. Emmerich, T. Bäck, S. Engell
  Derivative-Free Chemical Process Synthesis by Memetic Algorithms Coupled to Aspen Plus Process Models
  Computer-Aided Chemical Engineering 38, Elsevier, 187-192 (2016)

Proceedings

- A. Gottu Mukkula, R. Paulen
  Optimal design of dynamic experiments for guaranteed parameter estimation
  Proc. American Control Conference 1826-1831 (2016)

- D. Haßkerl, M. Arshad, R. Hashemi, S. Subramanian, S. Engell
  Simulation Study of the Particle Filter and the EKF for State Estimation of a Large-scale DAE-system with Multi-rate Sampling
  11th IFAC Symposium on Dynamics and Control of Process Systems, including Biosystems, IFAC PapersOnline 49 (7), Elsevier, 490-496 (2016)

- D. Haßkerl, S. Markert, S. Engell
  Application of Model-based Experimental Design for the Calibration of Online Composition Measurement by Near-infrared Spectroscopy
  Proc. IEEE Mediterranean Conference on Control and Automation, 967-972 (2016)

- L. Hebing, T. Neymann, T. Thüte, A. Jockwer, S. Engell
  Effcient Generation of Models of Fed-Batch Fermentations for Process Design and Control
  11th IFAC Symposium on Dynamics and Control of Process Systems, including Biosystems, IFAC PapersOnline 49 (7), Elsevier, 621-626 (2016)

- C. Nentwich, S. Engell
  Application of surrogate models for the optimization and design of chemical processes, Proc. IEEE World Congress of Computational Intelligence
  International Joint Conference on Neural Networks (IJCNN), 1291-1296 (2016)

- S. Subramanian, A. Ahmad, S. Engell
  Robust control of a supermarket refrigeration system using multi-stage NMPC
  11th IFAC Symposium on Dynamics and Control of Process Systems, including Biosystems, IFAC-PapersOnLine Bd. 49 (7), Elsevier, 2016, 901-906 (2016)

- T. Siwczyk, S. Engell
  Solving two-stage stochastic mixed-integer linear problems by ordinal optimization and evolutionary algorithms
  Proc. IEEE Congress on Evolutionary Computation, CEC 2016, 2836-2843 (2016)

- A. Tatuela-Codrean, D. Haßkerl, M. Urselmann, S. Engell
  Steady-state Optimization and Nonlinear Model-predictive Control of a Reactive Distillation Process using the Software Platform do-mpc1
  Proc. IEEE Conference on Control Applications (CCA), 1513-1518 (2016)

- T. Goerke, S. Engell
  Application of evolutionary algorithms in guaranteed parameter estimation
  Proc. IEEE Congress on Evolutionary Computation (CEC), 5100-5105 (2016)

- C. Lindscheid, D. Haßkerl, A. Meyer, A. Potschka, H.-G. Bock, S. Engell
  Parallelization of modes of the Multi-Level Iteration Scheme for Nonlinear Model-Predictive Control of an Industrial Process
  Proc. IEEE Conference on Control Applications (CCA), 1506-1512 (2016)

- R. Paulen, S. Nazari, S.A. Shahidi, C. Sonntag, S. Engell
  Primal and Dual Decomposition for Distributed MPC – Theory, Implementation, and Comparison in a Tailored Validation Framework
  Proc. 24th Mediterranean Conference on Control and Automation, Institute of Electrical and Electronics Engineers Inc., 286-291 (2016)

- M. Urselmann, C. Foussette, T. Janus, S. Tlatlik, A. Gottschalk, M.T.M. Emmerich, S. Engell, T. Bäck
  Selection of a DFO Method for the Efficient Solution of Continuous Constrained Sub-Problems within a Memetic Algorithm for Chemical Process Synthesis
  Proc. Genetic and Evolutionary Computation Conference (GECCO), 1029-1036 (2016)

- R. Hashemi, S. Engell
  Effect of Sampling Rate on the Divergence of the Extended Kalman Filter for a Continuous Polymerization Reactor in Comparison with Particle Filtering
  11th IFAC Symposium on Dynamics and Control of Process Systems, including Biosystems, IFAC PapersOnLine 49 (7), Elsevier, 365-370 (2016)

- T. Ebrahim, R. Hernandez, S. Subramanian, M. Kalliski, S. Krämer, S. Engell
  NCO-Tracking with Changing Set of Active Constraints using Multiple Solution Models
  11th IFAC Symposium on Dynamics and Control of Process Systems, including Biosystems IFAC PapersOnLine 49 (7), Elsevier, 79-84 (2016)

- S. Wegerhoff, S. Engell
  Control of the production of Saccharomyces cerevisiae on the basis of a reduced metabolic model
  6th IFAC Conference on Foundations of Systems Biology in Engineering, 49(26), Elsevier 201-206 (2016)

2015

- M. Urselmann, S. Engell
  A Memetic Algorithm for the Efficient Optimization of Chemical Process Synthesis Problems with Structural Restrictions
  Computers & Chemical Engineering 72 - Special Issue: Mixed Integer Nonlinear Optimization – A Tribute to Ignacio E. Grossmann's Contributions to the Field of Process Systems Engineering, 87–108 (2015)

- M. Behrens, H.G. Bock, S. Engell, P. Khobkhun, A. Potschka
  Real-Time PDE Constrained Optimal Control of a Periodic Multicomponent Separation Process
  In: Leugering, G., Benner, P., Engell, S., Griewank, A., Harbrecht, H., Hinze, M., Rannacher, R., Ulbrich, S., (Hrsg.): Trends in PDE Constrained Optimization, Heidelberg, Springer, 521-537 (2015)

- T. Goerke, S. Engell
  Analysis of the transfer of radical co-polymerization systems from semi-batch to continuous plants
  Computer Aided Chemical Engineering 37, 227-232 (2015)

- H. Hadera, I. Harjunkoski, G. Sand, I.E. Grossmann, S. Engell
  Optimization of steel production scheduling with complex time-sensitive electricity cost
  Computers and Chemical Engineering 76, 117-136 (2015)

- H. Hadera, R. Labrik, S. Engell, I. Harjunkoski
  An Improved Energy-awareness Formulation for General Precedence Continuous-time Scheduling Models
  Industrial and Engineering Chemistry Research 55, 1336-1346 (2016)

- H. Hadera, P. Wide, I. Harjunkoski, J. Mäntysaari, J. Ekström, S. Engell
  A Mean Value Cross Decomposition Strategy for Demand-side Management of a Pulping Process
  Computer Aided Chemical Engineering 37, 1931-1936 (2016)

- M. Jelemenský, R. Paulen, M. Fikar, Z. Kovacs
  Time-Optimal Operation of Multi-Component Batch Diafiltration
  Computers & Chemical Engineering 85, 131 – 138 (2015)

- M. Jelemenský, A. Sharma, R. Paulen, M. Fikar
  Time-optimal Operation of Diafiltration Processes in the Presence of Fouling
  Computer Aided Chemical Engineering 37, 1577-1582 (2015)

- M. Kalliski, D. Krahé, B. Beisheim, S. Krämer, S. Engell
  Resource efficiency indicators for real-time monitoring and optimization of integrated chemical production plants
  Computer Aided Chemical Engineering 37, 1949-1954 (2015)

- M. Kalliski, D. Krahé, N. Melchert, S. Engell
  Real-time Resource Efficiency Indicators for Monitoring and Optimization of Batch-Processing Plants
  The Canadian Journal of Chemical Engineering 95 (2), ECCE10 Special Issue, 265-280 (2015)

- R. Marti, S. Lucia, D. Sarabia, R. Paulen, S. Engell, C. de Prada
  Improving scenario decomposition algorithms for robust nonlinear model predictive control
  Computers & Chemical Engineering 79, 30-45 (2015)

- S. Nazari, C. Sonntag, G. Stojanovski, S. Engell
  A Modelling, Simulation, and Validation Framework for the Distributed Management of Large-scale Processing Systems
  Computer Aided Chemical Engineering 37, 269-274 (2015)

- R. Paulen, M. Jelemenský, Z. Kovacs, M. Fikar
  Economically optimal batch diafiltration via analytical multi-objective optimal control
  Journal of Process Control 28, 73–82 (2015)

- C. Schoppmeyer, C. Sonntag, S. Gajjal
  Optimal Management of Shuttle Robots in a Laboratory Automation System of a Cement Plant
  Computer Aided Chemical Engineering 37, 1895-1900 (2015)

- J. Steimel, S. Engell
  Conceptual design and optimization of chemical processes under uncertainty by two-stage programming
  Computers and Chemical Engineering 81, 200-217 (2015)

- P.H. Taskinen, J. Steimel, L. Gräfe, S. Engell, A. Frey
  A Competency Model for Process Dynamics and Control and Its Use for Test Construction at University Level
  Peabody Journal of Education 90, 477-490 (2015)

- M. Urselmann, S. Engell
  Design of memetic algorithms for the efficient optimization of chemical process synthesis problems with structural restrictions
  Computers and Chemical Engineering 72, 87-108 (2015)

Proceedings

- B. Chachuat, B. Houska, R. Paulen, N. Peric, J. Rajyaguru, M. Villanueva
  Set-Theoretic Approaches in Analysis, Estimation and Control of Nonlinear Systems
  Proc. 9th IFAC Symposium on Advanced Control of Chemical Processes ADCHEM 2015, IFAC Papers OnLine 48 (8), Elsevier, 981-995 (2015)

- S. Engell, R. Paulen, M.A. Reniers, H. Thompson, C. Sonntag
  Core Research and Innovation Areas in Cyber-Physical Systems of Systems: Initial Findings of the CPSoS project
  Lecture Notes in Computer Science Bd. 9361, Springer Amsterdam, 11-13 (2015)

- T. Goldschmidt, M. Murugaiah, C. Sonntag, B. Schlich, S. Biallas, P. Weber
  Cloud-Based Control: A Multi-Tenant, Horizontally Scalable Soft-PLC
  Proc. 8th IEEE International Conference on Cloud Computing, new York, USA, 909 – 916 (2015)

- W. Gao, S. Wenzel, S. Engell
  Integration of gradient adaptation and quadratic approximation in real-time optimization
  Proc. 34th Chinese Control Conference, Hangzhou, China, 2780 – 2785 (2015)

- W. Gao, S. Wenzel, S. Engell
  Comparison of modifier adaptation schemes in real-time optimization
  Proc. 9th IFAC Symposium on Advanced Control of Chemical Processes ADCHEM 2015, IFAC Papers OnLine 48 (8), 182–187 (2015)

- W. Gao, S. Wenzel, S. Engell
  Modifier Adaptation with Quadratic Approximation in Iterative Optimizing Control
  Proc. 2015 European Control Conference, 15-17 (2015)

- R. Hashemi, R. Schilling, S. Engell
  Optimizing Control of a Tubular Polymerization Reactor: Comparison of Single Shooting and Full Discretization
  Proc. 9th IFAC Symposium on Advanced Control of Chemical Processes ADCHEM 2015, IFAC Papers OnLine 48 (8), 557 – 562 (2015)

- M. Jelemenský, A. Sharma, R. Paulen, M. Fikar
  Multi-Objective Optimization of Batch Dialfiltration Processes in the Presence of Membrane Fouling,
  M. Fikar, M. Kvasnica (Hrsg.): Proceedings of the 20th International Conference on Process Control Slovak Chemical Library, Štrbské Pleso, Slovakia, 84–89 (2015)

- R. Marti, S. Lucia, D. Sarabia, R. Paulen, S. Engell, C. de Prada:
  An Efficient Distributed Algorithm for Multi-Stage Robust Nonlinear Predictive Control
  Proc. European Control Conference 2015, Linz, Austria, 2669–2674 (2015)

- S. Nazari, C. Sonntag, S. Engell
  A Modelica-based Modeling and Simulation Framework for Large-scale Cyber-physical Systems of Systems
  Proc. MATHMOD 2015, IFAC PapersOnLine 48 (1), 920-921. (2015)

- R. Paulen
  On the Design of a Guaranteed Extended Kalman Filter using Set Inversion Techniques
  Proc. 54th IEEE Conference on Decision and Control Osaka, Japan, 5014-5019 (2015)

- A. Sharma, M. Jelemenský, R. Paulen, M. Fikar
  Modelling and Optimal Control of Membrane Process with Partial Recirculation
  in: M. Fikar, M. Kvasnica (Hrsg.): In Proceedings of the 20th International Conference on Process Control Slovak Chemical Library, Štrbské Pleso, Slovakia, 90–95 (2015)

- S. Subramanian, S. Lucia, S. Engell
  Economic Multi-stage Output Feedback NMPC using the Unscented Kalman Filter
  Proc. 9th IFAC Symposium on Advanced Control of Chemical Processes ADCHEM 2015, IFAC-PapersOnLine, 48 (8), 38-43 (2015)

- S. Subramanian, S. Lucia, S. Engell
  Handling Structural Plant-model Mismatch via Multi-stage Nonlinear Model Predictive Control
  Proc. European Control Conference (ECC) 2015, 1596-1601 (2015)

- S. Subramanian, S. Lucia, S. Engell
  Adaptive Multi-stage Output Feedback NMPC using the Extended Kalman Filter for time varying uncertainties applied to a CSTR
  Proc. 5th IFAC Conference on Nonlinear Model Predictive Control NMPC 2015, IFAC-PapersOnLine 48 (23), Elsevier, 242-247 (2015)

- S. Subramanian, S. Lucia, R. Paulen, S. Engell
  Robust Output Feedback NMPC with Guaranteed Constraint Satisfaction
  Proc. 8th IFAC Symposium on Robust Control Design, IFAC-PapersOnLine 48 (14), Elsevier, 325–330 (2015)

- S.A. Shahidi, R. Paulen, S. Engell
  Two-layer Hierarchical Predictive Control via Negotiation of Active Constraints
  Proc. 5th IFAC Conference on Nonlinear Model Predictive Control, IFAC PapersOnLine 48 (23), Elsevier, 404–409 (2015)

- S. Thangavel, S. Lucia, R. Paulen, S. Engell
  Towards Dual Robust Nonlinear Model Predictive Control: A Multi-stage Approach
  Proc. 2015 American Control Conference, Chicago, IL, USA, 428–433 (2015)

- S. Wenzel, W. Gao, S. Engell
  Handling Disturbances in Modifier Adaptation with Quadratic Approximation
  Proc. 6th IFAC Workshop on Control Applications of Optimization CAO'2015, IFAC-PapersOnLine 48 (25), Elsevier, 132-137 (2015)

- G. Stojanovski, L.S. Maxeiner, S. Krämer, S. Engell
  Real-time Shared Resource Allocation by Price Coordination in an Integrated Petrochemical Site
  Proc. 14th European Control Conference, Linz, Austria, 1498-1503 (2015)

- S. Lucia, S. Engell
  Potential and Limitations of Multi-stage Nonlinear Model Predictive Control
  Proc. 9th IFAC Symposium on Advanced Control of Chemical Processes ADCHEM, Canada, IFAC Papers OnLine 48 (8), Elsevier, 1015-1020 (2015)

- D. Kampert, S. Nazari, C. Sonntag, U. Epple, S. Engell
  A Framework for Simulation, Optimization and Information Management of Physically-Coupled Systems of Systems
  Proc. 15th IFAC Symposium on Information Control Problems in Manufacturing, Ottawa, Canada, IFAC Papers OnLine 28 (3), Elsevier, 1553-1558 (2015)

2014

- S. Engell, T. Finkler, M. Kawohl, U. Piechottka
  Realisierung von Advanced Control in einem Polymerproduktionsprozess
  at-Automatisierungstechnik 62, 124-140 (2014)

- T. Finkler, M. Kawohl, U. Piechottka, S. Engell
  Realization of online optimizing control in an industrial semi-batch polymerization
  Journal of Process Control 24, 399-414 (2014)

- H. Hadera, I. Harjunkoski, I.E. Grossmann, G. Sand, S. Engell
  Steel Production Scheduling Optimization under Time-sensitive Electricity Costs
  Computer Aided Chemical Engineering, Bd. 33. Elsevier, 373-378 (2014)

- I. Harjunkoski, C. Maravelias, P. Bongers, P. M. Castro, S. Engell, I.E. Grossmann, J. Hooker, C. Méndez, G. Sand, J. Wassicki
  Scope for industrial applications of production scheduling models and solution methods
  Computers and Chemical Engineering 62, Elsevier, 161–193 (2014)

- R. Hernández, L. Simora, R. Paulen, C. de Prada, S. Engell
  Optimal integrated operation of a sugar production plant
  Computer Aided Chemical Engineering 33, Elsevier, 637-642 (2014)

- S. Lucia, J. Andersson, H. Brandt, M. Diehl, S. Engell
  Handling Uncertainty in Economic Nonlinear Model Predictive Control
  Journal of Process Control 24, 1247-1259 (2014)

- R. Mazaeda, L. Acebes, A. Rodriguez, S. Engell, C. de Prada
  Sugar Crystallization Benchmark
  Computer Aided Chemical Engineering, Bd. 33. Elsevier Ltd., 613-618 (2014)

- R. Paulen, B. Benyahia, M.A. Latifi, M. Fikar
  Analysis of optimal operation of a fed-batch emulsion copolymerization reactor used for production of particles with coreshell morphology
  Computers & Chemical Engineering 66, 233-243 (2014)

- C. Schoppmeyer, S. Fischer, J. Steimel, N. Wang, S. Engell
  Embedding of Timed Automata-based Schedule Optimization into Recipe Driven Production
  Computer Aided Chemical Engineering 33, 415-420 (2014)

- J. Steimel, M. Harrmann, G. Schembecker, S. Engell
  A framework for the modeling and optimization of process superstructures under uncertainty
  Chemical Engineering Science 115, 225-237 (2014)

- C. Schoppmeyer, S. Subbiah, J.M. De La Fuente Valdès, S. Engell
  Dynamic scheduling of shuttle robots in the warehouse of a polymer plant based on dynamically configured timed automata models
  Industrial and Engineering Chemistry Research 53, 17135-17154 (2014)

- J. Steimel, S. Engell
  Conceptual Design and Optimisation of Chemical Processes under Uncertainty by Two-Stage Programming
  Computers & Chemical Engineering 81, Elsevier, 200-2017 (2014)

- R. Paulen, M. E. Villanueva, B. Chachuat
  Guaranteed parameter estimation of non-linear dynamic systems using high-order bounding techniques with domain and CPU-time reduction strategies
  IMA Journal of Mathematical Control and Information 33 (3), 563–587 (2014)

Proceedings

- M. Behrens, P. Khobkhun, A. Potschka, S. Engell
  Optimizing set point control of the MCSGP process
  Proc. 2014 European Control Conference, ECC 2014, 1139-1144 (2014)

- R. Hashemi, S. Engell
  Optimizing Control and State Estimation in a tubular Polymerization Reactor
  Proc. The 19th IFAC World Congress 47 (3), 4873-4878 (2014)

- R. Lemoine-Nava, S. Engell
  Individual Column State and Parameter Estimation in the Simulated Moving Bed Process: an Optimization-based Method
  Proc. The 19th IFAC World Congress 47 (3), 9376-9381 (2014)

- S. Lucia, J. Andersson, H. Brandt, A. Bouaswaig, M. Diehl, S. Engell
  Efficient Robust Economic Nonlinear Model Predictive Control of an Industrial Batch Reactor
  Proc. The 19th IFAC World Congress 47 (3), 11093-11098 (2014)

- S. Lucia, S. Engell, R. Paulen
  Multi-stage Nonlinear Model Predictive Control with Verified Robust Constraint Satisfaction
  Proc. 54th IEEE Conference on Decision and Control, 2816-2821 (2014)

- S. Lucia, A. Tatulea-Codrean, C. Schoppmeyer, S. Engell
  An Environment for the Efficient Testing and Implementation of Robust NMPC
  Proc. 2014 IEEE Multi-conference on Systems and Control, Antibes, 1843-1848 (2014)

- S. Lucia, S. Engell
  Control of Towing Kites under Uncertainty using Robust Economic Nonlinear Model Predictive Control
  Proc. ECC 2014, 1158-1163 (2014)

- S. Subramanian, S. Lucia, S. Engell
  Economic Multi-stage Output Nonlinear Model Predictive Control
  Proc. IEEE Multi-conference on Systems and Control, 1837-1842 (2014)

Solids Process Engineering (FSV)

Equipment Qualification for Fused Deposition Modeling 3D Printers in Pharmaceutical Applications

A Qualification Framework for Fused Deposition Modeling 3D Printers has been Developed

Tim Feuerbach, Stefanie Kock, Markus Thommes

Fused Deposition Modeling (FDM) is a promising 3D printing technique in the pharmaceutical and medical research and the number of potential applications in these fields is increasing rapidly. The applications are mainly drug dosage forms as well as implants while the stated advantages in comparison to conventional manufacturing methods are the possibility of a patient tailored drug dosage personalization and implant customization. A widespread production and availability of 3D printed products is prevented by a lacking regulatory approval concept for 3D printed devices.

FDM is a 3D printing technique, in which thermoplastic materials are plasticized and extruded through a small nozzle. The extruded strands are deposited on a build platform in order to create three-dimensional objects in a layer by layer. Advantages of this technique in comparison to conventional manufacturing methods are the possibility of manufacturing complex geometries with no or small quantities of waste material as well as economy for small scale production.

The specific advantages in pharmaceutical and medical applications include the patient individual personalization of drug dosages and customization of implants. The lacking regulatory approval concept for 3D printed products prevents a widespread application. A first step to approach this problem is the development of an equipment qualification framework for FDM 3D printers which is suggested in this work.
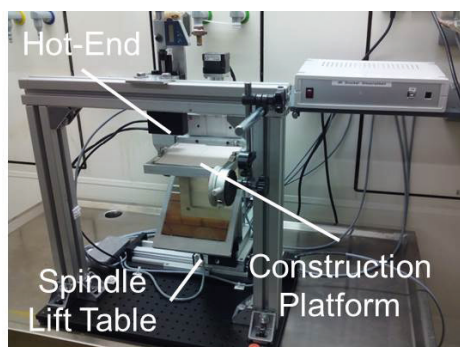

Figure 1: Illustration of the in-house developed FDM 3D printer. The construction platform is movable in all spatial directions due to a spindle lift table while the Hot-End is stationary.

The presented framework considers several important printing parameters and printer properties which have to be in accordance with the specification in order to ensure a reproducible 3D-printed product. The approach to investigate the printer performance and to evaluate if the specifications are statistically met is the application of the ICH Q2(R1) methodology in validating analytical procedures (see Figure 1).

The equipment qualification framework was applied to an in-house developed FDM 3D printer as well as two commercially available open-source printers: Ultimaker 2 (Ultimaker 2, Netherlands) and PRotos v3 (RepRap, Germany). The results for the positioning accuracy in one horizontal direction are exemplarily shown in Figure 2. While the in-house developed printer has the highest movement resolution it also shows the highest accuracy and precision. The PRotos v3 is not shown in this figure as its minimal movement distance amounts to 100 µm. The residual deviations are representative for the mechanical tolerances of the printers.
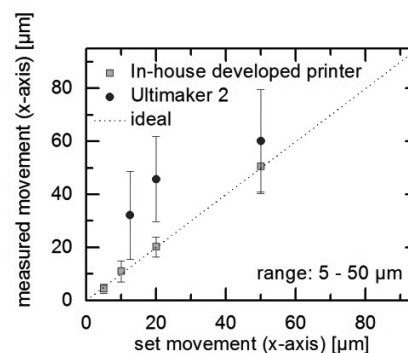
Figure 2: Positioning accuracy measurements (n = 20) in horizontal x-direction measured with a 1/1000 mm dial gauge. The measurements were conducted with a movement speed of 4 mm s^{-1}.

The developed framework confirms the capability of FDM 3D printers to meet manufacturing specifications reproducibly and can therefore lead to a facilitation and acceleration of the approval procedure as well as a better comparability of FDM 3D printers among themselves. The suitability of a printer for a specific product can also be evaluated based on the results of the equipment qualification.

Contact:
tim.feuerbach@bci.tu-dortmund.de
markus.thommes@bci.tu-dortmund.de

Spray Dried Submicron Sized Particles for Pharmaceutical Application

A Spray Drying Concept Contains an Aerosol Conditioning Step for Fine Droplets and an Electrostatic Precipitator for the Separation of Submicron Particles

Adrian Dobrowolski, Ramona Gorny, Gerhard Schaldach, Peter Walzel, Markus Thommes

Submicron sized particles are widely applied as catalysts, coating materials or in food and pharmaceutical industries. The preparation of submicron sized particles in the range of 0.1-1 µm is one possibility to increase the bioavailability of low water soluble drugs.

Due to the low water solubility of more than 40% of newly identified active pharmaceutical ingredients (API), new formulation methods were developed. The extent of an API that enters the systemic circulation, described by the bioavailability, is mainly limited by the dissolution rate. According to the Nernst-Brunner equation, the particle size reduction increases the specific surface area and in turn enhances the dissolution rate.

Spray drying processes for submicron sized particles are challenging regarding small ($d_{50,3}<3\mu m$) and uniform droplets and the precipitation of submicron sized particles.

In this work, the aerosol is firstly generated by a pneumatic atomizer and is subsequently conditioned by a cyclone separator. An optimal cyclone with a small cut-off size of about 2.6 µm was developed. Only the part of the aerosol with a drop size below the cut-off diameter reaches the drier. Afterwards the particles were separated with an electrostatic precipitator.

A 10 wt.-% mannitol solution was atomized using compressed air with a constant gas inlet pressure of $\Delta p = 5$ bar. The difference in the droplet size distribution is illustrated in figure 1 with the cumulative volume distribution Q_3 of both the primary aerosol, generated by the pneumatic atomizer and the conditioned aerosol.
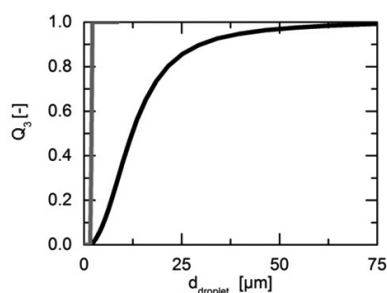
The investigations show, that the droplet separation process is independent of the liquid loading and the concentration or the viscosity of the liquid. The yield of the conditioned aerosol depends on the characteristics of the pneumatic atomizer, since only 1% is in the usable range. Submicron particles tend to follow the gas flow in appearing turbulences. Therefore the separation of these small particles is very challenging. By means of electrostatic precipitation the spray dried particles are charged and collected. For this purpose a taylor made two-stage electrostatic precipitator is designed. The main advantage dividing the charging and separation zone is the avoidance of turbulences. A simple design allows easy cleaning and quick changes in the setup. This allows the examination of various effects in the electrostatic precipitation process. To characterize the efficiency of the complete process long term tests are realized. The partition coefficient in the submicron range after 1 separation hour exceeds 99% and is shown in figure 2.
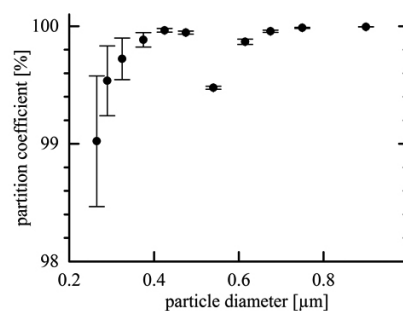
Figure 2: Precipitation experiments with mannitol particles at 20 kV and 7.5 mA/m² at t=0 for 1 h, n=6.

Figure 1: Volumetric cumulative droplet size distribution of the primary (black) and the conditioned (grey) aerosol (10 wt-mannitol solution, $\dot{m}_L$=100 mL/min).

Investigations show that submicron particles can be produced and collected with a rate of 1 g/h at highest separation efficiencies for at least 10 hours. Future research will help to increase the production rate as well as stabilizing a long term precipitation process.

Contact:
ramona.gorny@bci.tu-dortmund.de
markus.thommes@bci.tu-dortmund.de

Development of a Model for the Mixing Capacity of a Twin-Screw-Granulator

The Systematic Damping of Feeder Fluctuations during Twin-Screw-Granulation is Characterized

Jens Wesholowski, Hendrik Hallfarth, Robin Meier, Markus Thommes

Twin-screw granulation is a significant technique for continuous manufacturing within the pharmaceutical technology. For a homogenous product typically a consistent feed is crucial. However, the twin-screw-granulation process is capable to compensate feeder fluctuations, which is related to its mixing capacity due to the residence time distribution of the process itself. For the modelling of these relations an approach of Danckwertz was utilized. Based on the model results suitable process conditions for a sufficient product quality are defined.

The continuous wet-granulation with twin-screw-granulators (TSG) is a commonly applied process in pharmaceutical technology and includes a preceded dosing step for powder and liquid as well as a down-streaming. For a homogenous product quality there are two critical unit operations: dosing and mixing. The distributive mixing capability of the TSG is related to the residence time density function $E(t)$ of the process and can be described by the Axial-Dispersion-Model (Bo < 100). Here τ is the mean residence time, Θ the dimensionless time ratio of t to τ. The Bodenstein-number Bo as characteristic parameter defines the ratio of plug flow

$$E(\Theta) = \frac{1}{2} \cdot \sqrt{\frac{Bo}{\pi\Theta}} \cdot \exp\left(\frac{-Bo \cdot (1-\Theta)^2}{4\Theta}\right)$$

(Bo→∞) to superimposed axial dispersion (Bo→0).
For a small Bo a process is capable of compensating fluctuations of the feed mass flow $\dot{m}_{in}$ (θ). Then the product mass flow $\dot{m}_{out}$ (θ) can be modeled by convolution of these two coupled functions according to the approach of Danckwertz.

$$\dot{m}_{out}(\theta) = \int_0^\infty \dot{m}_{in}(\theta - \theta') \cdot E(\theta)\, d\theta$$

For the disturbed feed flow a systematic deviation in form of a sinus function was assumed. So the mean feed rate $\dot{m}$ is superimposed by a characteristic amplitude A and the disturbance time t_s. Here T describes the disturbance ratio between τ and t_s.

$$\dot{m}_{in}(\theta) = \bar{\dot{m}} + A \cdot \sin\left(2\pi \cdot \frac{\Theta}{T}\right)$$

The ratio of the amplitudes of the feed (A_{in}) and product mass-flow (A_{out}) is then directly related to the mixing capability of the TSG process and is defined as damping ratio $damp_{Modell}$.

$$damp_{Modell} = 1 - \frac{A_{aus}}{A_{ein}}$$

The model results are given within figure 1. The damping factor is constant for amplitudes < 1 and only dependent on the parameters Bo and T. For increasing Bo-numbers a higher damping ratio is achieved and for T≤0.3 fluctuations are totally compensated within the investigated Bo-range. For T → ∞ fluctuations cannot be reduced anymore by the TSG, so $damp_{Modell}$→0.

Contact:
jens.wesholowski@bci.tu-dortmund.de
markus.thommes@bci.tu-dortmund.de
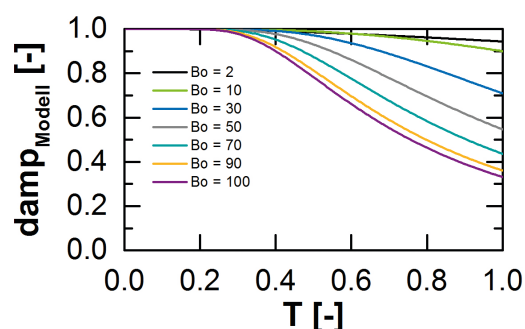
Figure 1: Theoretical damping of feed fluctuations based on the developed model.

Based on these results the so-called mass default plot can be created. First for any disturbance time t_s the theoretical damping ratio is calculated according to the developed model. Then a maximum disturbance amplitude for the feeder $A_{in,rel.,max}$ is determined related to a defined variation range of the component mass contents for a sufficient product quality. The mass default Δm_{norm} is then plotted against the duration time of the fluctuation $\Delta t = 0.5\, t_s$.
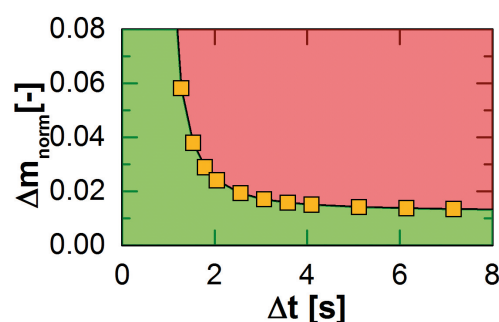
Figure 2: Mass default plot for a TSG process.

The calculated values (orange squares) symbolize critical feeder fluctuations for a certain disturbance time. If a mass default for a certain Δt is higher (red area), then the product quality does not match the specified criteria concerning the homogeneity anymore.

Publications:
R. Meier, M. Thommes, N. Rasenack, K.P. Moll, M. Krumme, P. Kleinebudde, Granule size distributions after twin-screw granulation – Do not forget the feeding systems, European Journal of Pharmaceutics and Biopharmaceutics, 106 (2016) 59-69.

J. Wesholowski, H. Hallfarth, R. Meier, M. Thommes, Charakterisierung der systemischen Dämpfung von kritischen Dosierschwankungen in der Doppelwellengranulation, DECHEMA Jahrestreffen: Fachgruppe Agglomerations- und Schüttguttechnik, Februar (2017).

Publications 2016 - 2014

2016

- D. T. Hegyesi, M. Thommes, P. Kleinebudde, T. Sovány, P. Jr Kása, A. Kelemen, K. Pintye-Hódi, G. Jr Regdon
  Preparation and Physicochemical Characterization of Matrix Pellets Containing APIs with Different Solubility via Extrusion Process
  Drug Development and Industrial Pharmacy dx.doi.org/10.1080/03639045 .2016.1261150 (2016)

- E. J. Laukamp, K. Knop, M. Thommes, J. Breitkreutz
  Micropellet-Loaded Rods with Dose-Independent Sustained Release Properties for Individual Dosing via the Solid Dosage Pen
  International Journal of Pharmaceutics 499, 271-279 (2016)

- R. Meier, M. Thommes, N. Rasenack, K.P. Moll, M. Krumme, P. Kleinebudde
  Granule Size Distributions after Twin-Screw Granulation - Do Not Forget the Feeding Systems
  European Journal of Pharmaceutics and Biopharmaceutics 106, 59-69 (2016)

2015

- F.E. Kiene, M. Pein, M. Thommes
  Orientation to Determine Quality Attributes of Flavoring Excipients Containing Volatile Molecules
  Journal of Pharmaceutical and Biomedical Analysis 110, 20-26 (2015)

- E.J. Laukamp, A.K. Vynckier, J. Voorspoels, M. Thommes, J. Breitkreutz
  Development of Sustained and Dual Drug Release Co-Extrusion Formulations for Individual Dosing
  European Journal of Pharmaceutics and Biopharmaceutics 89, 357-364 (2015)

- G.F. Petrovick, M. Pein, M. Thommes, J. Breitkreutz
  Spheronization of Solid Lipid Extrudates: A Novel Approach on Controlling Critical Process Parameters
  European Journal of Pharmaceutics and Biopharmaceutics 92, 15-21 (2015)

- J. Ronowicz, M. Thommes, P. Kleinebudde, J. Krysinski
  A Data Mining Approach to Optimize Pellets Manufacturing Process Based on a Decision Tree Algorithm
  European Journal of Pharmaceutical Science 73, 44-48 (2015)

- M. W. Tackenberg, C. Geisthovel, A. Marmann, H.P. Schuchmann, P. Kleinebudde, M. Thommes
  Mechanistic Study of Carvacrol Processing and Stabilization as Glassy Solid Solution and Microcapsule
  International Journal of Pharmaceutics 478, 597-605 (2015)

- M. W. Tackenberg, R. Krauss, A. Marmann, M. Thommes, H.P. Schuchmann, P. Kleinebudde
  Encapsulation of Liquids Using a Counter Rotating Twin Screw Extruder
  European Journal of Pharmaceutics and Biopharmaceutics 89, 9-17 (2015)

2014

- D. R. Ely, R. E. Garcia, M. Thommes
  Ostwald-Freundlich Diffusion-Limited Dissolution Kinetics of Nanoparticles
  Powder Technology 257, 120-123 (2014)

- C. Krueger, M. Thommes, P. Kleinebudde
  Influence of Storage Condition on Properties of MCC II-Based Pellets with Theophylline-Monohydrate
  European Journal of Pharmceutics and Biopharmceutics 88, 483-491 (2014)

- E. J. Laukamp, M. Thommes, J. Breitkreutz
  Hot-Melt Extruded Drug-Loaded Rods: Evaluation of the Mechanical Properties for Individual Dosing via the Solid Dosage Pen
  International Journal of Pharmaceutics 475, 344-350 (2014)

- C. Muehlenfeld, M. Thommes
  Small-scale twin-screw extrusion - evaluation of continuous split feeding
  Journal of Pharmacy and Pharmacology 66, 1667-1676 (2014)

- E. Reitz, D. Djuric, K. Kolter, M. Thommes
  Tablet Formulation Containing Solid Dispersions from SoluplusR
  Die Pharmzeutische Industrie 76, 286-296 (2014)

- T. Sakai, M. Thommes
  Investigation into Mixing Capability and Solid Dispersion Preparation using the DSM Xplore Pharma Micro Extruder
  Journal of Pharmacy and Pharmacology 66, 218-231 (2014)

- M. W. Tackenberg, A. Marmann, M. Thommes, H. P. Schuchmann, P. Kleinebudde
  Orange Terpenes, Carvacrol and α-Tocopherol Encapsulated in Maltodextrin and Sucrose Matrices via Batch Mixing
  Journal of Food Engineering 135, 44-52 (2014)

- M. W. Tackenberg, M. Thommes, H. P. Schuchmann, P. Kleinebudde
  Solid State of Processed Carbohydrate Matrices From Maltodextrin and Sucrose
  Journal of Food Engineering 129, 30-37 (2014)
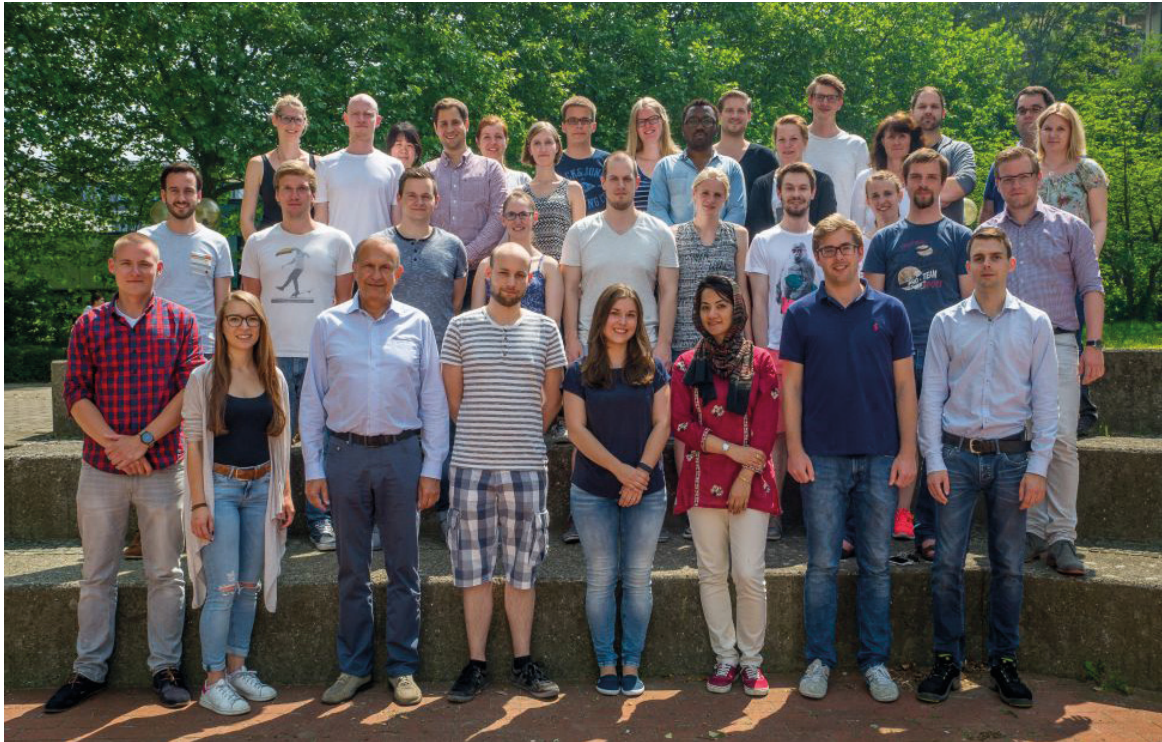
Fluid Separations (FVT)

Enzyme Accelerated Carbon Capture

Investigation of Different Contacting Equipment in a Comparative Study

Mathias Leimbrink, Kolja Neumann, Katharina Kupitz, Kai Groß, Andrzej Górak, Mirko Skiborowski

The Intergovernmental Panel on Climate Change (IPCC) states, that global CO_2 emissions have to be cut by at least 50 % until 2050 in order to limit average global temperature rise to less than 2°C. Despite the increasing utilization of renewable energy sources, fossil fuels still play an important role in power generation. Since the growing global energy demand cannot fully be covered by renewable energy, in short to medium term other technologies have to be applied to reach the IPCC goal. CO_2 capture is one tool to provide a sustainable and ecological solution by reducing the amount of emitted CO_2 when burning fossil fuels.

The state-of-the-art technologies for CO_2 capture are still not applied in the industry because of lowering the overall efficiency of the power plant. We develop two different approaches to intensify reactive absorption which is most mature capture technology (Figure 1). The first approach is use of a new solvent i.e. the combination of tertiary amine methyldiethanolamine (MDEA) with a highly efficient biocatalyst, the enzyme Carbonic Anhydrase (CA).

The second one is the application of new intensified contacting devices (ICD) for contacting of gas and liquid streams. Those are: membrane contactors (MC) and rotating packed beds (RPB) which are promising alternatives to standard packed columns.
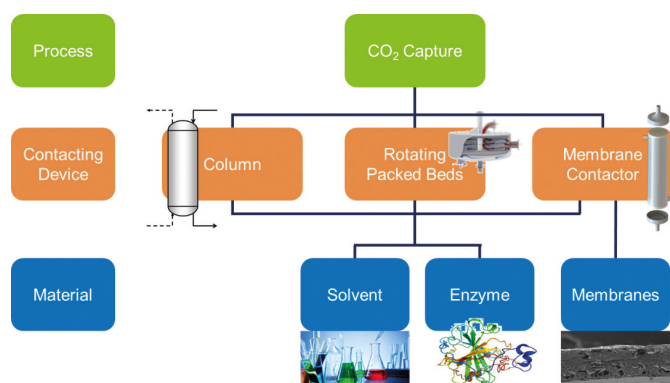

Figure 1: Overview of contacting devices and materials investigated.

In conventional operation, without enzyme, all three devices show a similar CO_2 absorption rate related to their specific area (Figure 2). CO_2 absorption increases substantially, if a combination of enzyme and amine is used. Catalytic effect of enzyme on absorption performance is the same for packed column and RPB, while a reduced performance was observed for the MC. It turned out that a combined application of enzyme and MC should not be recommended for industrial applications.
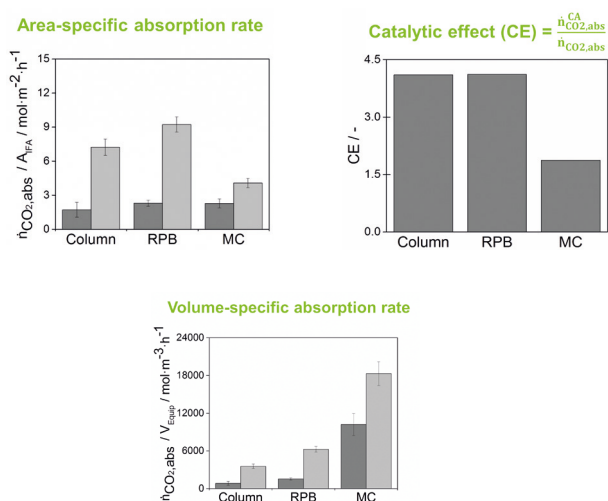
Figure 2: An aqueous amine solution with 30 wt.-% MDEA is investigated in this study without (■) and with *0.2 wt.-% dissolved CA* (■); 26 m^3 m^{-2} h^{-1} liquid load, 40 °C at inlet; Gas: humidified mixture of CO_2 and air, CO_2 partial pressure of 15 kPa at a gas load of 0.93 $Pa^{0.5}$.

Both ICDs outperform the packed column regarding the volume specific performance. By application of MC the required volume could be reduced by ~75% compared to a packed column, while the rotating packed bed would require half of the space of a packed column.

Future work will focus on investigation of ICDs at optimal operating conditions in order to exploit the full advantage of these technologies. Furhermore, model development and validation will be done to enable the conceptual process design and evalution of innovative capture processes based on enzyme-accelerated absorption in ICDs.

Contact:
kolja.neumann@bci.tu-dortmund.de
mathias.leimbrink@bci.tu-dortmund.de
andrzej.gorak@bci.tu-dortmund.de

Optimization-based Process Design

Efficient Optimization-based Design of Energetically Intensified Distillation Processes

Thomas Waltermann, Mirko Skiborowski

Although suffering from low energy efficiency, distillation is still the most widespread separation technique in industry. In order to improve the energy efficiency of distillation processes different means, such as heat-pump assisted and thermally coupled distillation columns, have been proposed. However, the comparison of these different configurations and the identification of the most energy or economically beneficial option for a specific separation is a tedious task. In order to resolve this problem an efficient optimization-based method for the evaluation of a broad range of different options for energetically intensified distillation processes is developed. In contrast to most previous approaches, the implemented superstructure formulation is further based on an equilibrium tray model including rigorous thermodynamics, such that the method can directly be applied to the separation of non-ideal mixtures.

In order to identify the most suitable distillation process for a given separation, several concepts for energetically intensified distillation are optimized. The investigated variants include conventional distillation, vapor recompression, thermally coupled columns as well as divided wall columns (DWC) for the direct, indirect and sloppy splits of a mixture into three products. Moreover, conventional heat integration by adjusting column pressure is also considered for the direct and indirect split. Based on a systematic initialization procedure 16 different process configurations are automatically screened for one specific separation task. The proposed method is based on a rigorous equilibrium tray model including non-ideal thermodynamics and does not require additional short-cut calculations for initialization.
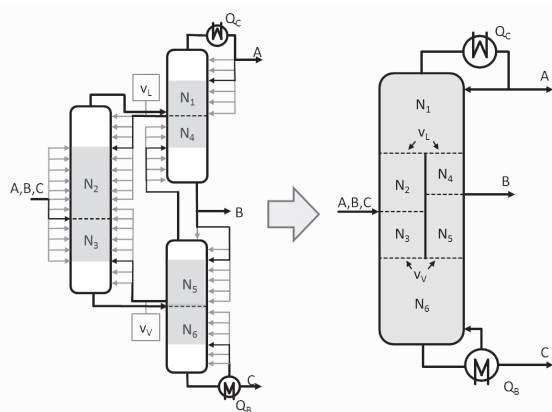

Figure 1: Illustration of the superstructure for the optimization of the fully thermally coupled configuration and transfer to the DWC design.

Each variant is optimized by means of a deterministic gradient-based optimization of a superstructure formulation, exemplarily illustrated in Figure 1 for the DWC column. All process variants are automatically initialized by means of a sequential procedure, in which the problem is finally solved as a sequentially relaxed mixed integer nonlinear programming problem.

All process variants are finally optimized for minimum total annualized costs.

The developed method is demonstrated by application to the separation of an equimolar mixture consisting of chloroform (C), benzene (B) and toluene (T) with a feed flowrate of 10 mol/s (cf. Figure 2).[1]
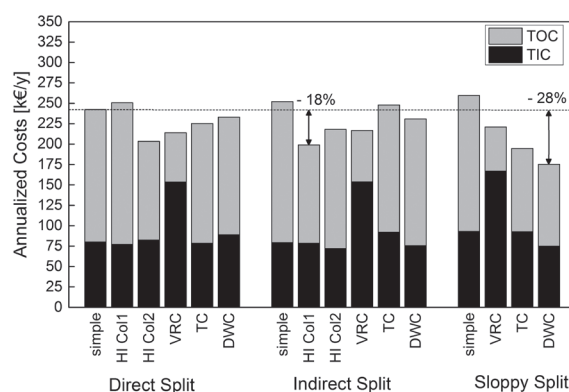
Figure 2: Annualized cost values of the different distillation configurations for the separation of an equimolar feed of CBT.

While multiple configurations result in significant improvements compared to a sequence of simple distillation columns, in this case a DWC with a central separating wall offers the highest savings of about 28% in terms of TAC in comparison to the best sequence of simple distillation columns.

The presented approach facilitates an efficient evaluation of a variety of energetically intensified distillation configurations within a computational time of less than 15 min and can further be used to evaluate the influence of different parameters to e.g. address the uncertainty related to the different cost factors. Future work will extend the method to extractive and heteroazeotropic distillation processes for the separation of azeotropic mixtures.

Publications:
[1] T. Waltermann, M. Skiborowski, in Computer Aided Chemical Engineering, Vol. 38 (Eds: Z. Kravanja, M. Bogataj), Elsevier, Amsterdam 2016.

Contact:
thomas.waltermann@bci.tu-dortmund.de
mirko.skiborowski@bci.tu-dortmund.de

Publications 2016 - 2014

2016

- J. Dreimann, P. Lutze, M. Zagajewski, A. Behr, A. Górak, A. J. Vorholt
  Highly integrated reactor–separator systems for the recycling of homogeneous catalysts
  Chemical Engineering and Processing: Process Intensification. 99, 124-131 (2016)

- T. Goetsch, P. Zimmermann, S. Enders, T. Zeiner
  Tuneable extraction systems based on hyperbranched polymers
  Chemical Engineering and Processing: Process Intensification. 99 (3), 175-182 (2016)

- T. Goetsch, P. Zimmermann, R. van den Bongard, S. Enders, T. Zeiner
  Superposition of Liquid–Liquid and Solid–Liquid Equilibria of Linear and Branched Molecules: Binary Systems
  Industrial & Engineering Chemistry Research. 55 (42), 11167-11174 (2016)

- M. M. Jaworska, A. Górak
  Modification of chitin particles with chloride ionic liquids
  Materials Letters. 164, 341-343 (2016)

- A. Kubiczek, W. Kamiński, A. Górak
  Modeling of single- and multi-stage extraction in the system of water, acetone, butanol, ethanol and ionic liquid
  Fluid Phase Equilibria. 425, 365-373 (2016)

- H. Kuhlmann, M. Skiborowski
  Synthesis of Intensified Processes from a Superstructure of Phenomena Building Blocks
  Computer Aided Chemical Engineering. 38, 697-702 (2016)

- K. Neumann, K. Werth, A. Martín, A. Górak
  Biodiesel production from waste cooking oils through esterification: Catalyst screening, chemical equilibrium and reaction kinetics
  Chemical Engineering Research and Design. 107, 52-62 (2016)

- R. Schulz, R. van den Bongard, J. Islam, T. Zeiner
  Purification of Terpenyl Amine by Reactive Extraction
  Industrial & Engineering Chemisty Research. 55 (19), 5763-5769 (2016)

- T. Waltermann, M. Skiborowski
  Efficient optimization-based design of energetically intensified distillation processes
  Computer Aided Chemical Engineering. 38, 571-576 (2016)

- M. Wierschem, S. Boll, P. Lutze, A. Górak
  Evaluation of the Enzymatic Reactive Distillation for the Production of Chiral Compounds
  Chem. Ing. Tech. 88 (1-2), 147-157 (2016)

- K. Groß, K. Neumann, K. Kupitz, M. Skiborowski, A. Górak
  HiGee-Technologie – Untersuchung von Hydrodynamik und Stofftransport
  Chemie-Ingenieur-Technik, 88 (9), p. 1283 (2016)

- J. Dreimann, P. Lutze, M. Zagajewski, A. Behr, A. Górak, A.J. Vorholt
  Highly integrated reactor-separator systems for the recycling of homogeneous catalysts
  Chemical Engineering and Processing: Process Intensification, 99, pp. 124-131 (2016)

- C. Kunde, D. Michaels, J. Micovic, P. Lutze, A. Górak, A. Kienle
  Deterministic global optimization in process design of distillation and melt crystallization
  Chemical Engineering and Processing: Process Intensification, 99,pp. 132-142 (2016)

2015

- T. Färber, R. Schulz, O. Riechert, T. Zeiner, A. Górak, G. Sadowski, A. Behr
  Different recycling concepts in the homogeneously catalysed synthesis of terpenyl amines
  Chemical Engineering and Processing: Process Intensification (98), 22–31 (2015)

- A. Kulaguin Chicaroux, A. Górak, T. Zeiner
  Demixing behavior of binary polymer mixtures
  Journal of Molecular Liquids. 209 (3), 42-49 (2015)

- A. Kulaguin Chicaroux, M. Plath, T. Zeiner
  Hyperbranched polymers as phase forming components in aqueous two-phase extraction
  Chemical Engineering and Processing: Process Intensification. 149 (3), 66-73 (2015)

- A. Kulaguin Chicaroux, T. Zeiner
  Investigation of interfacial properties of aqueous two-phase systems by density gradient theory
  Fluid Phase Equilibria. 149 (2015)

- A.-K. Kunze, P. Lutze, M. Kopatschek, J. F. Maćkowiak, J. Maćkowiak, M. Grünewald, A. Górak
  Mass transfer measurements in absorption and desorption: Determination of mass transfer parameters
  Chemical Engineering Research and Design. 104, 440-452 (2015)

- A.-K. Kunze, G. Dojchinov, V. S. Haritos, P. Lutze
  Reactive absorption of CO_2 into enzyme accelerated solvents: From laboratory to pilot scale
  Appl. Energy (156), 676-685 (2015)

- M. Leimbrink, A.-K. Kunze, D. Hellmann, A. Górak, M. Skiborowski
  Conceptual Design of Post-Combustion CO_2 Capture Processes - Packed Columns and Membrane Technologies
  Computer Aided Chemical Engineering. 37, 1223-1228 (2015)

- J. Muendges, A. Zalesko, A. Górak, T. Zeiner
  Multistage aqueous two-phase extraction of a monoclonal antibody from cell supernatant
  Biotechnology Progress. 31 (4), 925-936 (2015)

- J. Muendges, I. Stark, S. Mohammad, A. Górak, T. Zeiner
  Single stage aqueous two-phase extraction for monoclonal antibody purification from cell supernatant
  Fluid Phase Equilibria. 385 (0), 227-236 (2015)

- A. Niesbach, N. Fink, P. Lutze, A. Górak
  Design of reactive distillation processes for the production of butyl acrylate: Impact of bio-based raw materials
  Chinese Journal of Chemical Engineering. 23 (11), 1840-1850 (2015)

- P. Rdzanek, S. Heitmann, A. Górak, W. Kamiński
  Application of supported ionic liquid membranes (SILMs) for biobutanol pervaporation
  Separation and Purification Technology. 155, 83-88 (2015)

- D. Sudhoff, M. Leimbrink, M. Schleinitz, A. Górak, P. Lutze
  Modelling, design and flexibility analysis of rotating packed beds for distillation
  Chemical Engineering Research and Design. 94, 72-89 (2015)

- K. Werth, K. Neumann, M. Skiborowski
  Computer-aided process analysis of an integrated biodiesel process incorporating reactive distillation and organic solvent nanofiltration
  Computer Aided Chemical Engineering. 37, 1277-1282 (2015)

- M. Wierschem, R. Heils, S. Schlimper, I. Smirnova, A. Górak, P. Lutze
  Enzymatic Reactive Distillation for the Transesterification of Ethyl Butyrate: Model Validation and Process Analysis
  Computer Aided Chemical Engineering 37, 2135-2140 (2015)

- K. Werth, P. Lutz, A.A. Kiss, A.I. Stankiewicz, G.D. Stefanidis, A. Górak
  A systematic investigation of microwave-assisted reactive distillation: Influence of microwaves on separation and reaction
  Chemical Engineering and Processing: Process Intensification, 93, pp. 87-97 (2015)

- M. Wierschem, M. Skiborowski, A. Górak
  Continuous enzymatic reactive distillation with immobilized enzyme beads
  Separations Division 2015 – Core Programming Area at the 2015 AIChE Annual Meeting, 2, pp. 648-655 (2015)

- D.K. Babi, J. Holtbruegge, P. Lutze, A. Górak, J.M. Woodley, R. Gani
  Sustainable process synthesis–intensification
  Computers and Chemical Engineering, 81, pp. 218-244 (2015)

2014

- K. Babi, J. Holtbruegge, P. Lutze, A. Górak, J. M. Woodley, R. Gani
  Sustainable process synthesis-intensification
  Proceedings of the 8th International Conference on Foundations of Computer-Aided Process Design – FOCAPD 2014. 34 (2014)

- R. Heils, A. Niesbach, M. Wierschem, D. Claus, S. Soboll, P. Lutze, I. Smirnova
  Integration of Enzymatic Catalysts in a Continuous Reactive Distillation Column: Reaction Kinetics and Process Simulation
  Industrial & Engineering Chemistry Research. 53 (50), 19612-19619 (2014)

- J. Holtbruegge, H. Kuhlmann, P. Lutze
  Conceptual Design of Flowsheet Options Based on Thermodynamic Insights for (Reaction−)Separation Processes Applying Process Intensification
  Industrial & Engineering Chemistry Research (53), 13413-13429 (2014)

- J. Holtbruegge, H. Kuhlmann, P. Lutze
  Process analysis and economic optimization of intensified process alternatives for simultaneous industrial scale production of dimethyl carbonate and propylene glycol
  Chemical Engineering Research and Design (2014)

- J. Holtbruegge, M. Wierschem, P. Lutze
  Synthesis of dimethyl carbonate and propylene glycol in a membrane-assisted reactive distillation process: Pilot-scale experiments, modeling and process analysis
  Chemical Engineering and Processing: Process Intensification. 84, 54-70 (2014)

- W. Kamiński, A. Górak, A. Kubiczek
  Modeling of liquid–liquid equilibrium in the quinary system of water, acetone, n-butanol, ethanol, and ionic liquid
  Fluid Phase Equilibria. 384 (3), 114-121 (2014)

- A. A. Kiss, R. Schmuhl, P. Lutze, A. Górak, G. Stefanidis, A. Stankiewicz
  Reactive Distillation Powered by Alternative Energy Sources, *NPT Procestechnolog, 11-13 (2014)*

- K. Koch, A. Górak
  Pervaporation of binary and ternary mixtures of acetone, isopropyl alcohol and water using polymeric membranes: Experimental characterisation and modelling
  Chemical Engineering Science. 115, 95-114 (2014)

- J. Micovic, K. Werth, P. Lutze
  Hybrid separations combining distillation and organic solvent nanofiltration for separation of wide boiling mixtures
  Chemical Engineering Research and Design. 92, 2131-2147 (2014)

- A. Prinz, J. Hönig, I. Schüttmann, H. Zorn, T. Zeiner
  Separation and purification of laccases from two different fungi using aqueous two-phase extraction
  Process Biochemistry. 49 (2), 335-346 (2014)

- A. Prinz, K. Koch, A. Górak, T. Zeiner
  Multi-stage laccase extraction and separation using aqueous two-phase systems: Experiment and model
  Process Biochemistry. 49 (6), 1020-1031 (2014)

- M. Puthirasigamany, I. Hamm, F. A. van Winssen, N. Nikbin, P. Kreis, A. Górak, T. Zeiner
  Purification of biomolecules combining ATPS and membrane chromatography
  Food and Bioproducts Processing. 92 (2), 152-160 (2014)

- P. Schmidt, J. Micovic, P. Lutze, A. Górak
  Organophile Nanofiltration - Herausforderungen und Lösungsansätze zur Anwendung eines innovativen Membrantrennverfahrens
  Chemie Ingenieur Technik. 86 (5), 602-610 (2014)

- P. Schmidt, E. L. Bednarz, P. Lutze, A. Górak
  Characterisation of Organic Solvent Nanofiltration membranes in multi-component mixtures: Process design workflow for utilising targeted solvent modifications
  Chemical Engineering Science. 115 (3), 115-126 (2014)

- P. Schmidt, J. Micovic, P. Lutze, A. Górak
  Organophile Nanofiltration - Herausforderungen und Lösungsansätze zur Anwendung eines innovativen Membrantrennverfahrens
  Chemie Ingenieur Technik. 86 (5), 602-610 (2014)

- D. Sudhoff, K. Neumann, P. Lutze
  An Integrated Design Method for Rotating Packed Beds for Distillation
  Computer Aided Chemical Engineering. 2014 (33), 1303-1308 (2014)

- K. Sundmacher, A. Górak, M. Kraume, G. Wozny
  Special issue: InPROMPT – Integrated chemical processes with liquid multiphase systems
  Chemical Engineering Science. 115 (3), 1-2 (2014)

- W. Kamiński, A. Górak, A. Kubiczek
  Modeling of liquid-liquid equilibrium in the quinary system of water, acetone, n-butanol, ethanol and ionic liquid
  Fluid Phase Equilibria, 384, pp. 114-121 (2014)

- P. Rdzanek, S. Heitmann, A. Górak, W. Kamiński
  Application of supported ionic liquid membranes (SILMs) for biobutanol pervaporation
  Separation and Purification Technology, 155, pp. 83-88 (2014)

- K. Sundmacher, A. Górak, M. Kraume, G. Wozny
  Special issue: InPROMPT - Integrated chemical processes with liquid multiphase systems
  Chemical Engineering Science, 115, pp. 1-2 (2014)

- A. Górak
  Preface to the Distillation Collection, Distillation: Fundamentals and Principles
  pp. vii-viii (2014)

- A. Górak, Z. Olujić
  Distillation: Fundamentals and Principles
  Distillation: Fundamentals and Principles pp. 1-506 (2014)

- A. Górak
  Preface to the Distillation Collection
  Distillation: Operation and Applications p. vii (2014)

- A. Górak, H. Schoenmakers
  Distillation: Operation and Applications
  Distillation: Operation and Applications, pp. 1-445 (2014)

- A. Górak
  Preface to the Distillation Collection
  Distillation: Equipment and Processes, pp. vii-viii (2014)

- A. Górak, Z. Olujić
  Distillation: Equipment and Processes
  Distillation: Equipment and Processes, pp. 1-351 (2014)

- C. A. González-Rugerio, R. Fuhrmeister, D. Sudhoff, J. Pilarczyk, A. Górak
  Optimal design of catalytic distillation columns: A case study on synthesis of TAEE
  Chemical Engineering Research and Design, 92 (3), pp. 391-404 (2014)

- P. Schmidt, J. Micovic, P. Lutze, A. Górak
  Organic Solvent nanofiltration - Challenges and approaches of an innovative membrane separation process [Organophile Nanofiltration - Herausforderungen und Lösungsansätze zur Anwendung eines innovativen Membrantrennverfahrens]
  Chemie-Ingenieur-Technik, 86 (5), pp. 602-610 (2014)

- D. K. Babi, J. Holtbruegge, P. Lutze, A. Górak, J.M. Woodley, R. Gani
  Sustainable process synthesis-intensification
  Computer Aided Chemical Engineering, 34, pp. 255-260 (2014)

Fluid Mechanics (SM)

Mass Transfer in Liquid/Liquid Slug Flow

Physical Modelling of Conjugated Mass Transfer in Capillary Micro Reactors

Christian Heckmann, Peter Ehrhard

Micro Reactors have been applied for the production of fine chemicals and pharmaceuticals for several years. Owing to the small size of the channels, especially the liquid/liquid slug flow pattern offers large specific areas and high mixing convection due to the segmented flow. Before, we introduced a new concept that can handle the hydrodynamics and the mass transfer of conjugated mass transfer systems, considering a high resolution at the free interface. In the next step the numerical concept is applied to a technical application to physically validate the numerical model. A detailed access to the mass transfer of the liquid/liquid Slug Flow pattern is achieved.

A periodic element of the slug flow pattern is used to model the capillary micro reactor, see figure 1. We set up a model consisting of two incompressible immiscible and Newtonian liquids, which are acting as solvents for a solute, which is extracted from one phase to the other. The hydrodynamics are simulated based on an imported steady-state interface. Separate static computational domains are arranged. The computational domains are coupled at the free interface. Only dilute concentrations are taken into account, so the back-coupling of the mass transfer to the hydrodynamics of the multiphase system is neglected, hence transport equation of a passive (scalar) concentration is solved at both sides of the interface.

Experiments are performed to physically validate the numerical model. The standard extraction system consisting of Water/Aceton/Butylacetate is used. An experimental test rig is set up based on the work of Kurt et. al [1]. The residence time unit consists of a FEP capillary with a cross-sectional flow diameter of 1mm. The lipophilic FEP capillary attracts the organic phase, so aqueous slug are formed in the continuous phase. In the experiment, Aceton is extracted from the aqueous to the organic phase. The extraction rate is evaluated by gas chromatography.
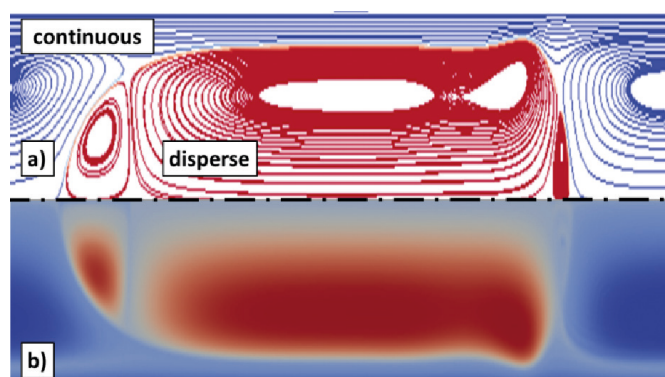

Figure 1: a) stream lines for $Ca_c=Ca_d=10^{-1}$, $Re_c=Re_d=100$, b) concentration distribution for $Pe_c=Pe_d=10^5$, Fo = 0.01.
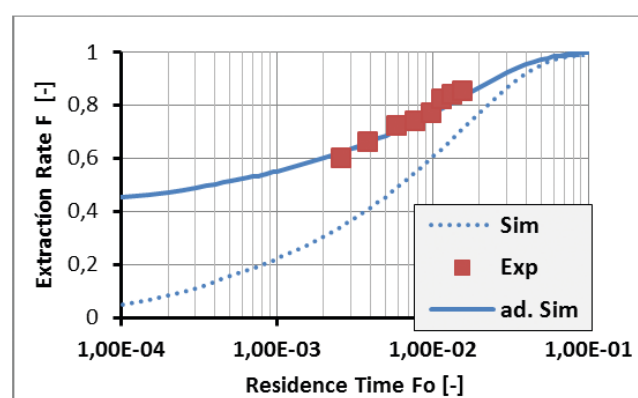

Figure 2: Extraction rate F over dimensionless time Fo: comparing the simulation (Sim) with the experiments (Exp) using the adapted extraction rate (ad. Sim).

Changing the length of the capillary reactor tube allows the evaluation of the extraction rate versus the residence time in the micro reactor. Physical parameters are taken over to set up specific simulations. Comparing the experimental and theoretical results shows that the extraction performance of the experiment is underestimated in the simulation, see figure 2. This contribution is introduced by the system immanent slug formation at the beginning of the extraction process in the experiment and not considered in the theoretical model. Adapting the definition of the simulative extraction rate allows the change of the initial concentration to fit the experimental data. The result shows that 36% of the extraction process are taking place during the slug formation.

[1] Kurt et al, Liquid–liquid extraction system with microstructured coiled flow inverter and other capillary setups for single-stage extraction applications, Chem. Ing J., 284 (2016), 764-777.

Contact:
christian.heckmann@bci.tu-dortmund.de
peter.ehrhard@bci.tu-dortmund.de

Multi-phase Flow in Bubble Columns

CFD-Modeling and Simulation of Rising Bubbles in Water

Ann Kathrin Höffmann, Peter Ehrhard

The energy consumption of waste-water-treatment plants in Germany appears to be substantial. Waste-water-treatment plants working with the activated-sludge process consume up to 80 % of their energy demand to aerate the respective basins. To identify saving potentials, numerical computations of the hydrodynamics and biochemical reactions in the aeration basins can be used. To validate the numerical computations, the results are compared to measurements at the Helmholtz-Zentrum Dresden-Rossendorf (HZDR). The following article presents the numerical model to compute rising bubbles in a bubble column based on the Euler-Euler method.

To compute the hydrodynamics of rising bubbles in a bubble column, a transient Euler-Euler method is engaged. Water is used as continuous phase and air as incompressible disperse phase with a bubble diameter of 2 mm. The isothermal computations neglect coalescence. As initial condition, the bubble column is filled with stagnant water and is aerated from the bottom with a defined air mass flow. To capture the interface momentum transfer, the drag force, the lift force, the wall-lubrication force, and the turbulent dispersion force are implemented. As boundary condition at the walls, a no-slip condition is chosen for the continuous phase and a free-slip condition is chosen for the disperse phase. The air leaves the domain at the top of the bubble column and a free-slip condition is used for the continuous water.

A sketch of the bubble column is shown on the left side of figure 1. On the right, the computed profile of the axial water velocity w_{water} is shown.

It can be seen, that the rising air bubbles induce a water flow in the upward direction in the middle-region of the column. At the near-wall region, the water flows in the downward direction, as expected. This velocity field is due to continuity reasons, since the water cannot leave the bubble column at the top.
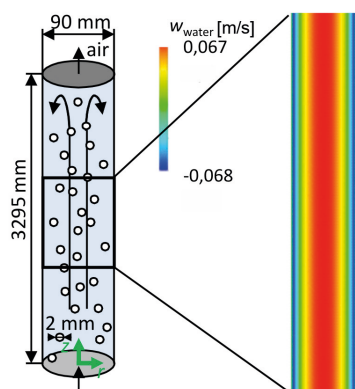
The computed axial air velocity w_{air} and air volume fraction φ_{air} can be evaluated at different column heights. Figure 2 shows e.g. the resulting radial profiles at a height of z = 1637 mm. Moreover, the measured data from the HZDR are plotted. Hence, the computed and the experimental profiles can be compared to judge whether the numerical model appears to be appropriate.
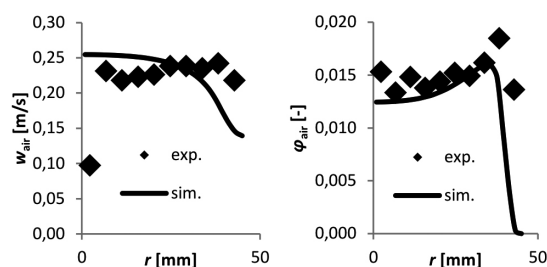

Figure 2: Axial air velocity profile (left) and air volume-fraction profile (right), both at a height of z = 1637 mm.

The computed profiles show a reasonably-good agreement with the measured data. Additionally, the specific mass-exchange surface is computed. The specific mass-exchange surface from the experiments is a = 32 m^{-1}, from the computations we infer a = 34 m^{-1}. The deviation from the measured value with +6 %, once more shows a reasonably-good agreement. The value of the specific mass-exchange surface is responsible for the amount of oxygen transferred from the air bubbles into the continuous water phase.

Next steps we consider the bubble rise in activated sludge, instead of water. This involves a non-Newtonian rheology of the continuous phase. Further, both computations and experiments will be conducted for larger basins, before the simulation of the full-scale aeration basins in the water treatment plant in Schwerte will be adressed.

Figure 1: Sketch of the computed bubble column (left) and axial velocity profile in the middle section of the bubble column (right).

Contact:
ann-kathrin.hoeffmann@bci.tu-dortmund.de
peter.ehrhard@bci.tu-dortmund.de

Experimental Analysis of Bell-atomized Waterborne Paint Sprays using Optical Measurement Methods

Analysis and Measurement of Non-Newtonian Jet Disintegration

Lutz Gödeke, Peter Ehrhard

High-speed rotary bell atomizers are used in a wide range of industrial processes due to their flexibility and overall performance. The major application fields are spray drying processes and the formation of highly-uniform paint coatings, with the latter being desirable in the automotive industry. Accordingly, this process needs to be viable for variable flow rates, bell speeds and different material properties, while maintaining well-defined droplet size distributions. The use of appropriate process parameters leads to the desired spray characteristics.

The current work investigates the main influencing process parameters and material properties for the formation and breakup of the emerging filaments and the resulting spray cone by using phase-Doppler-anemometry (PDA), time shift measurements (TS), and high speed imaging (HS) (Figure 1). Furthermore, we investigate the influence of effect particles on the PDA measurement results. The analyzed materials are fully opaque, of non-Newtonian character and differ in their filament breakup due to their rheological behavior based on composition.
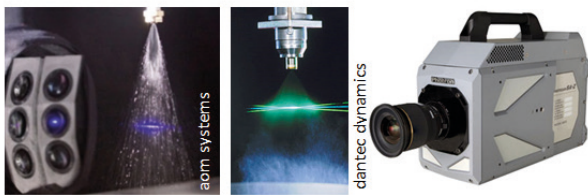

Figure 1: Measurement devices used for detecting droplet size and filament characteristics. AOM SpraySpy (TS), Dantec phase-Doppler anemometer (PDA), Photron Fastcam SA-Z (HS).

The overall process can be split up into four regimes: the film flow underneath the bell, the filament formation and breakup, the spray deployment and the droplet impact at the substrate surface. Of course, all those regimes must be investigated in detail to fully understand the complete process. The flow underneath the bell is being characterized using the lubrication approximation, solved numerically to obtain an estimate for the shear rate (film thickness 20-40 μm, radial velocity 1-10 m/s, shear rate 10^5 - 10^6 Pas). This directly leads to a way to estimate the effective viscosity during the following atomization process. Depending on the main parameters (flowrate Q, bell speed ω, bell diameter R) the film disintegrates at the bell edge by formation of direct droplets, lamella, or filaments (Figure 2). These droplets are measured using the available techniques (PDA, TS, HS) at specific points and are characterized by the Sauter mean diameter (SMD or D_{32}, Figure 3), the diameter of a sphere with the mean volume to surface ratio of the true distribution.
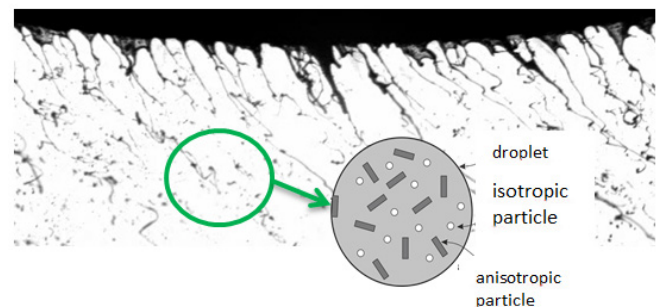

Figure 2: Filament buildup and disintegration at the edge of the rotating bell. Schematic overview of droplet composition.

Detailed information about the process-dependent droplet size and velocity allows for the analysis of the resulting paint film distribution on the substrate and the susceptibility for surface defects like pinholes or orange-peel effects. Pinholes e.g. are due to bubble entrapment in the liquid film and are dependent on the impact of droplets and their rheological behavior. The surface waviness (orange peel) on the other hand is influenced by local Marangoni flows in the film, which can be avoided by a uniform solvent distribution. Evaporation effects, droplet impact, and substrate deposition can be evaluated only based on detailed experimental data and a subsequent analysis.
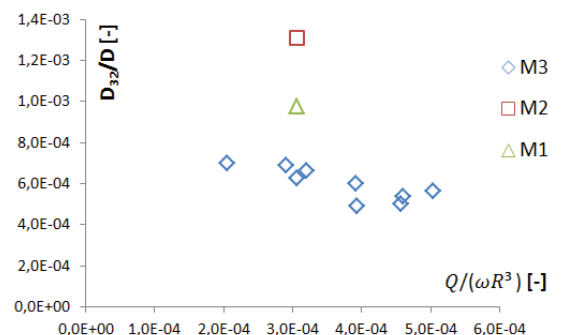

Figure 3: SMD as a function of the discharge coefficient $Q/(wR^3)$ for different materials M1-3, flow rates *200-400 ml/min*, bell speed 20-50 *krpm*, R = 32.5 mm.

Contact:
lutz.goedeke@bci.tu-dortmund.de
peter.ehrhard@bci.tu-dortmund.de

Publications 2016 - 2014

2016

- P. Ehrhard
  Mikroströmungen
  in: Prandtl-Führer durch die Strömungslehre, ed. H.H. Oertel, 14. Auflage, 663-714, Springer Vieweg, Wiesbaden (2016)

- M. Meier
  Modellierung und Simulation von Strömungen und biologischen Reaktionen innerhalb eines Belebtschlammbeckens
  Chemie Ingenieur Technik 88, 1128-1137 (2016)

- P. Lakshmanan, P. Ehrhard
  Enhanced mass transfer in micro-capillary two-phase flow
  Proc. Angewandte Mathematik und Mechanik 16, 603 (2016)

- A.K. Höffmann, P. Lakshmanan, P. Ehrhard, Th. Ostermann
  The Jungebad apparatus for the production of oil-dispersion baths
  Proc. Angewandte Mathematik und Mechanik 16, 599 (2016)

- T. Neumann, K. Boettcher, P. Ehrhard
  Numerical investigation into a liquid displacing a gas in thin porous layers
  Proc. Angewandte Mathematik und Mechanik 16, 605 (2016)

- Ch. Heckmann, P. Ehrhard
  Simulation of mass transfer in liquid/liquid slug flow
  Proc. Angewandte Mathematik und Mechanik 16, 597 (2016)

2015

- W. Tillmann, J. Pfeiffer, N. Sievers, K. Boettcher
  Analysis of the spreading kinetics of AgCuTi melts on silicon carbide below 900 °C, using a large-chamber SEM
  Colloids and Surfaces A: Physicochemical Engineering Aspects 468, 167-173 (2015)

- T. Neumann, K. Boettcher, P. Ehrhard
  Numerical investigation of a liquid displacing a gas in thin porous layers
  Proc. Angewandte Mathematik und Mechanik 15, 517 (2015)

- K. Boettcher, T. Externbrink
  Linear stability of a thin non-isothermal droplet spreading on a rotating disk
  Proc. Angewandte Mathematik und Mechanik 15, 503 (2015)

- Ch. Heckmann, P. Lakshmanan, P. Ehrhard
  Simulation of mass transfer at free liquid/liquid interfaces
  Proc. Angewandte Mathematik und Mechanik 15, 509 (2015)

- P. Lakshmanan, P. Ehrhard
  Gas bubbles in micro capillaries – hydrodynamics and mass transfer
  Proc. Angewandte Mathematik und Mechanik 15, 513 (2015)

2014

- M. Blank, P. Ehrhard
  Experiments on the spreading of silicone oil droplets on horizontal rotating plates
  Proc. Angewandte Mathematik und Mechanik 14, 677 (2014)

- M. Fischer, P. Ehrhard
  Numerical study of a particle separation method based on the Segré-Silberberg effect
 *Proc. Angewandte Mathematik und Mechanik 14, 669 (2014)*

Technical Biochemistry (TB)

Discrimination of Wild Types and Hybrids of *Duboisia myoporoides* and *Duboisia leichhardtii* at Different Growth Stages Using ^{1}H NMR-based Metabolite Profiling

Sophie Friederike Ullrich, Oliver Kayser

Metabolic profiling is an important tool for the elucidation metabolic pathways and the detection of relevant biomarkers in plants. Duboisia R.Br., used in this study, contains tropane alkaloids which are utilised as anticholinergic drugs in human medicine, thereof scopolamine being economically most important. As only little is known about the metabolite composition among the different species, ^{1}H NMR-based metabolic profiling was done in order to elucidate primary and secondary metabolism in Duboisia especially focusing on the tropane alkaloid pathway.

Duboisia R.Br., which belongs to the family of *Solanaceae*, is indigenous to Australia and used as principal source of the medicinally active tropane alkaloid scopolamine (Figure 1). Until today, its full chemical synthesis is very complex and low yielding. Moreover, no alkaloid levels competitive to field grown plants could be achieved by overexpressing biosynthetic genes in regenerated plants or by using cell culture systems so far. Thus, the industrial production providing scopolamine is largely based on agricultural field cultivation of *Duboisia* hybrids.
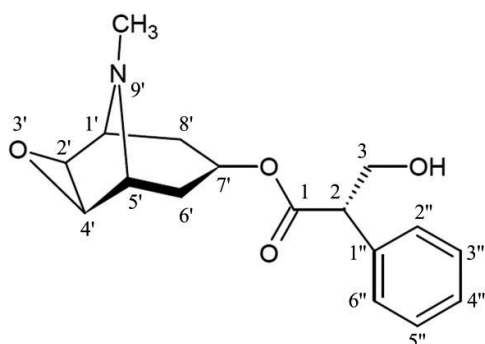
(-)-Scopolamine ((-)-Hyoscine)
IUPAC name: (1R,2R,4S,5S,7S)-9-Methyl-3-oxa-9-azatricyclo[3.3.1.0^{2,4}]non-7-yl (2S)-3-hydroxy-2-phenylpropanoate
Molecular formula: $C_{17}H_{21}NO_4$

Figure 1: Structure, IUPAC name and molecular formula of scopolamine.

For optimizing the breeding process and the plant cultivation, ^{1}H NMR-based metabolic profiling was applied as it allows a deeper insight into the primary and secondary metabolism of *Duboisia*. For this purpose, plants of five different genotypes (*Duboisia myoporoides*, *D. leichardtii* and hybrids of *D. myoporoides* and *D. leichhardtii*) were cultivated under strictly controlled conditions in climate chambers and harvested after 3 and 6 months. All in all, 14 different metabolites including sugars, amino acids and secondary metabolites like flavonoids or tropane alkaloids were identified in the leaves of *Duboisia* with the help of 1D- and 2D-NMR technique (Figure 2).
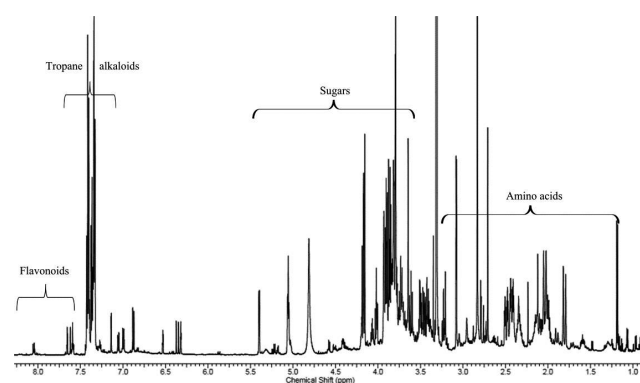

Figure 2: ^{1}H NMR spectrum of a *Duboisia* leaf extract demonstrating the signal richness and the wide range in metabolites.

The application of principal component analysis (PCA) for the comparison of the different genotypes based on the NMR data of the leaf extracts allowed a clear distinction between the *Duboisia* hybrids and the wild types, which were further sub grouped into *D. myoporoides* and *D. leichhardtii*. Thereby, scopolamine and its precursors were found in higher levels in *Duboisia* hybrids, except of hyoscyamine, which was predominant in *D. leichhardtii*. Sugars like glucose or sucrose and amino acids like proline or threonine were more abundant in *D. myoporoides* and *D. leichhardtii*. The average content in scopolamine increased significantly from month 3 to 6 in *Duboisia* hybrids contrary to the wild.

This NMR analysis allows a fast and easy comparison of different samples of *Duboisia* by grouping them based on their metabolite composition. In addition, it can be applied in order to select promising genotypes and optimised cultivation conditions for the production of scopolamine.

Contact:
oliver.kayser@bci.tu-dortmund.de

Influence of Light Intensity, Illumination Time and Temperature on Growth and Scopolamine Biosynthesis in *Duboisia* Species

Sophie Friederike Ullrich, Oliver Kayser

Duboisia *species contain tropane alkaloids as secondary plant components, thereof quantitatively as well as economically most important scopolamine. In order to optimise its production, the effect of abiotic factors, namely light and temperature, on biomass and biosynthesis of scopolamine was studied.*

Duboisia is a native Australian plant belonging to the family of Solanaceae and contains tropane alkaloids which are utilised as anticholinergic drugs. Thereof pharmaceutically most valued and increasingly demanded is scopolamine, which is for example applied in form of scopolamine-N-butylbromide for the treatment of abdominal pain and bladder spasms. Until today, industrial manufacturing operations providing scopolamine are largely based on field plant cultivation of *Duboisia* hybrids. As it is of great interest to optimise the farming by increasing the knowledge concerning the impact of environmental factors on growth and scopolamine biosynthesis, plants of three different genotypes (wild type of *Duboisia myoporoides* R.Br., hybrids of *Duboisia myoporoides* R.Br. and *D. leichhardtii* F.Muell.) were grown in climate chambers. In order to systematically analyse the influence of temperature (20, 24, 28 °C) and light (50 – 300 µmol/m²·s, 12, 18, 24 hours per day) on scopolamine and biomass production strictly controlled conditions were applied using a central composite face centered (CCF) – design (Figure 1).
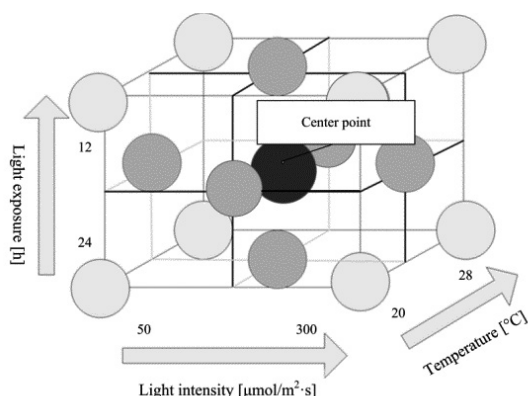

Figure 1: Experimental design of the cultivation parameters light and temperature.

replicates/cultivation condition) under different experimental settings (temperature [°C],
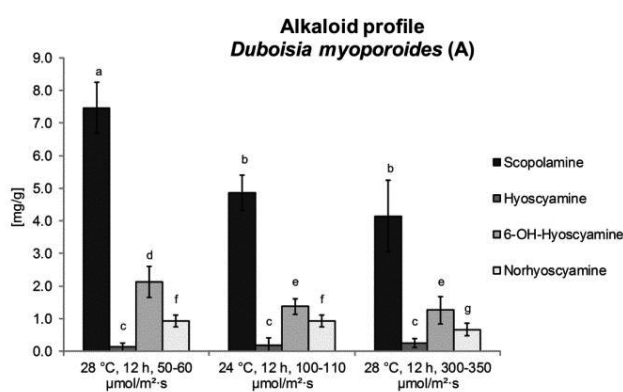
daily exposure to light [h], light intensity [µmol/m²·s]), Kruskal-Wallis test with P = 0.05 (different letters = statistical significant differences).

The HPLC-MS analysis of all plants under investigation hereby reveals that scopolamine is significantly decreased with strengthened illumination time and light exposure (Figure 2). In contrast, biomass production is enhanced by using light of high intensity and elevated temperature, as this increases the photosynthetic activity. Regarding the hybrids, longer illumination time has an additional positive effect on biomass production contrary to *Duboisia myoporoides*.

All in all, it can be concluded that especially the light intensity is an important regulating variable which can be applied in a targeted manner for influencing the scopolamine and biomass production.

Figure 2: Alkaloid profile of 7-week-grown *Duboisia myoporoides* plants (A) (5-6

Contact:
oliver.kayser@bci.tu-dortmund.de

Publications 2016 - 2014

2016

- Ullrich, S.F., Hagels, H., Kayser O.
  Scopolamine: a journey from the field to clinics
  Phytochem Rev 2016, DOI: 10.1007/211101-016-9477-x

- Sasse, J., Schlegel, M., Borghi, L., Ullrich, F., Lee, M., Liu, G.-W., Giner, J.-L., Kayser, O., Bigler, L., Martinoia, E., Kretzschmar
  T. Petunia hybrida PDR2 is involved in herbivore defense by controlling steroidal contents in trichomes
  Plant, Cell & Environment 2016, DOI: 10.1111/pce. 12828

- Ullrich, S.F., Averesch, N.J.H., Castellanos, L., Choi, Y.H., Rothauer, A. and Kayser, O.
  Discrimination of wild types and hybrids of *Duboisia myoporoides* and *Duboisia leichhardtii* at different growth stages using $_1$H NMR-based metabolite profiling and tropane alkaloidstargeted HPLC-MS analysis
  Phytochemistry 2016, 131: 44-56

- Hariharan, C., Kayser, O.
  Innovative and rapid detection of marihuana consumption from direct breath analysis
  PITTCON 2016, Atlanta, Georgia, USA, March 6-10

- Happyana, N., Kayser, O.
  Monitoring metabolite profiles of Cannabis sativa L. trichomes during flowering period using ^{1}H NMR-based metabolomics and Real-Time PCR
  Planta Med 2016, DOI: 10.1055/s-0042-108058

- Wang, W.-X., Kusari, S., Laatsch, H., Golz, C., Kusari, P., Strohmann, C., Kayser, O., Spiteller, M.
  Antibacterial azaphilones from an endophytic fungus, *Colletotrichum* sp. BS4
  J Nat Prod 2016, 79: 704-710

2015

- Gruchattka, E., Kayser, O.
  ***In vivo* validation of *in silico* predicted metabolic engineering strategies in yeast: disruption of alpha-ketoglutarate dehydrogenase and expression of ATP-citrate lyase for terpenoid production**
  PLoS One. 2015, 10(12): e0144981

- Farag, S., Kayser, O.
  Cultivation and breeding of *Cannabis sativa L.*
  In: Medicinal and aromatic plants of the world. Vol. 1, Springer Netherlands, Dordrecht, ISBN 978-94-017-9810-5, 2015, 165-186

- Farag, S., Kayser, O.
  Cannabinoids production by hairy root cultures of *Cannabis sativa L.*
  Am. J. Plant Sciences 2015, 6: 1874-1884

- Li, G., Kusari, S., Kusari, P., Kayser, O., Spiteller, M.
  Endophytic *Diaporthe* sp. LG23 produces a potent antibacterial tetracyclic triterpenoid
  J. Nat. Prod. 2015, 78: 2128-2132

- Zirpel, B., Stehle, F., Kayser, O.
  Production of Delta-9-tetrahydrocannabinolic acid from cannabigerolic acid by whole cells of Pichia (*Komagataella*) pastoris expressing Delta-9-tetrahydrocannabinolic acid synthase from *Cannabis sativa l.*
  Biotechn. Lett. 2015. doi: 10.1007/s10529-015-1853-x

- Kusari, P., Kusari, S., Spiteller, M., Kayser, O.
  Implications of endophyte-plant crosstalk in light of quorum responses for plant biotechnology
  Appl. Microbiol. Biotechnol. 2015, 99: 5383-5390

- Wang, W.-X., Kusari, S., Sezgin, S., Lamshöft, M., Kusari, P., Kayser, O., Spiteller, M.
  Hexacyclopeptides secreted by an endophytic fungus Fusarium solani N06 act as crosstalk molecules in *Narcissus tazetta*
  Appl. Microbiol. Biotechnol. 2015, 99: 7651-7662

2014

- Kusari, S., Lamshöft, M., Kusari, P., Gottfried, S., Zühlke, S., Louven, K., Hentschel, U., Kayser, O., Spiteller, M.
  Endophytes are hidden producers of maytansine in *Putterlickia roots*
  J. Nat. Prod. 2014, 77: 2577-2584 (selected as ACS editor's choice article)

- Kusari, P., Kusari, S., Spiteller, M., Kayser, O.
  Biocontrol potential of endophytes harbored in *Radula marginata* (liverwort) from the New Zealand ecosystem
  Antonie van Leeuwenhoek 2014, 106: 771-788

- Kusari, P., Kusari, S., Lamshöft, M., Sezgin, S., Spiteller, M., Kayser, O.
  Quorum quenching is an antivirulence strategy employed by endophytic bacteria
  Appl Microbiol Biotechnol May 2014, 98: 7173-7183

- El Fahmi, S., Woerdenbag, H.-J., Kayser, O.
  Indonesian traditional herbal medicine towards rational phytopharmacological use.
  Herbal Med. 2014, 4: 51-73

- Kusari, P., Spiteller, M., Kayser, O., Kusari, S.
  Recent advances in research on *Cannabis sativa* L. endophytes and their prospect for the pharmaceutical industry
  In: Kharwar, R.N. et al. (eds.) Microbial Diversity and Biotechnology in Food Security, Springer India, 2014, Book Part I, 3-15. ISBN: 978-81-322-1800-5

- Staniak, A., Bouwmeester, H., Fraser, P.D., Kayser, O., Martens, S., Tissier, A., van der Krol, S., Wessjohann, L., Warzecha, H.
  Natural products - learning chemistry from plants
  Biotechnol J. 2014, 9(3): 326-336

Technical Biology (TBL)

Anticancer Drugs

A concise synthetic route provides access to novel 5-lipoxygenase inhibitors

Sebastian Schieferdecker, Markus Nett

The enzyme human 5-lipoxygenase (5-LO) catalyzes two initial steps in the conversion of arachidonic acid into leukotrienes, which are well-known mediators of inflammatory and allergic reactions. Increasing evidence suggests that leukotrienes also play an important role in tumorigenesis. Recently, the bacterial natural product myxochelin A was identified both as a potent inhibitor of 5-LO and as an antileukemic agent. The original assumption that the biological activity of myxochelin A is due to the complexing properties of its catechol moieties could be disproven after the testing of myxochelin analogues, which had been generated by precursor-directed biosynthesis. This unexpected finding prompted efforts to establish a low-cost method for the preparation of myxochelin A.

A step-economical synthesis of myxochelin A from commercially available starting materials has been achieved using a biomimetic strategy, in which the 2,3-dihydroxybenzoate residues were linked with a lysine moiety prior to the reduction of the central carboxylate group (Figure 1). In terms of yield, the developed method was clearly superior to a previously published route, in which the reduction reaction preceded the attachment of the aromatic moieties.
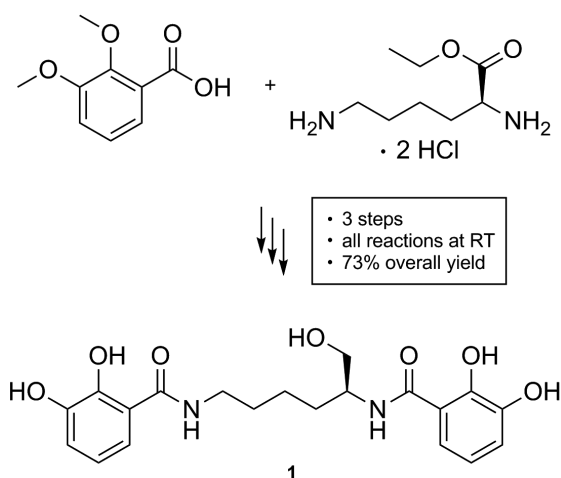

Figure 1: General scheme for the synthesis of myxochelin A (1).

To further explore the structure-activity relationship (SAR) of myxochelin, 48 non-natural derivatives were prepared according to the protocol depicted in Figure 1. Because modification of the ring substitution pattern was not very permissive in terms of 5-LO inhibition in a cell-free assay, we turned our attention to the lysinol motif, which linked the two aromatic moieties. This study revealed that the secondary alcohol function and only chiral center of myxochelin A is not required for biological activity and can be omitted. Furthermore, it was possible to generate myxochelin derivatives with improved activity by expanding the diaminoalkane linker of the two catechol residues.
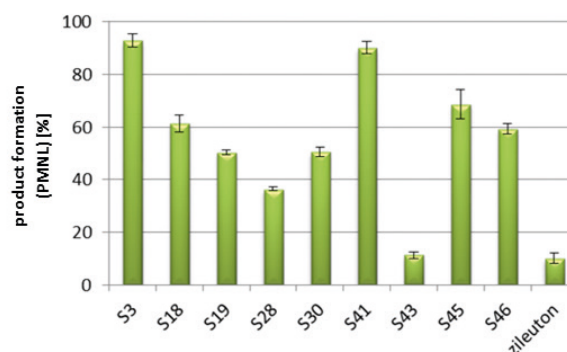

Figure 2: 5-LO activity in PMNL cells after treatment with synthetic myxochelin analogues (10 µM). The 5-LO inhibitor zileuton (10 µM) was used as a control.

The most active myxochelin analogues (*i.e.*, S3, S18, S19, S28, S30, S41, S43, S45, and S46) were eventually tested in a cell-based assay using human polymorphonuclear leukocytes (PMNL) stimulated with the Ca^{2+} ionophore A23187. While the derivatives S3 and S41 completely failed to inhibit 5-LO product formation in PMNL, myxochelins S18, S19, S28, S30, S45, and S46 showed partial inhibition (Figure 2). The most potent cellular 5-LO inhibitor was myxochelin S43, which decreased 5-LO product formation by 88.7% at 10 µM, comparable to the FDA-approved drug zileuton. In comparison, myxochelin A was found to be much less efficient in the PMNL assay (inhibition of 5-LO product formation at 10 µM by only 26.5%).

In summary, a convenient route for the preparation of myxochelin A was developed. The new methodology could be exploited not only for clarifying the SAR of this natural product, but also for the generation of a derivative with superior bioactivity.

Contact:
markus.nett@bci.tu-dortmund.de

Publications:
S. Schieferdecker, M. Nett,
Tetrahedron Lett. 57, 1359-1360 (2016).
S. Schieferdecker, S. König, S. Pace, O. Werz, M. Nett,
ChemMedChem 12, 23-27 (2017).

Biosynthesis of Lipopeptide Siderophores

Unveiling hidden metabolic properties in bacteria of the genus *Variovorax*

Colette Kurth, Hirokazu Kage, Markus Nett

Almost all life forms depend on iron as an essential micronutrient that is needed for electron transport and metabolic processes. Siderophores are low-molecular-weight iron chelators that safeguard the supply of this important metal to bacteria, fungi and graminaceous plants. Although animals and the majority of plants do not utilize siderophores and have alternative means of iron acquisition, siderophores have found important medical and agricultural applications. In this project, we investigated the potential of different bacteria for the production of novel siderophores using a genome mining approach.

Siderophore biosynthesis involves the preparation of suitable ligand groups and their incorporation into a larger molecular scaffold that can accommodate a ferric ion. For this, the structural backbone must integrate defined spacer groups to support the creation of an octahedral binding site. The biosynthetic linkage of ligand and spacer groups involves amide or ester bond formations, which are often carried out by large, multifunctional enzyme complexes: The nonribosomal peptide synthetases (NRPS) exhibit a modular organization and follow an assembly-line logic, in which the arrangement of catalytic domains determines the sequence of enzymatic reactions. In consequence, the chemical structures of many siderophores can be predicted from an analysis of their biosynthesis enzymes or genes, respectively. This approach allows fermentation studies to be focused on strains that possess a high probability of producing new siderophores.
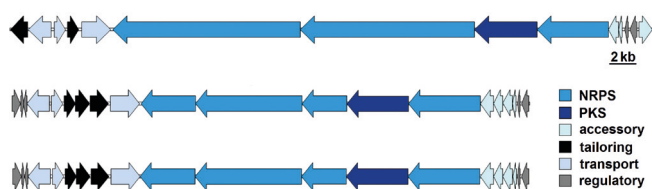

Figure 1: Siderophore biosynthesis gene clusters detected in the genomes of three *Variovorax* spp.

Analysis of the genomic sequences from soil-derived and plant-associated proteobacteria revealed that bacteria of the genus *Variovorax* possess unique siderophore biosynthesis pathways, featuring polyketide synthase (PKS) genes (Figure 1). To test the secretion of iron-chelating metabolites, five *Variovorax* strains available in our laboratory were grown under iron-limited conditions and subjected to the CAS assay, in which the presence of siderophores is detected by the decolorization of an iron-chrome azurol S complex. Extracts of all tested strains produced the distinctive color change from blue to red, thereby indicating the production of iron-chelating agents.
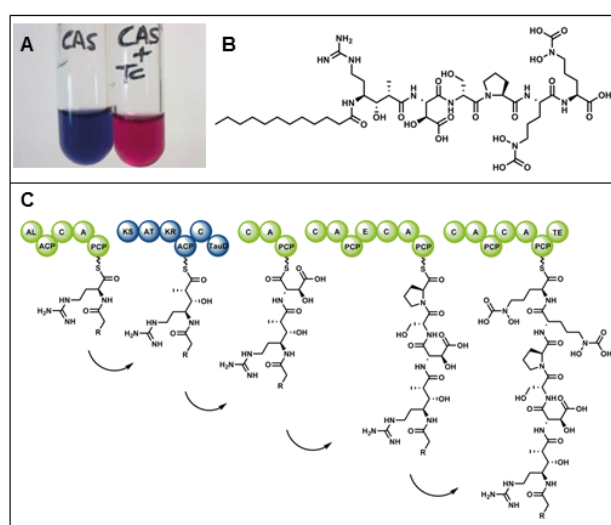
Figure 2: CAS assay in the absence and presence of a siderophore (A). Chemical structure (B) and proposed assembly-line biosynthesis (C) of the new siderophore variochelin A.

Variovorax boronicumulans BAM-48, which gave the strongest response in the CAS assay, was subsequently chosen for an in-depth chemical investigation. Exploiting the structure prediction from the bioinformatics analysis, a customized separation process for the purification of the siderophore could be devised. NMR and MS analyses confirmed the novelty of the retrieved molecule. Furthermore, a biosynthetic model was deduced (Figure 2).

Contact:
markus.nett@bci.tu-dortmund.de

Publications 2016 - 2014

2016

- S. Schieferdecker, S. König, S. Pace, O. Werz, M. Nett
  Myxochelin-inspired 5-lipoxygenase inhibitors: synthesis and biological evaluation
  ChemMedChem, doi: 10.1002/cmdc.201600536 (2016)

- D. Braga, D. Hoffmeister, M. Nett
  A non-canonical peptide synthetase adenylates 3-methyl-2-oxovaleric acid for auriculamide biosynthesis
  Beilstein Journal of Organic Chemistry 12, 2766-2770 (2016)

- E. Walther, S. Boldt, H. Kage, T. Lauterbach, K. Martin, M. Roth, C. Hertweck, A. Sauerbrei, M. Schmidtke, M. Nett
  Zincophorin – biosynthesis in *Streptomyces griseus* and antibiotic properties
  GMS Infectious Diseases 4, 08.20161128 (2016)

- I. Seccareccia, A. T. Kovacs, R. Gallegos-Monterrosa, M. Nett
  Unraveling the predator-prey relationship of *Cupriavidus necator* and Bacillus subtilis
  Microbiological Research 192, 231-238 (2016)

- C. Kurth, H. Kage, M. Nett
  Siderophores as molecular tools in medical and environmental applications
  Organic & Biomolecular Chemistry 14 (35), 8212-8227 (2016)

- D. Kalb, T. Heinekamp, S. Schieferdecker, M. Nett, A. A. Brakhage, D. Hoffmeister
  An iterative O-methyltransferase catalyzes 1,11-dimethylation of *Aspergillus fumigatus* fumaric acid amides
  ChemBioChem 17 (19), 1813-1817 (2016)

- J. Korp, M. S. Vela-Gurovic, M. Nett
  Antibiotics from predatory bacteria
  Beilstein Journal of Organic Chemistry 12, 594-607 (2016)

- A. M. Schaible, R. Filosa, V. Krauth, V. Temml, S. Pace, U. Garscha, S. Liening, C. Weinigel, S. Rummler, S. Schieferdecker, M. Nett, A. Peduto, S. Collarile, M. Scuotto, F. Roviezzo, G. Spaziano, M. de Rosa, H. Stuppner, D. Schuster, B. D'Agostino, O. Werz
  The 5-lipoxygenase inhibitor RF-22c potently suppresses leukotriene biosynthesis in cellulo and blocks bronchoconstriction and inflammation *in vivo*
  Biochemical Pharmacology 112, 60-71 (2016)

- D. Schwenk, P. Brandt, R. A. Blanchette, M. Nett, D. Hoffmeister
  Unexpected metabolic versatility in a combined fungal fomannoxin/vibralactone biosynthesis
  Journal of Natural Products 79 (5), 1407-1414 (2016)

- C. Kurth, S. Schieferdecker, K. Athanasopoulou, I. Seccareccia, M. Nett
  Variochelins, lipopeptide siderophores from *Variovorax boronicumulans* discovered by genome mining
  Journal of Natural Products 79 (4), 865-872 (2016)

- S. Schieferdecker, M. Nett
  A fast and efficient method for the preparation of the 5-lipoxygenase inhibitor myxochelin A
  Tetrahedron Letters 57 (12), 1359-1360 (2016)

2015

- H. Kage, E. Riva, J. S. Parascandolo, M. F. Kreutzer, M. Tosin, M. Nett
  Chemical chain termination resolves the timing of ketoreduction in a partially reducing iterative type I polyketide synthase
  Organic & Biomolecular Chemistry 13 (47), 11414-11417 (2015)

- J. S. Bauer, M. G. K. Ghequire, M. Nett, M. Josten, H.-G. Sahl, R. De Mot, H. Gross
  Biosynthetic origin of the antibiotic pseudopyronines A and B in *Pseudomonas putida* BW11M1
  ChemBioChem 16 (17), 2491-2497 (2015)

- J. Korp, S. König, S. Schieferdecker, H.-M. Dahse, G. M. König, O. Werz, M. Nett
  Harnessing enzymatic promiscuity in myxochelin biosynthesis for the production of 5-lipoxygenase inhibitors
  ChemBioChem 16 (17), 2445-2450 (2015)

- M. H. Medema, R. Kottmann, P. Yilmaz, ..., M. Nett, …, R. Breitling, E. Takano, F. O. Glöckner
  Minimum information about a biosynthetic gene cluster
  Nature Chemical Biology 11 (9), 625-631 (2015)

- I. Seccareccia, C. Kost, M. Nett
  Quantitative analysis of *Lysobacter* predation
  Applied and Environmental Microbiology 81 (20), 7098-7105 (2015)

- S. Schieferdecker, N. Domin, C. Hoffmeier, D. A. Bryant, M. Roth, M. Nett
  Structure and absolute configuration of auriculamide, a natural product from the predatory bacterium *Herpetosiphon aurantiacus*
  European Journal of Organic Chemistry (14), 3057-3062 (2015)

- E. C. Barnes, P. Bezerra-Gomes, M. Nett, C. Hertweck
  Dandamycin and chandrananimycin E, benzoxazines from *Streptomyces griseus*
  Journal of Antibiotics 68 (7), 463-468 (2015)

- S. Schieferdecker, S. König, A. Koeberle, H.-M. Dahse, O. Werz, M. Nett
  Myxochelins target human 5-lipoxygenase
  Journal of Natural Products 78 (2), 335-338 (2015)

2014

- D. Schwenk, M. Nett, H.-M. Dahse, U. Horn, R. A. Blanchette, D. Hoffmeister
  Injury-induced biosynthesis of methyl-branched polyene pigments in a white-rotting basidiomycete
  Journal of Natural Products 77 (12), 2658-2663 (2014)

- M. Nett
  Genome mining: concept and strategies for natural product discovery
  Progress in the Chemistry of Organic Natural Products 99, 199-245 (2014)

- S. Schieferdecker, S. König, C. Weigel, H.-M. Dahse, O. Werz, M. Nett
  Structure and biosynthetic assembly of gulmirecins, macrolide antibiotics from the predatory bacterium *Pyxidicoccus fallax*
  Chemistry – A European Journal 20 (48), 15933-15940 (2014)

- J. Pauly, M. Nett, D. Hoffmeister
  Ralfuranone is produced by an alternative aryl-substituted γ-lactone biosynthetic route in *Ralstonia solanacearum*
  Journal of Natural Products 77 (8), 1967-1971 (2014)

- S. Schieferdecker, T. Exner, H. Gross, M. Roth, M. Nett
  New myxothiazols from the predatory bacterium *Myxococcus fulvus*
  Journal of Antibiotics 67 (7), 519-525 (2014)

- C. Otzen, B. Bardl, I. D. Jacobsen, M. Nett, M. Brock
  ***Candida albicans* utilises a modified β-oxidation pathway for the degradation of toxic propionyl-CoA**
  Journal of Biological Chemistry 289 (12), 8151-8169 (2014)

- M. F. Kreutzer, H. Kage, J. Herrmann, J. Pauly, R. Hermenau, R. Müller, D. Hoffmeister, M. Nett
  Precursor-directed biosynthesis of micacocidin derivatives with activity against *Mycoplasma pneumoniae*
  Organic & Biomolecular Chemistry 12 (1), 113-118 (2014)

Patents

- F. Surup, H. Steinmetz, K. Mohr, K. Viehrig, R. Müller, M. Nett, S. Schieferdecker, H.-M. Dahse, M. Wolling, A. Kirschning
  Novel macrolide antibiotics *Pub. No.: WO/2016/005049 (2016)*

Technical Chemistry (TC)

A Hybrid Separation Approach for the Recovery of Homogeneous Transition Metal Catalysts

Jens M. Dreimann, Mirko Skiborowski, Andreas J. Vorholt, Andrzej Górak, Arno Behr

The application of homogeneous transition metal catalysts usually allows for mild reaction conditions and high selectivity. Difficult and insufficient recovery of these catalysts may hinder their application in chemical production processes. Thermomorphic solvent systems and the organic solvent nanofiltration are separation techniques which are promising for efficient catalyst recovery. So-called hybrid catalyst separation can even increase the recovery of these catalysts.

Homogeneous transition metal catalysts (TMC) allow for mild reaction conditions as well as high selectivity, but separation and recycling of these can be difficult. One method for efficient combination of reaction and catalyst recovery is the application of thermomorphic solvent systems (TMS), which consist of two solvents having a highly temperature dependent miscibility gap. With this, a homogeneous reaction mixture is present at elevated temperature and two phases are present at low temperature. Additionally, reactants and products need to be present in one solvent and the transition metal catalyst in the other.

Another approach for the recovery of TMCs is application of organic solvent nanofiltration (OSN) membranes. While solvent, reactants and products pass the membrane the TMC is rejected and recycling to the reactor can be achieved. Mild separation conditions and low energy demand of this separation technology is beneficial.

However, even the loss of small amounts of the TMC is crucial for the development of industrial production processes. The combination of two different separation techniques in a hybrid separation process to outperform single stage catalyst recovery can increase the efficiency of the recovery of TMCs. We investigated the combination of TMS and OSN in a continuously operated miniplant process for the hydroformylation of 1-dodecene using a Rh/Biphephos-catalyst (Figure 1).
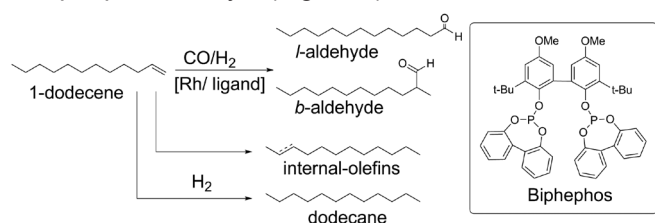

Figure 1: Hydroformylation and side reactions of 1-dodecene and structure of the Biphephos ligand.

The substrate 1-dodecene was hydroformylated in the miniplant process presented in figure 2. This process consists of a continuously stirred tank reactor, a decanter for the separation of the two liquid phases of the TMS system and an OSN-unit (membrane unit and hold-up).
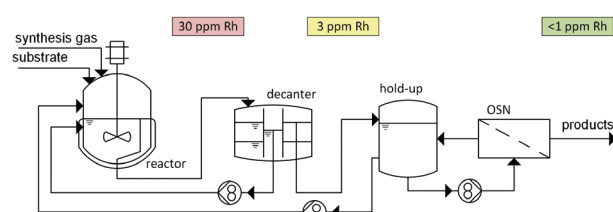

Figure 2: Process flowsheet.

With this setup the catalyst loading of the reaction mixture was reduced in a first stage from 30 ppm rhodium to 3 ppm rhodium in the product stream using the TMS approach. In the second stage the catalyst loading of the product stream was reduced below 1 ppm. Preserving excellent catalyst recovery the process was operated continuously for 50 h as shown in figure 3 at maximum yields of the linear aldehyde of 70% and excellent *l/b*-ratio of 99/1.
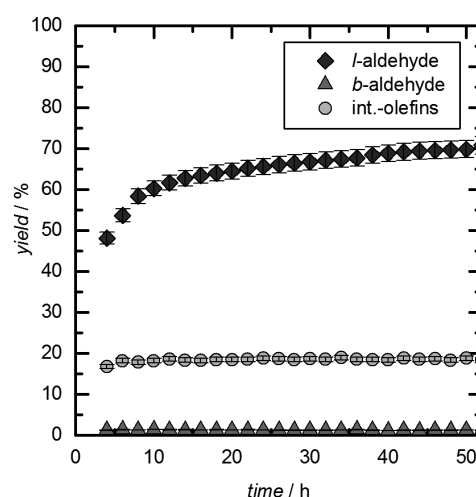
Figure 3: Yields of the hydroformylation reaction of 1-dodecene obtained in continuous miniplant operation.

In summary, highly efficient catalyst recovery was achieved in a hybrid separation process combining a thermomorphic solvent system and organic solvent nanofiltration. In further investigations steady state operation is desired.

Contact:
jens.dreimann@bci.tu-dortmund.de
andreas.vorholt@bci.tu-dortmund.de
arno.behr@bci.tu-dortmund.de

Terpene Derived Surfactants – The Hydroaminomethylation of β-Myrcene

Thiemo A. Faßbach, Tom Gaide, Michael Terhorst, Arno Behr, Andreas J. Vorholt

A catalytic system was developed to enable the use of industrially-available terpenes in hydroaminomethylation to obtain renewable building blocks for surfactants in two steps. This homogeneously, tandem-catalyzed reaction includes both a hydroformylation and an enamine condensation, followed by a hydrogenation. The terpene-derived amines obtained were further functionalized to quaternary ammonium compounds (quats), which are widely used as surfactants. The synthesized products show surface active activity that is quite similar to that of industrially available compounds.

The term hydroaminomethylation refers to a tandem catalyzed reaction, incorporating the hydroformylation of an olefin to an aldehyde, followed by an enamine condensation and a subsequent hydrogenation. If a 1,3-diene, like β-myrcene, is employed as olefin, the reaction sequence is as depicted in Figure 1.
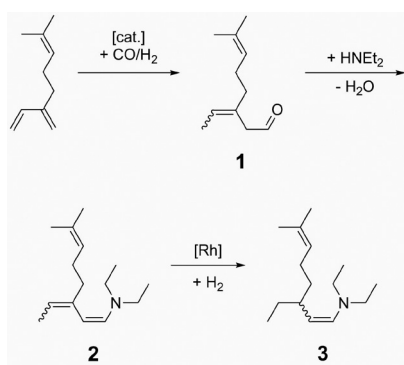

Figure 1: The hydroaminomethylation of β-myrcene with diethylamine.

Preliminary studies showed that the use of the catalytic system $[Rh(cod)Cl]_2$/dppe (= diphenylphosphinoethane) is capable of a fast and highly selective hydroformylation, yielding the unsaturated aldehyde **1**. Subsequent reductive amination proceeds by the hydrogenation of the diene-amine **2** to finally yield the enamine **3**.
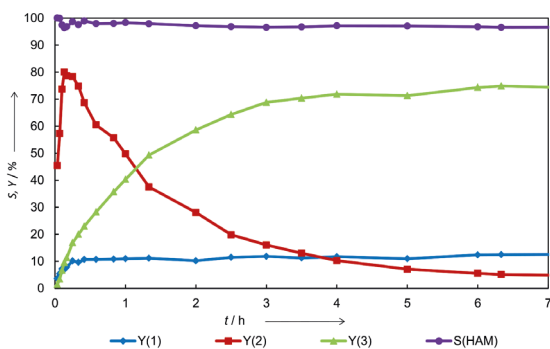

Figure 2: Yield-time-plot of the hydroaminomethylation of myrcene with diethylamine. *Reaction conditions:* Precursor: $[Rh(cod)Cl]_2$, 1 mol% Rh based on myrcene; ligand: DPPE, M/P = 1/5; $n_{myrcene}$ = 75 mmol, n_{amine} = 300 mmol, $m_{toluene+amine}$ = 107 g, p_{CO}/p_{H2} = 1/4; p_{syngas} = 40 bar, T = 140°C, 600 rpm, after 40 min. the reactor was pressurized with 40 bar H_2, S(HAM) = (Y(**1**)+Y(**2**)+Y(**3**))/X(myrcene)), results determined by GC-FID.

surprisingly fast, leading to a complete conversion of myrcene already after 8 minutes. Furthermore, the regio isomer **1**, shown in Figure 1 is formed almost exclusively (S > 97%). The hydrogenation of the formed diene-amine **2** to the enamine **3** yields 70% after a total reaction time of 3 h. The reaction was developed well for the model substrates myrcene and diethylamine. In order to establish a general procedure to obtain surfactant building blocks from terpenes, the sesquiterpene farnesene was also employed. Furthermore the use of dimethylamine as the nucleophile leads to a more polar head of the resulting surfactant. All combinations of the substrates mentioned were employed successfully in the hydroaminomethylation and subsequent hydrogenation and methylation led to the surfactants aimed for (Figure 3).

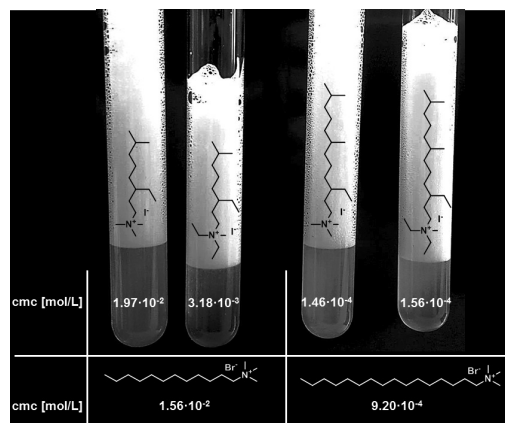Figure 3: CMCs of the surfactants derived from the hydroaminomethylation of β-myrcene and β-farnesene with diethylamine and dimethylamine.

The CMCs of the derived quats are well aligned with the ones of long known cationic surfactants. Thus, the hydroaminomethylation of terpenes is a valuable contribution to the green synthesis of cationic surfactants.

Contact:
thiemo.fassbach@bci.tu-dortmund.de
arno.behr@bci.tu-dortmund.de

Tertiary Amines as Ligands in a Four-Step Tandem Reaction of Hydroformylation and Hydrogenation: an Alternative Route to Industrial Diol Monomers

Sarah Fuchs, Dominik Lichte, Morten Dittmar, Arno Behr and Andreas J. Vorholt

A highly selective synthesis of diols is presented via simple auto-tandem catalysis to connect hydroformylation and hydrogenation reactions by a rhodium-catalyst and tertiary amines as ligands. This system allows the hydroformylation/hydrogenation of non-conjugated cyclic olefins to selectively provide diols under mild reaction conditions. As model substrate, the industrial relevant dicyclopentadiene (dcpd) was chosen.

TCD-diol **6**, also known as tricyclodecanedimethanol, is of high industrial interest as an additive in adhesives, sealants, plasticizers, high ester lubricating oils, perfume compositions and acid sterilization-resistant polyester coatings. We describe the optimisation of the hydroformylation/hydrogenation sequence toward high activities and chemoselectivities for the hydrogenation of aldehydes to alcohols using dcpd **1** (figure 1).
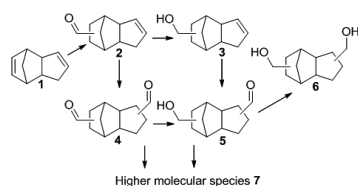

Figure 1: Industrial approach from dcpd 1 to TCD-diol 6 vs new route.

With a rhodium-precursor in combination with tertiary amines as ligands, possible undesired side reactions in hydroformylation such as olefin hydrogenation and aldol addition sought to be reduced. Different rhodium catalysts and amines as ligands were investigated and all showed hydrogenation activity (table 1).

Table 1: Variation of different ligands.

Entry	ligand	Yield [%]					
		Y_2	Y_3	Y_4	Y_5	Y_6	Y_7
1.1	Et$_3$N	0	5	0	1	51	43
1.2	-	8	0	32	0	0	60
1.3[a,b]	PPh$_3$	4	0	68	0	0	28
1.4[a]	Et$_3$N + PPh$_3$	14	0	41	0	0	45
1.5[b]	Et$_3$N	0	1	0	0	79	20

Reaction conditions: 1 mmol dcpd **1**, 0.5 mol % [Rh(octanoate)$_2$]$_2$, 3 mmol Et$_3$N, 5 mL toluene, t = 4 h, T = 120°C, p = 60 bar CO/H$_2$ (1:1), 450 rpm. [a] Rh:P 1:10 P = PPh$_3$, [b] = 70 bar CO/H$_2$. Yield (Y) is given as sum of the isomers and reported in % determined with dibutylether as internal standard based on GC–FID analysis.

The best rhodium-amine catalytic reaction system (entry 1.5) was revealed to be [Rh(octanoate)$_2$]$_2$ and triethylamine obtaining 79% TCD-diol 6 within 4 h under mild reaction conditions.

To obtain a better understanding of the reaction network, the reaction progress was examined over 16 hours (figure 2). The time/yield plot shows that the first hydroformylation step, forming TCD monoaldehyde 2 and subsequent hydrogenation to the TCD-monool 3 occurred prior to the second hydroformylation giving rise to the intermediate TCD-monoalcohol-monoaldehyde 5. Which was then hydrogenated resulting in TCD-diol 6.
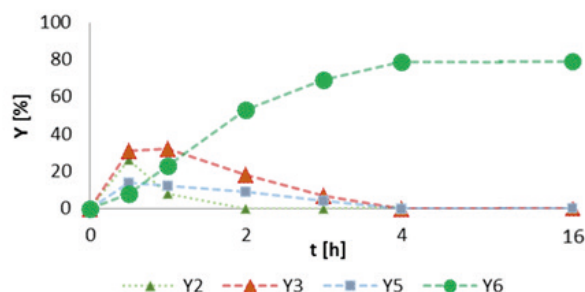
Figure 2: Reaction progress over time.

Reaction conditions: 1 mmol dcpd **1**, 0.5 mol% [Rh(octanoate)$_2$]$_2$, 3 mmol Et$_3$N, 5 mL toluene, t = 4 h, T = 120°C, p = 70 bar CO:H$_2$ (1:1), 450 rpm. Yield (Y) is given as sum of the isomers and reported in % determined with dibutylether as internal standard based on GC FID analysis.

The scope of the reaction was evaluated and the optimised reaction conditions were successfully scaled up to a 2 L reactor. Finally, the Rh/amine catalyst complex was recycled by a simple water extraction of the diol-product.

Contact:
sarah.fuchs@bci.tu-dortmund.de
andreas.vorholt@bci.tu-dortmund.de

Isomerization/Hydroformylation Tandem Reaction of a Decene Isomeric Mixture with Subsequent Catalyst Recycling in Thermomorphic Solvent Systems

Tom Gaide, Andreas Jörke, Kim E. Schlipköter, Christof Hamel, Andreas Seidel-Morgenstern, Arno Behr, Andreas J. Vorholt

Herein we report about an efficient isomerization / hydroformylation tandem reaction to convert a technical mixture of decene isomers selectively into the linear undecanal in a thermomorphic solvent system. By applying a rhodium / BIPHEPHOS catalyst a high turnover frequency of 375h^{-1} and a high regioselectivity of 92% for the linear product are achieved. Yields up to 70% of the linear aldehyde are obtained. The catalyst can be successfully separated from the product using a thermomorphic solvent system of dimethyl formamide (catalyst phase) and dodecane (product phase). The leaching of the rhodium (0.6% of the initial amount) and phosphorus (1.2% of the initial amount) is very low. The catalyst was successfully recycled five times.

The hydroformylation is the most important reaction for the homogeneously catalyzed synthesis of linear aldehydes, which are intermediates of high interest in the chemical industry (e.g. in the synthesis of surfactants, plasticizers or perfumes). Essentially, linear as well as branched aldehydes can be synthesized from a terminal double bond. The hydroformylation of internal double bonds leads to the formation of branched aldehydes. Often the linear aldehydes are of particular interest in technical chemistry. Unfortunately, technical grade olefin feedstocks are often complex mixtures of different olefin isomers, predominately internal olefins. In order to convert these mixtures into linear aldehydes a tandem reaction sequence of double bond isomerization and highly *n*-selective hydroformylation is necessary. Catalysts, which are able to catalyze this tandem reaction in an efficient manner, are expensive rhodium complexes with tailored ligands. Therefore, an efficient catalyst recycling is necessary in view of a technical application.

A promising catalyst recycling approach is the use of thermomorphic multicomponent solvent (TMS) systems. The TMS concept takes advantage of the temperature dependent miscibility gap of a polar and a non-polar solvent. The reaction mixture is homogeneous at reaction temperature, so there are no mass transport limitations during the reaction. Cooling down after reaction leads to formation of a polar, catalyst containing phase and a non-polar product phase.

Herein, we present the development of the tandem isomerization / hydroformylation of a technical grade mixture of internal decene isomers (figure 1) in a TMS system consisting of DMF (catalyst solvent) and dodecane (product solvent) (w50/50) with subsequent catalyst recycling.

Application of a rhodium / biphephos catalyst leads to 70% of the desired linear aldehyde after 3 h. Low catalyst leaching values are achieved by use of the TMS system. Only 0.6% of the rhodium and 1.2% of the ligand leached into the product phase. The catalyst was successfully recycled five times, demonstrating the applicability of the developed system.
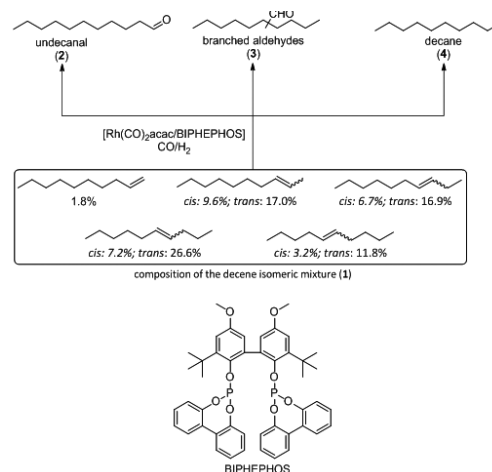

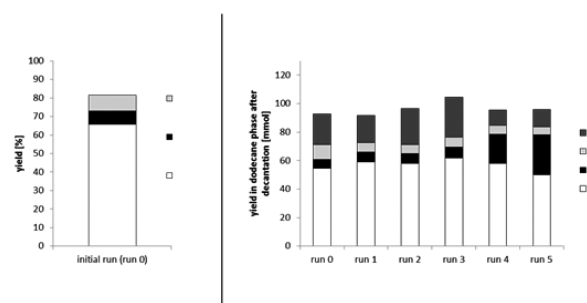Figure 1: Isomerization / hydroformylation of decene isomers.

Figure 2: Results of the reaction and catalyst recycling.

Conditions: 0.2 mol% Rh(CO)2acac, 0.8 mol% BIPHEPHOS, 50 mL DMF, 50 mL dodecane, 150 mmol **1**, 15 bar syngas, T= 135 °C, reaction time = 3h.

Contact:
andreas.vorholt@bci.tu-dortmund.de
tom.gaide@bci.tu-dortmund.de
arno.behr@bci.tu-dortmund.de

Conversion of Carbon Dioxide to *N,N*-Dimethylformamide in Miniplant Scale

Process development for the carbon dioxide based continuous synthesis of formamides

René Kuhlmann, Anna Prüllage, Manuel Nowotny, Arno Behr

The catalytic hydrogenation of carbon dioxide is a promising option to form methanol, formic acid or formamides. Especially formamides are popular solvents for the syntheses of polymers or are used as intermediates in organic fine chemistry. Our investigations in a continuously operated miniplant showed that a synthesis of N,N-dimethylformamide (DMF) with a recycling of the homogeneous ruthenium catalyst is feasible. While the formed product DMF was extracted in-situ into an aqueous phase, the catalyst stayed in the nonpolar alcoholic phase consisting of 2-ethylhexanol.

The utilization of carbon dioxide as C_1-building block for valuable chemicals is an attractive alternative to common carbon sources. Due to its abundancy and high concentrations in flue gas, carbon dioxide can be obtained with low costs. Since CO_2 is non-toxic and non-flammable it turns out to be an attractive green chemical. One potential application is the utilization as surrogate for toxic carbon monoxide in industrial applications, e. g. the synthesis of formamides. Formamides are yet produced via the carbonylation of amines, since no economical carbon dioxide based processes have been developed so far.

The synthesis of formamides via CO_2 involves the homogeneous catalyzed hydrogenation of carbon dioxide (Figure 1).
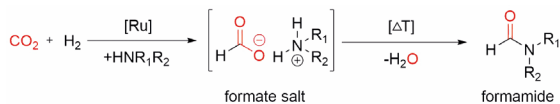

Figure 1: Synthesis of formamides from CO_2.

Even though the reaction itself is well studied, the integration into a continuously operated process remains a challenge. While formamides are in general excellent solvents for many components, the homogeneous catalyst has still to be separated from these products.
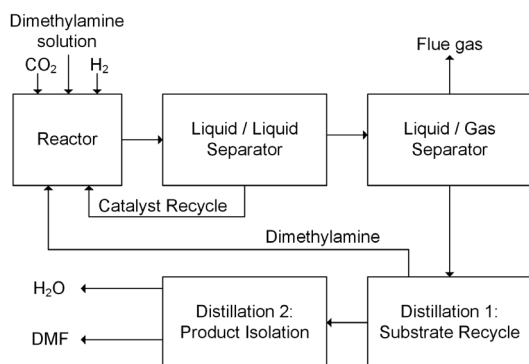
Figure 2: Simplified flow-sheet of the continuously operated miniplant.

Our investigations show that a catalyst for the synthesis of *N,N*-dimethylformamide (DMF) can easily be recycled by a liquid-liquid multiphase system, containing the nonpolar alcohol 2-ethylhexanol as catalyst solvent and an aqueous phase as product extraction agent (Figure 2).

Investigations were made in the miniplant in order to demonstrate the long-term stability and activity of the developed reaction system (Figure 3).
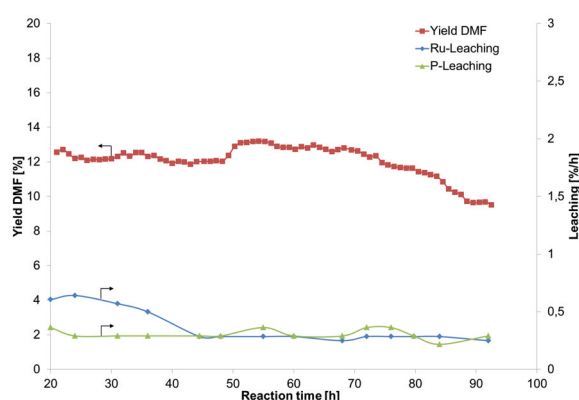
Figure 3: Influence of the reaction temperature on the process stability. Reaction conditions: 2.5 mmol/l $RuCl_3$, 2.0 mmol/l BISBI, τ = 3.15 h, $p_{CO2/H2}$ = 20/20 bar, $V_{2-ethylhexanol}$ = $V_{dimethylamine-solution}$ = 0.8 ml/min, V_{liquid} = 310 ml.

The process showed a stable operation over at least 90 hours. An increase of the reaction temperature resulted in a slightly higher reactivity but did not influence the catalyst leaching at all. Besides the intermediate formate no other byproducts were observed.

Contact:
rene.kuhlmann@bci.tu-dortmund.de
arno.behr@bci.tu-dortmund.de

Preparation of a Synthetic Polyester in a Resource Efficient Manner by Means of Carbonylative Tandem Reactions

Bis-Hydroaminomethylation of Renewable Resources under Sustainable and Holistic Process Contemplation from Oleochemicals to a Polymer

Thomas Seidensticker, Hanna Busch, Christopher Diederichs, Jork Jonas von Dincklage, Andreas J. Vorholt

Resource-efficient bis-hydroaminomethylation of the castor oil derived renewables methyl 10-undecenoate and 10-undecene-1-ol with piperazine furnished linear, bifunctional molecules. A structured and sustainable path towards a novel polyester from these monomers was developed. Key to success was the selective crystallization of the linear product directly from the crude reaction mixture in >98% purity. Additionally, with this methodology, the homogeneous Rh catalyst was retained in the supernatant and was successfully recycled. Finally, polycondensation yielded a novel piperazine-linked polyester.

Oleo chemicals are very attractive substrates for polymer applications. This is due to their broad availability, comparably low price, easy processing and their general chemical structure consisting of a long linear alkyl chain and an additional functional group. Furthermore, a major part of these substrates is unsaturated and offers potential for further functionalization.

In this regard, methyl 10-undecenoate (**1**) and 10-undecen-1-ol (**2**) are very interesting owing to their terminal double bond. Both are accessible from cracking castor oil derived methyl ricinoleate (Scheme 1).
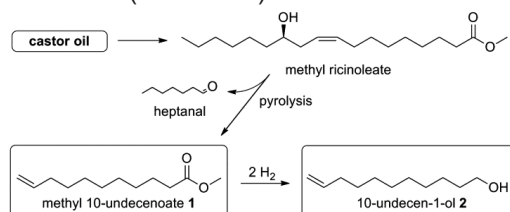

Figure 1: Methyl 10-undecenoate (**1**) and 10-undecene-1-ol (**2**) as renewable terminal unsaturated compounds from castor oil.

1 and **2** were successfully transformed within a rhodium-catalyzed auto-tandem *bis*-hydroaminomethylation into linear bifunctional molecules in a resource-efficient fashion (linear diester **3** and linear diol **4**, Scheme 2). *Bis*-HAM consisted of initial Rh-catalyzed hydroformylation to form the intermediate linear aldehyde, which *in situ* underwent rhodium-catalyzed reductive amination at both nitrogen atoms of the diamine piperazine.

An integrated and sustainable isolation procedure for the monomers from the crude, toluene-containing mixture was attempted in order to provide a high-purity monomer and selectively retaining the precious rhodium catalyst in the liquid phase for recycling purposes. Precipitation from the reaction solvent was generally observed upon workup, and hence, a temperature-regulated, selective crystallization seemed a promising isolation approach to meet the aforementioned desires.
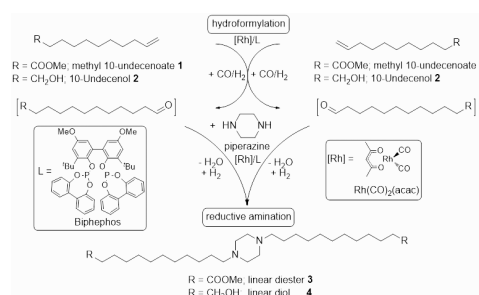
Figure 2: *Bis*-hydroaminomethylation of **1** and **2** for the synthesis of **3** and **4**, respectively.

88% of the linear diester **3** were successfully crystallized directly from the crude reaction mixture with an initial purity of 98% *via* this innovative approach.

The rhodium catalyst system retained in the liquid phase and showed catalytic activity in additional recycling runs after the reaction mixture has been replenished with fresh substrate.

Finally, the corresponding, novel piperazine-linked polyester was synthesized and showed molecular weights (M_n) of typically 2.4×10^4 g mol^{-1} (Mw/Mn ≈ 2.6), which was confirmed by analysis of the end group by ^{1}H-NMR spectroscopy.

In conclusion, a novel and holistic path from oleo chemicals to novel polymers has been developed under consideration of sustainability aspects such as atom-economy and catalyst recycling.

Contact:
andreas.vorholt@bci.tu-dortmund.de

A General and Efficient Method for the Palladium-Catalyzed Conversion of Allylic Alcohols into their Corresponding Dienes

Development of a Highly Selective Palladium Catalyst System for the Dehydration of Allylic Alcohols into Dienes

Dennis Vogelsang, Karoline A. Ostrowski, Andreas J. Vorholt

A general method was established, converting a broad range of allylic alcohols directly and quantitatively into their corresponding dienes. The developed protocol allows the direct use of allylic alcohols, circumventing the need for their derivatization into more reactive precursors, thereby minimizing waste production with water as the sole co-product.

Conjugated dienes frequently serve as substrates for conversion into highly functionalized molecules *via* numerous organic reactions, e.g. Diels-Alder, telomerisation, hydroformylation and carbonylation reactions. Furthermore, dienes and allylic compounds can be found in natural products, e.g. terpenes, which make them attractive as both substrates and products.

Herein, we present the development of a palladium catalyzed reaction to convert allylic alcohols quantitatively into their corresponding dienes (Figure 1).
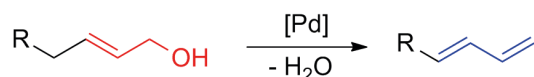

Figure 1: Elimination reaction of water from an allylic compound yielding a conjugated diene.

Based on the model reaction, the palladium catalyzed dehydratization of 2,7-octadienol into octatriene, which has been observed in preliminary studies, the essential reaction conditions for a quantitative conversion were successively determined (Table 1).

Table 1: Model elimination reaction for determining the optimum conditions.

Entry	Cat.	Lig.	TFA	MeOH	CO	Y
2.1	+	+	+	+	+	>99
2.2	+	+	+	+	-	0
2.3	+	+	+	-	+	>99
2.4[a]	+	+	+	-	+	>99
2.5[b]	+	+	+	-	+	>99
2.6[c]	+	+	+	-	+	77
2.7	+	+	-	+	+	0
2.8	+	+	-	-	+	0
2.9[d]	+	+	+	-	-	83
2.10[d]	-	+	+	-	-	0

Cond.: 2 mmol, 10 mol% trifluoric acetic acid (TFA), cat.:1 mol% Pd(acac)$_2$, Lig.: 1.1 mol% Xantphos, 1.2 eq MeOH, 40 bar CO, 2.5 ml toluene, T = 105 °C, t = 18 h, 500 rpm, reaction performed in a 20 mL autoclave, results in %; the presence/addition of a compound is marked as "+" and the absence is marked as "-", [a] t = 3 h. [b] reaction was performed with 10 bar CO in a pressure tube, [c] 5 times flushed with CO, reaction under CO atmosphere, [d] with 1 mol% Ru$_3$CO$_{12}$ as CO source, which was performed in a glass flask.

For a highly selective conversion of the 2,7-octadienol into the corresponding octatriene with yields higher than 99%, a catalytic system consisting of palladium acetylacetonate, Xantphos as ligand and trifluoric acetic acid under a carbon monoxide atmosphere is required.

In Table 2 the wide application of the developed catalytic system is shown, which tolerates several kinds of allylic alcohols.

Table 2: Substrate scope.

Entry	Substrate	Product[b]	Y$_{product}$[c]
3.1			85[a]
3.2			>99
3.3			>99
3.4			96
3.5			>99
3.6			>99
3.7			>99
3.8			>99
3.9			98

Cond.: 2 mmol substrate, 10 mol% TFA, 1 mol% Pd(acac)$_2$, 1.1 mol% Xantphos, 40 bar CO, 2.5 ml toluene, T = 105 °C, t = 18 h, 500 rpm, reaction performed in a 20 mL autoclave, results in %; [a] yield of the product butadiene was determined via the conversion of crotyl alcohol; [b] major isomers are displayed; [c] yield including all isomers.

A broad range of allylic alcohols could be succesfully converted into their corresponding dienes by application of the developed palladium catalyst system, exceptional allylic alcohols with substituents in position R^3. Probably, this additional group is hindering the formation of the η^3-palladium complex, which is a crucial intermediate in the mechanism.

By usage of Ru$_3$CO$_{12}$ as an alternative CO resource, this reaction can be carried out in commercial glassware and the gap between technical autoclave chemistry and organic laboratories can be closed.

Contact:
dennis.vogelsang@bci.tu-dortmund.de
andreas.vorholt@bci.tu dortmund.de

Utilising Innovative Reactor Types to Accelerate Multiphasic Homogenous Reactions

Helge Warmeling, Marco-Tobias Bürger, Arno Behr, Andreas J. Vorholt

The biphasic aqueous hydroformylation of the long chain olefin 1-octene is taken as model for a multiphase and non-mass-transfer-limited reaction. In this work it was shown that it can be accelerated by the creation of large interfacial areas between the substrate phase and the catalyst phase. The increase in reaction rate is most probably induced due to the elevated substrate concentration in the mixing zone of the surface compared to the bulk of the catalyst phase. To exploit this effect the innovative jet loop reactor, which is known to create large interfacial areas, was applied and compared to a standard stirred tank reactor.

The biphasic aqueous hydroformylation is a homogenously catalysed reaction in which an alkene (e.g. 1-octene) is converted under syngas pressure to form linear and branched aldehydes as shown in equation (1). With an annual production of >10 mio t this reaction is of industrial relevance. To enable an efficient recycling of the homogenous rhodium catalyst it is immobilized in an aqueous catalyst phase by application of water soluble phosphine salts. Until now the biphasic reaction system was considered to slow for alkenes longer than pentene due to the decreasing solubility of the substrate in water.
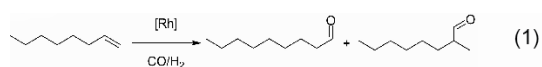
To overcome this limitation severall studies have been published in the literature, mostly focusing heavily on the application of chemical additives to increase substrate solubility. To avoid the downcomes of the use of additives like complicated downstreaming, high costs or increased catalyst leaching we focused on a strictly procedural approach. Additionally the investigation was carried out incorporating principles of green chemistry in order to develop a sustainable process for long chain hydroformylation.

In a first step the reaction was carried out in standard stirred tank reactors on laboratory and miniplant scale with different stirrer types (Figure 1) and energy inputs. The goal of the experiments was to increase the interfacial area between substrate and catalyst phase by intensifying the applied mixing technique [1].
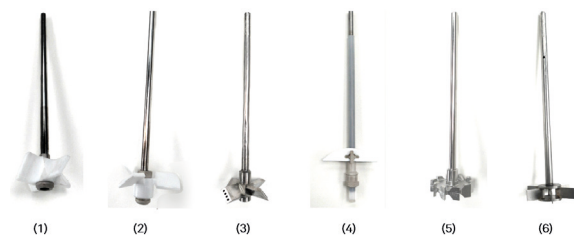
Figure 1: Different stirrer types applied to intensify the mixing.

It was shown that the rate of reaction was linearly dependent (Fig 3, blue) on the interfacial area, most likely due to the elevated substrate concentration in the film volume compared to the bulk of the catalyst phase.

To benefit from these interesting results the reaction was transferred to a jet loop reactor. This reactor type is well known for its ability to create large interfacial areas between all three applied phases (l/l/g) [2]. Herein a part of the reaction media is taken out of the reactor and is reinjected through a nozzle at the reactor head creating fine dispersions through the shear stress (reactor schemes in Figure 2).
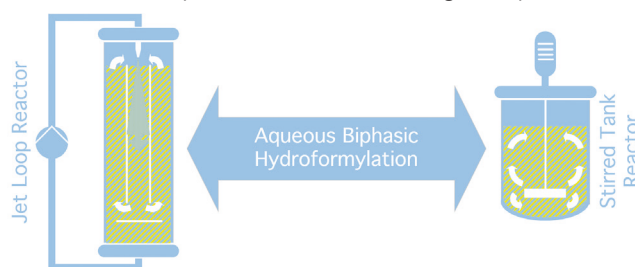
Figure 2: Compared reactor types, Jet loop reactor (JLR, left) and stirred tank reactor (STR, right).

The rate of reaction in the jet loop was compared to the results obtained with the stirred tank reactor as shown in Figure 3. In the JLR reactor the turn over frequency was more than doubled with 3225 h^{-1} compared to the stirred tank with 1370 h^{-1}.
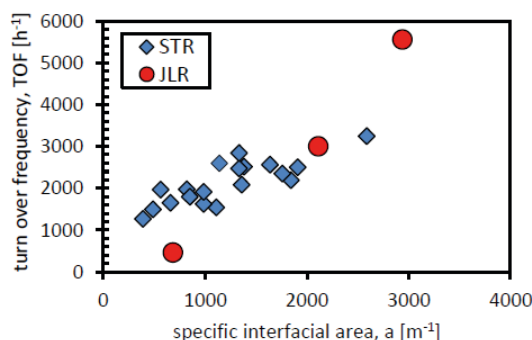
Figure 3: Turnover frequency (mol product per mol catalyst and time) of the aqueous biphasic rhodium catalyzed hydroformylation of 1-octene in a jet loop reactor compared to a stirred tank reactor.

Contact:
helge.warmeling@tu-dortmund.de
andreas.vorholt@tu-dortmund.de

Publications 2016 - 2014

2016

- A. Kämper, P. Kucmierczyk, T. Seidensticker, A.J. Vorholt, R. Franke, A. Behr
  Ruthenium-Catalyzed Hydroformylation: From Laboratory to Continuous Miniplant Scale
  Catal. Sci. Technol., 2016, 6, 8072-8079, DOI: 10.1039/C6CY01374K

- J. M. Dreimann, M. Skiborowksi, A. Behr, A.J. Vorholt
  Recycling homogeneous catalysts simply via organic solvent nanofiltration: New ways to efficient catalysis
  ChemCatChem, 2016, 8 (21), 3330-3333, DOI: 10.1002/cctc.201601018

- A.J. Vorholt, S. Immohr, K.A. Ostrowski, S. Fuchs, A. Behr
  Catalyst Recycling in the Hydroaminomethylation of Methyl Oleate: A Route to Novel Polyamide Monomers
  Eur. J. Lipid Sci. Technol., 2016, accepted, DOI: 10.1002/ejlt.201600211

- T. Seidensticker, H. Busch, C. Diederichs, J.J. von Dincklage, A.J. Vorholt
  From Oleo Chemicals to Polymer: Bis-Hydroaminomethylation as a Tool for the Preparation of a Synthetic Polymer from Renewables
 *Chemcatchem, 2016, 8 (18), 2890-2893, DOI: 10.1002/cctc.201600629*

- J.M. Dreimann, H. Warmeling, J.N. Weimann, K. Künnemann, A. Behr, A.J. Vorholt
  Increasing selectivity of the hydroformylation in a miniplant catalyst, solvent and olefin recycle in two loops
  AIChE J., 2016, DOI: 10.1002/aic.15345

- T. Färber, O. Riechert, T. Zeiner, G. Sadowski, A. Behr, A.J. Vorholt
  Homogeneously Catalyzed Hydroamination in a Taylor-Couette Reactor using a Thermormorphic Multicomponent Solvent System
  Chem. Eng. Res. Des., 2016, 112, 263–273; DOI: 10.1016/j.cherd.2016.06.022

- J. Dreimann, A.J. Vorholt, M. Skiborowski, A. Behr
  Removal of homogeneous precious metal catalysts via organic solvent nanofiltration, Chemical Engineering Transactions
  Chem. Eng. Trans., 2016, 47, 343-348; DOI:10.3303/CET1647058

- T. A. Faßbach, R. Kirchmann, A. Behr, St. Romanski, D. Leinweber, A.J. Vorholt
  Telomerization of 1,3-Butadiene with highly substituted Alcohols Using Pd/NHC-Catalysts − Structure-Reactivity-Relationship of the O-Nucleophile
  J. Mol. Catal. A: Chem. 2016, accepted; DOI:10.1016/j.molcata.2016.05.002

- H. Warmeling, A. Behr, A.J. Vorholt
  Jet loop reactors as a versatile reactor set up - Intensifying catalytic reactions: A review
  Chem. Eng. Sci., 2016, 149, 229–248; DOI:10.1016/j.ces.2016.04.032

- P. Neubert, I. Meier, T. Gaide, A. Behr
  Additive-Free Palladium-Catalysed Hydroamination of Piperylene with Morpholine
  Synthesis 48 (2016), A-G

- A. Behr, L. Johnen, A. Wintzer, A. G. Cetin, P. Neubert, L. Domke
  Ruthenium-Catalyzed Cross Metathesis of β-Myrcene and its Derivatives with Methyl Acrylate
  ChemCatChem 8 (2016), 515-522

- A. Kämper, S.J. Warrelmann, K. Reiswich, R. Kuhlmann, R. Franke, A. Behr
  First iridium-catalyzed hydroformylation in a continuously operated miniplant
  Chem. Eng. Sci. 144 (2016), 364-371

- P. Neubert, I. Meier, T. Gaide, R. Kuhlmann, A. Behr
  First telomerisation of piperylene with morpholine using palladium-carbene catalysts
  Catalysis Comm. 77 (2016), 70-74

- J. Haßelberg, A. Behr, C. Weiser, J.B. Bially, I. Sinev
  Process development for the synthesis of saturated branched fatty derivatives: Combination of homogeneous and heterogeneous catalysis in miniplant scale
  Chem. Eng. Sci. 143 (2016), 256-269

- J. Haßelberg, A. Behr
  Saturated branched fatty compounds Proven industrial processes and new alternatives
  Eur. J. Lipid Sci. Technol. 118 (2016) 36-46

- A. Behr, Z. Bayrak, G. Samli, D. Yildiz, S. Peitz, G. Stochniol
  Oligomerization of n-butenes in a two phase reaction system with homogeneous Ni/Al-catalysts
  Chem. Eng. Technol. 39 (2016), 263-270

- M. Zagajewski, J. Dreimann, M. Thönes, A. Behr
  Rhodium catalyzed hydroformylation of 1-dodecene using an advanced solvent system: Towards highly efficient catalyst recycling
  Chem. Eng Process. 99 (2016), 115-123

- K. A. Ostrowski, D. Vogelsang, A.J. Vorholt
  A general and efficient method for the palladium-catalysed conversion of allylic alcohols into their corresponding dienes
  Catal. Sci. Technol., 2016, accepted. DOI: 10.1039/C5CY02096D

- T. Gaide, J. Dreimann, A. Behr, A.J. Vorholt
  Overcoming Phase-Transfer Limitations in the Conversion of Lipophilic Oleo Compounds in Aqueous Media-A Thermomorphic Approach
  Angew. Chem. Int. Ed., 2016, 55, 2924–2928, DOI: 10.1002/anie.201510738

- T. Seidensticker, J. M. Vosberg, K. A. Ostrowski, A.J. Vorholt
  Rhodium-Catalyzed Bis-Hydroaminomethylation of Linear Aliphatic Alkenes with Piperazine
  Adv. Synth. Catal., 2016, 358, 610–621, DOI: 10.1002/adsc.201500896

- K. A. Ostrowski, D. Vogelsang, T. Seidensticker, A.J. Vorholt
  Direct Synthesis of an α,ω-Diester from 2,7-Octadienol as Bulk Feedstock in Three Tandem Catalytic Steps
  Chem. Eur. J. 2016, 22, 1840-1846. DOI: 10.1002/chem.201503785

- T. Seidensticker, D. Möller, A.J. Vorholt
  Merger of Johnson–Claisen rearrangement and alkoxycarbonylation for atom efficient diester synthesis
  Tetrahedron Lett., 2016, 57, 371-374. DOI: 10.1016/j.tetlet.2015.12.032

- K. A. Ostrowski, D. Lichte, M. Stuck, A.J. Vorholt
  A comprehensive investigation and optimisation on the proteinogenic amino acid catalysed homo aldol condensation
  Tetrahedron, 2016, 72, 592-598. DOI: 10.1016/j.tet.2015.11.069

- T. Gaide, A. Behr, M. Terhorst, A. Arns, F. Benski, A.J. Vorholt
  Katalysatorvergleich bei der Hydroesterifizierung von 10-Undecensäuremethylester in thermomorphen Lösungsmittelsystemen
  Chem. Ing. Tech., 2016, 88, 158-167. DOI: 10.1002/cite.201500096

- D.L.L. Pingen, C. Altintas, M. Schaller, D. Vogt
  A Ruthenium Racemisation Catalyst for Synthesis of Primary Amines from Secondary Amines
  Dalton Trans. 2016, 45, 11765-11771. http://dx.doi.org/10.1039/C6DT01525E, first published on the web 10 June, 2016

2015

- A. Behr, A. Wintzer
  Hydroaminomethylation of the Renewable Limonene with Ammonia in an Aqueous Biphasic Solvent System
  Chem. Eng. Technol. 12 (2015), 2299-2304

- T. Färber, R. Schulz, O. Riechert, T. Zeiner, A. Górak, G. Sadowski, A. Behr
  Different recycling concepts in the homogeneously catalysed synthesis of terpenyl amines
  Chem. Eng. Process. 98 (2015), 22-31

- A. Behr, A. Kämper, M. Nickel, R. Franke
  Crucial role of additives in iridium-catalyzed hydroformylation
  Appl. Catal. A:General 505 (2015), 243-248

- A. Behr, D. Levikov, E. Nürenberg
  Rhodium-catalyzed hydroaminimethylation of cyclopentadiene
  RSC Adv. 5 (2015), 60667-60673

- P. Neubert, M. Steffen, A. Behr
  Three step auto-tandem catalysed hydroesterification: Access to linear fruity esters from piperylene
  J. Mol. Catal. A: Chem. 407 (2015), 122-127

- P. Neubert, S. Fuchs, A. Behr
  Hydroformylation of piperylene and efficient catalyst recycling in propylene carbonate
  Green Chem. 17 (2015), 4045-4052

- A. Behr, D. Levikov, D. Vogelsang
  First rhodium-catalyzed hydroformylation of cyclopentadiene
  J. Mol. Catal. A: Chem. 406 (2015), 114-117

- A. Behr, T. Färber
  Application of a Taylor-Couette Reactor in Homogeneous Catalysis
  Chem. Ing. Trans. 43 (2015), 835-840

- A. Behr, K. A. Irawadi
  Glycerin-Oxidation mit magnetisch abtrennbaren Nanokatalysatoren
  Chem. Ing. Tech. 87 (2015)

- A. Behr, Z. Bayrak, S. Peitz, G. Stochniol, D. Maschmeyer
  Oligomerization of 1-butene with a homogeneous catalyst system based on allylic nickel complexes
  RSC Adv. 5 (2015), 41372-41376

- A. Behr, A. Wintzer, C. Lübke, M. Müller
  Synthesis of primary amines fron the renewable compound citronellal via biphasic reductive amination
  Journal of Molecular Catalysis A: Chemical 404 (2015), 74-82

- A. Behr, D. Levikov, E. Nürenberg
  Rhodium catalyzed one-step hydroamidation of cyclopentadiene and dicyclopentadiene
  Catal. Sci. Technol. 5 (2015), 2783-2787

- A. Behr, S. Toepell
  Comparison of Reactivity in the Cross Metathesis of Allyl Acetate-Derivates with Oleochemical Compounds
  J Am Oil Chem Soc 92 (2015), 603–611

- K. A. Ostrowski, D. Lichte, M. Terhorst, A.J. Vorholt
  Two sides of the same amino acid-development of a tandem aldol condensation/epoxidation by using the synergy of different catalytic centres in amino acids
  Appl. Catal., A, 2015, 509, 1–7. DOI: 10.1016/j.apcata.2015.10.018

- T. Seidensticker, M. R. L. Furst, R. Frauenlob, J. Vondran, E. Paetzold, U. Kragl, A.J. Vorholt
  Palladium-Catalyzed Aminocarbonylation of Aliphatic Alkenes with N,N-Dimethylformamide as an In Situ Source of CO
  ChemCatChem, 2015, 7, 4085-4090. DOI: 10.1002/cctc.201500824.

- A. Behr, A. Kämper, R. Kuhlmann, A.J. Vorholt, R. Franke
  First efficient catalyst recycling for the iridium-catalysed hydroformylation of 1-octene
  Catal. Sci. Technol., 2015, 6, 208-214. DOI: 10.1039/C5CY01018G

- T. Seidensticker, A.J. Vorholt, A. Behr
  The mission of addition and fission – catalytic functionalization of oleochemicals
  Eur. J. Lipid Sci. Technol., 2016, 118, 3-25. DOI: 10.1002/ejlt.201500190

- K.A. Ostrowski, T.A. Faßbach, D. Vogelsang, A.J. Vorholt
  The Quest for Decreasing Side Products and Increasing Selectivity in Tandem Hydroformylation/Acyloin Reaction
  ChemCatChem, 2015, 7, 2607-2613. DOI: 10.1002/cctc.201500727

- J. Dreimann, P. Lutze, M. Zagajewski, A. Behr, A. Górak, A.J. Vorholt
  Chemical Engineering and Processing, Highly Integrated Reactor-Separator Systems for the Recycling of Homogeneous Catalysts
  Chem. Eng. Proc. 2016, 99, 124-131. DOI:10.1016/j.cep.2015.07.019

- K. McBride, T. Gaide, A.J. Vorholt, A. Behr, K. Sundmacher
  Chemical Engineering and Processing, Thermomorphic Solvent Selection for Homogeneous Catalyst Recovery based on COSMO-RS
  Chem. Eng. Proc. 2015, 99, 97-106. DOI:10.1016/ j.cep.2015.07.004

- T. Gaide, A. Behr, A. Arns, F. Benski, A.J. Vorholt
  Chemical Engineering and Processing, Hydroesterification of methyl 10-undecenoate in thermomorphic multicomponent solvent systems-Process development for the synthesis of sustainable polymer precursors
  Chem. Eng. Proc., 2015, 99, 197-204. DOI: 10.1016/j.cep.2015.07.009

- K.A. Ostrowski, T.A. Faßbach, A.J. Vorholt
  Tandem Hydroformylation/Acyloin Reaction – The Synergy of Metal Catalysis and Organocatalysis Yielding Acyloins Directly from Olefins
  Adv. Synth. Catal., 2015, 357, 1374–1380. DOI: 10.1002/adsc.201401031

- A. Behr, A.J. Vorholt, T. Seidensticker
  An Old Friend in a New Guise-Recent Trends in Homogeneous Transition Metal Catalysis
  ChemBioEng Rev. 2015, 2, 6-21. DOI: 10.1002/cben.201400034

- A. Falk, A. Cavalieri, D. Vogt, H.-G. Schmalz
  Enantioselective Nickel-Catalyzed Hydrocyanation using Chiral Phosphine-Phosphite Ligands: Recent Improvements and Insights,
  Adv. Synth. Catal. 2015, 357, 3317-3320. http://dx.doi.org/10.1002/ adsc.201500644, first published on the web 14 Oct, 2015

- E.H. Boymans, P.T. Witte, D. Vogt
  Study on the Selective Hydrogenation of Nitroaromatics to N-aryl hydroxylamines using a Supported Pt Nanoparticle Catalyst
  Catal. Sci. Technol. 2015, 5, 176-183. http://dx.doi.org/10.1039/ C4CY00790E, first published on the web 29 Aug, 2014

2014

- A. Behr, A.J. Vorholt, K.A. Ostrowski, T. Seidensticker
  Towards recource efficient chemistry: tandem reactions with renewables
  Green Chem. 2014, 16, 982-1006, DOI: 10.1039/C3GC41960

- A. Behr, A.J. Vorholt
  Neue Trends in der homogenen Übergangsmetallkatalyse
  Chem. Ing. Tech., 2014, 86, 2089–2104, DOI: 10.1002/cite.201400109

- J. Esteban, A.J. Vorholt, A. Behr, M. Ladero, F. Garcia-Ochoa
  Liquid-liquid equilibria for the system acetone + solketal + glycerol
  J. Chem. Eng. Data, 2014, 59, 2850-2855, DOI: 10.1021/je500469a

- A. Behr, T. Seidensticker, A.J. Vorholt
  Diester monomers from methyl oleate and proline via tandem hydroaminomethylation-esterification sequence with homogeneous catalyst recycling using TMS-technique
  Eur. J. Lipid Sci. Technol., 2014, 166, 477-485, DOI: 10.1002/ejlt.201300224

- A. Behr, N. Rentmeister, T. Seidensticker, T.A. Faßbach, S. Peitz, D. Maschmeyer
  Nickel catalyzed dimerization reactions of vinylidene compounds: Head-to-head couplings and catalyst stabilization
  Journal of Molecular Catalysis A: Chemical 395 (2014), 355-363

- A. Behr, A. Lux
  Ein einfacher Syntheseweg zu Lösungsmittelstabilisierten Metallnanopartikeln und ihre Anwendung in der Hydrierung
  Chem. Ing. Tech. 86 (2014), 1-9

- A. Behr, N. Rentmeister, D. Möller, J. Vosberg, S. Peitz, D. Maschmeyer
  Dimerization reactions with iron and cobalt bis(imino)pyridine catalysts: A substrate based approach
  Catalysis Communications 55 (2014), 38-42

- M. Zagajewski, A. Behr, P. Sasse, J. Wittman
  Continously operated miniplant for the rhodium catalyzed hydroformylation of 1-dodecene in a thermomorphic multicomponent solvent system (TMS)
  Chem. Eng. Sci. 115 (2014), 88-94

- A. Rost, Y. Brunsch, A. Behr, R. Schomäcker
  Comparison of the Activity of a Rhodium-Biphephos Catalyst in Thermomorphic Solvent Mixtures and Microemulsions
  Chem. Eng. Technol. 37 (2014), 1055-1064

- M. Zagajewski, J. Dreimann, A. Behr
  Verfahrensentwicklung vom Labor zur Miniplant: Hydroformylierung von 1-Dodecen in thermomorphen Lösungsmittelsystemen
  Chem. Ing. Tech. 86 (2014), 449-457

- A. Behr, S. Toepell, S. Harmuth
  Cross-metathesis of methyl 10-undecenoate with dimethyl maleate: an efficient protocol with nearly quantitative yields
  RSC Adv. 4 (2014), 16320-16326

- A. Behr, H. Witte, A. Kämper, J. Haßelberg, M. Nickel
  Entwicklung und Untersuchung eines Verfahrens zur Herstellung verzweigter Fettstoffe im Miniplant-Maßstab
  Chem. Ing. Tech. 86 (2014), 458-466

- A. Behr, P. Neubert
  Piperylene – A Versatile Basic Chemical in Catalysis
  ChemCatChem 6 (2014), 412-428

- A. Behr, Z. Bayrak, S. Peitz, D. Maschmeyer, G. Stochniol
  Rhodium-catalyzed codimerization of n-butenes with allylic halides
  Applied Catalysis A: General 476 (2014), 68-71

- A. Behr, N. Rentmeister, T. Seidensticker, J. Vosberg, S. Peitz, D. Maschmeyer
  Highly Selective Dimerization and Trimerization of Isobutene to Linearly Linked Products by Using Nickel Catalysts
  Chem. Asian J. 9 (2014), 596-601

- A. Behr, A. Wintzer
  From Terpenoids to Amines: A Critical Review
  in: New Developments in Terpenes Research, Ed.: J. Hu, Nova Science Publishers, Inc., Chapt. 6, p. 113-134, 2014

- A. Behr, K. Nowakowski
  Catalytic Hydrogenation of Carbon Dioxide to Formic Acid, Advances in Inorganic Chemistry
  Vol. 66, Elsevier, Chapt. 7, p. 223-258, 2014

- C. Hendriksen, E. Pidko, G. Yang, B. Schäffner, D. Vogt
  Catalytic Formation of Acrylate from Carbon Dioxide and Ethene
  Chem. Eur. J. 2014, 20, 12037-12040. http://dx.doi.org/10.1002/chem.201404082, first published on the web 12 Aug, 2014

- D.L.L. Pingen, T. Lebl, M. Lutz, G.S. Nicol, P.C.J. Kamer, D. Vogt
  Catalytic Activity and Fluxional Behavior of Complexes based on RuHCl(CO)(PPh₃)₃ and Xantphos-Type Ligands
  Organometallics 2014, 33, 2798-2805.http://dx.doi.org/10.1021/om5003182, first published on the web 28 May, 2014

- D. Pingen, M. Lutz, D. Vogt
  Mechanistic Study on the Ru-Catalyzed Direct Amination of Alcohols
  Organometallics 2014, 33, 1623-1629. http://dx.doi.org/10.1021/om4011998, first published on the web 17 Mar, 2014

- S. Güven, M.M. L. Nieuwenhuizen, B. Hamers, R. Franke, M. Priske, M. Becker, D. Vogt
  Kinetic Explanation for the Temperature Dependence of Regioselectivity in Neohexene Hydroformylation
  ChemCatChem 2014, 6, 603-610. http://dx.doi.org/10.1002/cctc.201300818, first published on the web 8 Jan, 2014

- S. Güven, B. Hamers, R. Franke, M. Priske, M. Becker, D. Vogt
  Kinetics of Cyclooctene Hydroformylation for Continuous Homogeneous Catalysis, *Catal. Sci. Technol. 2014, 4, 524-530 http://dx.doi.org/10.1039/C3CY00676J, first published on the web 13 Dec, 2013*

- D. Pingen, D. Vogt
  Amino-alcohol cyclization: selective synthesis of lactams and cyclic amines from amino-alcohols
  Catal. Sci. Technol. 2014, 4, 47-52. http://dx.doi.org/10.1039/C3CY00513E, first published on the web 17 Sep, 2013

- C.F. Czauderna, D.B. Cordes, A.M.Z. Slawin, C. Müller, J.I. van der Vlugt, D. Vogt, P.C.J. Kamer
  Synthesis and Reactivity of Chiral Wide Bite Angle Hybrid Diphosphorus Ligands
  Eur. J. Inorg. Chem. 2014, 10, 1797-1810. http://dx.doi.org/10.1002/ejic.201301255, first published on the web 3 Dec, 2013

Proceedings

- A. Behr, A.J. Vorholt, T. Gaide, J. Dreimann
  Process Development for the Hydroformylation/Hydroesterification of Methyl-10-Undecenoate - From Laboratory to Miniplant Scale
  DGMK-Tagungsbericht 2015-2. 119-125, ISBN 978-3-941721-56-2

- A. Behr, N. Tenhumberg, A. Wintzer
  Selective Oxidation and Functionalisation of Renewables
  DGMK-Tagungsbericht 2014-3, 11-15

Books & Bookarticles

- P.C.J. Kamer, D. Vogt, J. Thybaut (Eds.)
  Contemporary Catalysis; Science, Technology and Applications
  RSC 2017, Eischeinungsdatum Mai 2017

Patents

- B. Schäffner, M. Blug, D. Vogt, C. Hendriksen, E. Pidko, (to Evonik Industries AG)
  Synthesis of α,β-ungesaturated carboxylic acid (meth)acrylates from olefins and CO₂
  WO 2014/198469 A1, priority date 12.05.2014

- D. Leinweber, S. Romanski, A.J. Vorholt, A. Behr, T.A. Faßbach
  DE 10 2016 224 089.7

- D. Leinweber, S. Romanski, X. Guo, A.J. Vorholt, A. Behr, T.A. Faßbach,
  EP 17156549.2

- S. Fuchs, A. Behr, A.J. Vorholt, G. Meier, H. Strutz
  Verfahren zur Hydroaminomethylierung zyklischer Diene zu Di-sekundären Aminen
  EP 17 153 047.0

- S. Fuchs, A. Behr, A.J. Vorholt, G. Meier, H. Strutz
  Verfahren zur Aminocarbonylierung zyklischer Diene
  DE 10 2017 101 371.7

- S. Peitz, Z. Bayrak, A. Behr, F. Geilen, D. Maschmeyer, G. Stochniol, M. Winterberg, C. Böing, **Ni(II) catalyst for dimerization of olefins**
  WO 2015/104185A1

- S. Peitz, Z. Bayrak, A. Behr, F. Geilen, D. Maschmeyer, G. Stochniol, M. Winterberg, C. Böing
  Dimerisierung von Olefinen, *DE 10 2014 200072A1*

- A. Behr, A. Gottschalk, A. Kämper, S. Tlatlik, R. Franke, D. Fridag, K.M. Dyball, F. Geilen **Verfahren zur Untersuchung der Langzeiteigenschaften Homogener Katalysatorsysteme im kontinuierlichen Betrieb**
  DE 15162342.8
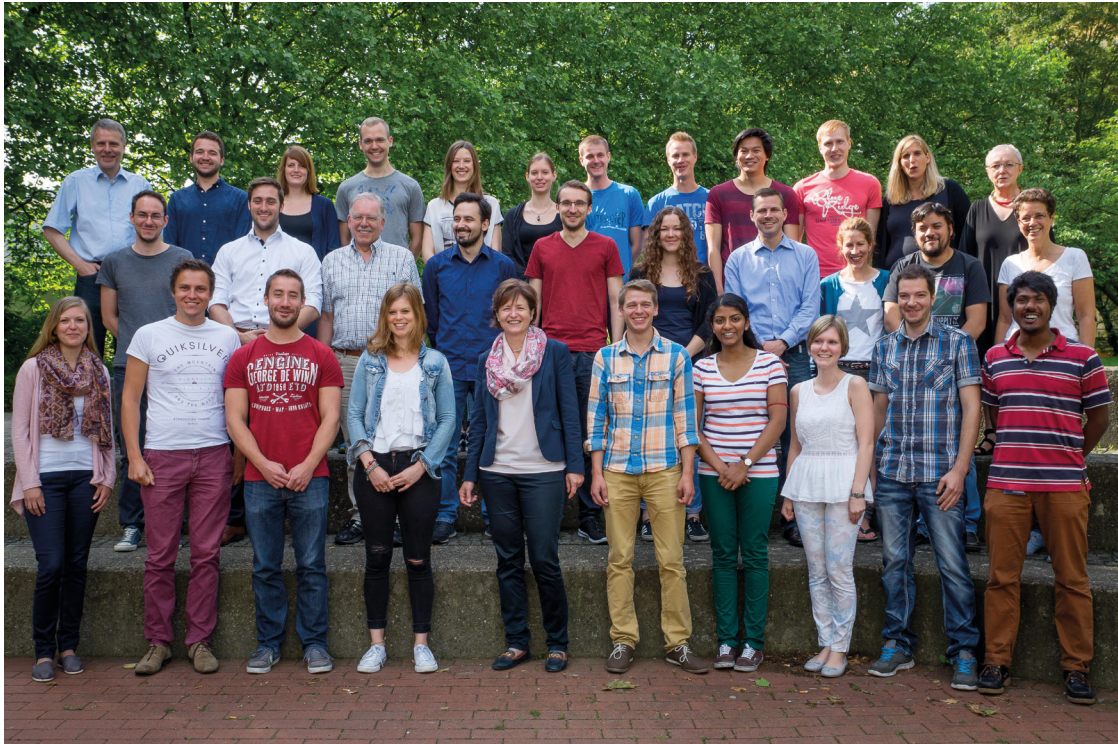
Thermodynamics (TH)

Predicting Solvent Effects on the 1-Dodecene Hydroformylation Reaction

Max Lemberg, Gabriele Sadowski

Due to molecular interactions with the reacting species, solvents can have a decisive influence on the position of reaction equilibria and therewith on the yield of the reaction. To account for this effect on the hydroformylation of 1-dodecene in a decane/ DMF-solvent system, a thermodynamic model was applied to predict the reactant equilibrium concentrations as function of solvent composition. Based on thermodynamic equilibrium constants derived from quantum-chemical calculations, the approach developed in this work allowed for predicting the solvent effect on the reaction equilibrium in very good agreement with the experimental data.

The knowledge of the solvent influence on reaction equilibria is of high importance for the design of efficient reaction systems. Reaction equilibria are thermodynamically accessible via the standard Gibbs energy of reaction $\Delta^R g^0$ for the ideal-gas standard state whereby $\Delta^R g^0$ is related to the thermo-dynamic equilibrium constant K_f via the following equation:

$$\Delta^R g^0 (T) = - RT \ln K_f (T) \qquad (1)$$

These two quantities depend on temperature only. $\Delta^R g^0$ can be obtained by quantum chemical calculations, e.g. applying the Møller-Plesset second order perturbation theory (MP2). Reaction engineering requires the concentrations of the reactants and products at equilibrium, usually described by K_x. The latter can be calculated based on K_f according to Eq. (2):

$$K_x = \frac{K_f}{K_\varphi} \cdot \left(\frac{p}{p^0}\right)^2 \qquad (2)$$

Herein K_φ is derived from the fugacity coefficients of reactants and products and therewith contains the information about the interactions between the different components in the reaction mixture (i.e. the solvent influence on reactants and products). In this work K_φ was calculated using the physical-sound thermodynamic model PC-SAFT (Fig. 1).
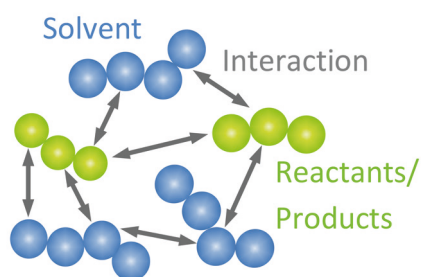

Figure 1: Interactions in a reaction mixture considered by PC-SAFT.

In contrast to K_f, K_φ obviously strongly depends on the solvent in which the reaction takes place.

Benefically, with K_f known form quantum-chemical calculations and K_φ calculated by PC-SAFT, the solvent effect on K_x can be predicted using Eq. (2). The results for the hydroformylation reaction are compared with experimental data in Figure 2.
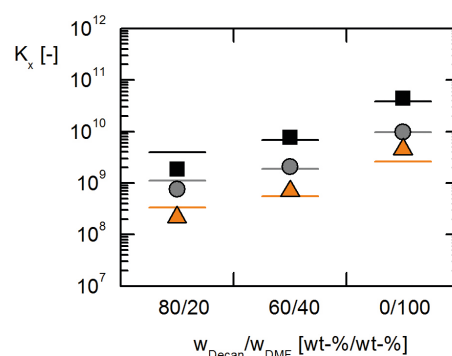

Figure 2: K_x values for the 1-dodecene hydroformylation at different compositions of the decane/DMF solvent system. The symbols are experimental data at 368 K (black squares), 378 K (grey circles) and 388 K (orange triangles). Lines are predictions using PC-SAFT.

As to be seen, prediction and experiment are in excellent agreement. Moreover, the value of K_x (10^8 to 10^{10}) indicates that the reaction equilibrium lies almost completely on the product side.

Concerning the solvent effect, experiments and modeling results show that K_x increases with increasing DMF content in the mixture. Depending on temperature, K_x is about 10 to 20 times higher in pure DMF (0/100) than in the 80/20 decane/ DMF-mixture, which is an immense solvent effect.

Using this approach of combining quantum-chemical calculations and a thermodynamic model accounting for the interactions between the components involved allows for almost quantitatively predicting of solvent effects on reaction equilibria. This significantly reduces the experimental effort required for identifying the best solvent candidate for a given reaction.

Contact:
max.lemberg@bci.tu-dortmund.de
gabriele.sadowski@bci.tu-dortmund.de

Long-Term Stability of Polymeric Pharmaceutical Formulations

Prediction and Experimental Validation of Amorphous-Amorphous Phase Separation and Recrystallization

Christian Luebbert, Gabriele Sadowski

Pharmaceutical formulations (PFs) have to be stable throughout their intended shelf-life. In order to provide the required stability, two phenomena have to be avoided: recrystallization of the active pharmaceutical ingredient (API) in the PF and amorphous-amorphous phase separation (AAPS) into two liquid phases (a polymer-rich phase and an API-rich phase). This work predicted the long-term stability conditions of PFs composed of poly (vinyl pyrrolidone) (PVP) and Ibuprofen (IBU) by means of thermodynamic calculations for storage temperatures and humidities of interest. Predicted conditions for the occurrence of AAPS and recrystallization were validated via measurements with Raman spectroscopy and X-ray diffraction. It was thus shown that thermodynamic modeling can successfully replace the usually applied trial-and-error methods for identifying polymers suitable for long-time stable PFs.

Numerous recently-developed active pharmaceutical ingredients (APIs) are poorly water soluble leading to an insufficient bioavailability. A typical method to overcome this solubility limitation is to use pharmaceutical formulations (PFs), which are formed by dissolving the APIs in suitable polymers. Authorities like the Federal Drug Administration require providing data on long-term stability studies at defined temperature and relative humidity (RH) conditions prior to administration of new PFs.

In this work, the long-term stability of a PF composed of poly (vinyl pyrrolidone) (PVP) and Ibuprofen (IBU) was investigated at 75% RH. The thermodynamic model Perturbed-Chain Statistical Associating Fluid Theory (PC-SAFT) was used to predict AAPS and the solubility of IBU in PVP (which determines the recrystallization region) at 75% RH (Figure 1).

To investigate the recrystallization behavior, PFs were analyzed by X-ray diffraction in recurring measurements during long-term storage (550 days) at 40°C. Figure 1 shows that recrystallized IBU was found in PFs with IBU loadings above 60 wt%.

AAPS was measured by two-dimensional X,Y-mapping using confocal Raman spectroscopy (Figure 2) showing an IBU-rich phase (IBU/PVP = 40/60) and an IBU-poor phase (IBU/PVP = 1/99). All PF lying in this concentration range undergo AAPS.

This means, that long-term stable PFs (neither crystallization nor AAPS) of IBU and PVP were experimentally found only for IBU loadings between 40 and 60 wt%.
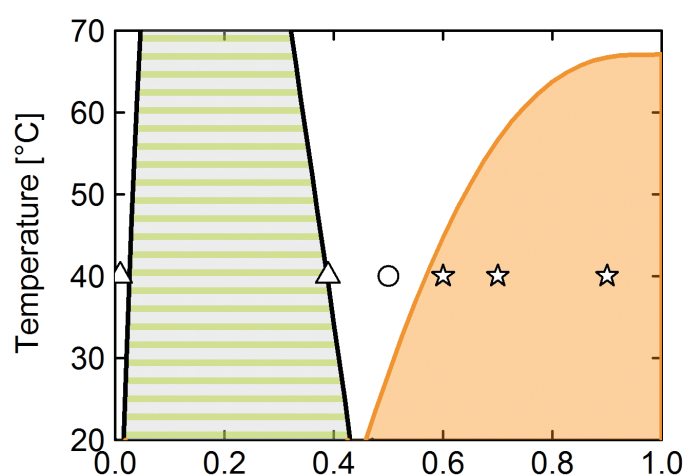

Figure 1: Phase diagram for the system PVP/IBU at 75% RH. Lines are predictions with PC-SAFT (orange: solubility, black: AAPS). Symbols are experimental results of long-term studies carried out at 40 °C (stars: recrystallization, triangles: AAPS compositions from Fig. 2, circle: stable formulation).
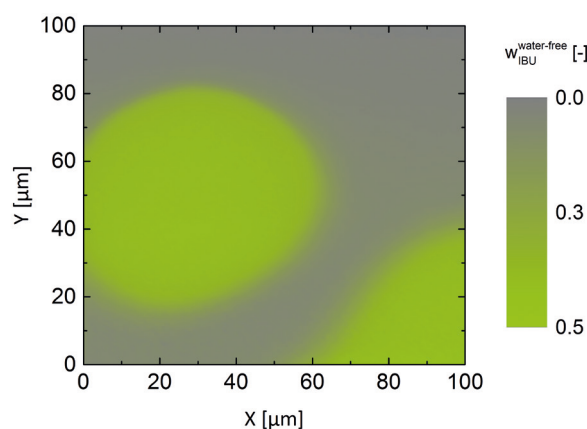

Figure 2: Raman scan of a pharmaceutical formulation of PVP/IBU at 40 °C and 75% RH showing AAPS.

As to be seen from Figure 1, the experimental findings perfectly validate the PC-SAFT predictions.

Thus, PC-SAFT allows predicting the concentration ranges for obtaining long-term stable PFs enabling a significant time reduction for evaluating thermodynamic stability in early stages of PF development.

Contact:
christian.luebbert@bci.tu-dortmund.de
gabriele.sadowski@bci.tu-dortmund.de

Numerical Simulation of the Appendix Gap in Stirling Cycle Machines

Jan Sauer, Hans-Detlev Kühl

One-dimensional differential models are an essential tool for the design optimization of Stirling cycle machines, and their accuracy is of course dependent on the characterization of the relevant loss mechanisms. Recent findings suggest that the thermal losses caused by the annular gap surrounding the displacer have been underestimated due to insufficient, too rigorously simplified modelling approaches. In this research work, an existing one-dimensional simulation program has therefore been extended by a differential model of the appendix gap.

Typically, Stirling cycle machines feature a cylinder-displacer system separating a hot and a cold temperature level, in which the so-called appendix gap works as an insulating layer between the displacer and the cylinder, as shown in Figure 1. This gap is usually closed by a seal at the cold end, whereas cyclic gas flows arise at the open hot end due to pressure fluctuations in the machine, resulting in the so-called enthalpy loss. Additionally, cyclic displacements of the axial temperature profiles in the displacer and the cylinder wall cause a thermal loss known as the shuttle loss. The sum of these loss mechanisms, which feature opposite dependencies on the gap width h, is known as the appendix gap loss and may amount up to 10% of the heat input of a Stirling machine. Several analytical models exist for these losses, which are partly based on questionable assumptions. Therefore a new analytical model has recently been developed.
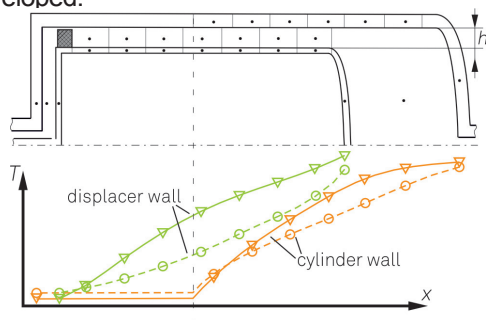

Figure 1: Discretization of the cylinder-displacer system featuring an appendix gap and calculated wall temperature profiles along the gap for a small gap width h (dashed lines) and a large gap width h (solid lines).

However, none of these models is capable of accounting for interactions between these losses and the thermodynamic cycle of a Stirling machine. Even in numerical simulations, where this would theoretically be possible, the appendix gap losses have so far been evaluated by analytical models usually. Now, an existing one-dimensional simulation program has been extended by a differential model of the entire appendix gap, including a discretization of the cylinder and the displacer wall (Figure 1).

Evidently, the appendix gap is subdivided into several evenly sized finite volumes. They are bound to the moving displacer wall, which is also subdivided into finite elements, as well as the non-moving cylinder wall. The wall elements have the same axial lengths as the finite volumes in the gap. In contrast, the cylinder volumes are treated as single ideally mixed volumes undergoing the volumetric changes as imposed by the displacer motion.

The results for the wall temperatures as well as the gas temperatures in the gap are highly dependent on the gap width h. This is also visualized in Figure 1 by the wall temperatures obtained with a small and a large gap width (dashed and solid lines, respectively). In turn, the appendix gap losses are also strongly dependent on the gap width. This is illustrated in Figure 2, where the appendix gap losses including axial heat conduction are plotted versus the gap width. The dash-dotted lines indicate the losses obtained by the new analytical model (black) and an older analytical model (grey), whereas the colored solid lines are results of the numerical simulation.
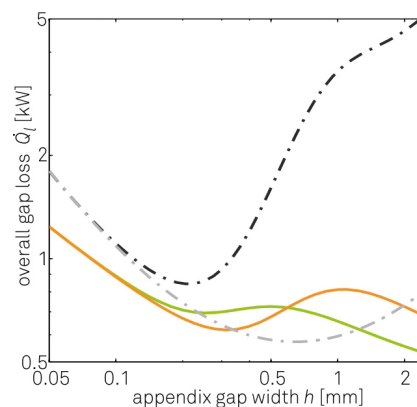

Figure 2: Simulated overall gap loss for different heat transfer models (solid colored lines) compared to the new analytical appendix gap loss (black line) and an older appendix gap loss model (grey line).

Due to the one-dimensional modelling approach, the heat exchange between the gas and the walls has to be described by separate model assumptions. The orange line is obtained assuming parabolic radial gas temperature profiles, whereas assuming steady-state heat conduction between the gas and the walls results in the green line. Obviously, the various models yield considerably different losses and optimum gap widths. Therefore, further theoretical and experimental investigations are pursued.

Contact:
jan.sauer@bci.tu-dortmund.de
hans-detlev.kuehl@bci.tu-dortmund.de

Light-Scattering Data as Novel Access to PC-SAFT Parameters

Development of a Novel Method for Estimating and Validating Perturbed Chain-Statistical Associating Fluid Theory Parameters for Proteins and Polymers Using Molecular Light-Scattering Data

Matthias Voges, Marcel Herhut, Christoph Held, Christoph Brandenbusch

The experimental effort in gathering phase-equilibrium data for polymer and/or protein solutions can be reduced by means of thermodynamic models. This work presents a new method for estimation and validation of parameters of thermodynamic models by means of molecular light-scattering data obtained by static-light-scattering (SLS) measurements. Perturbed-Chain Statistical Associating Fluid Theory (PC-SAFT) was used to successfully predict the isothermal SLS data of buffered PEG/lysozyme/ water solutions in dependence of concentration of PEG and lysozyme and of molecular weight of PEG. On the one hand, the accuracy of the novel approach allows predicting SLS data of complex solutions. On the other hand, the method provides an access to the estimation of model parameters by means of experimental SLS data, which are accessible with much less effort than experimental phase-equilibrium data of complex macromolecular solutions.

Design and optimization of industrial separation processes require knowledge of phase-equilibrium data. Caused by high viscosity of polymer solutions and by high costs of proteins, measuring phase-equilibrium data is time-consuming and cost-intensive. To reduce this effort, thermodynamic models (e.g. PC-SAFT) have been developed and applied for the calculation of phase diagrams of solutions containing macromolecules. However, these models require a lot of experimental data such as densities, phase equilibria or activity coefficients as input in order to adjust parameters.

In this work, a new approach was developed serving as an access to model parameters based on experimental SLS data (see Figure 1) since SLS measurements are very fast and show a high sensitivity even at low polymer or protein concentrations (about 5 wt-%). A model system containing poly ethylene glycol (PEG) and lysozyme was chosen for demonstration.
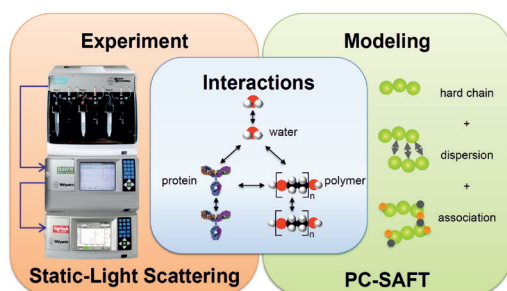

Figure 1: Static-light-scattering data of solutions containing macromolecules are specific for the respective macromolecule and its interactions with surrounding molecules in a multi-component solution. These interactions and, thus, static-light-scattering data can be predicted by means of PC-SAFT.

Experimental light-scattering signals (excess Rayleigh ratio $\Delta R_{SLS} / K_{SLS}$) were determined using pure-component PC-SAFT parameters of water, PEG and lysozyme, as well as the binary interaction parameter between water/PEG and water/lysozyme taken from literature. The binary PEG/ lysozyme interaction parameter was fitted to experimental SLS signals of buffered PEG/lysozyme/water solutions. Parameters were then used to predict the SLS signals of buffered PEG/lysozyme/water solutions at different concentrations of PEG and lysozyme as well as of different molecular weights of PEG (see Figure 2). These predictions are in excellent agreement with the experimental results.
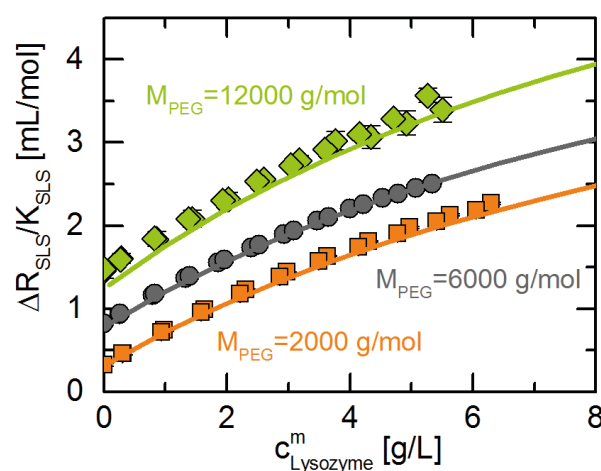
Figure 2: Excess Rayleigh ratio $\Delta R_{SLS} / K_{SLS}$ of PEG/lysozyme/ buffer solutions versus concentration of lysozyme at 298.15 K, pH 4.6 and c^m_{PEG}= 10 g/L for different molecular weights of PEG. Symbols represent experimental data, lines represent PC-SAFT predictions.

This novel method allows for a fast and efficient validation and estimation of PC-SAFT parameters for (bio) macromolecules. Compared to conventional methods, this means a clear advantage for model applications to polymer and protein solutions. Based on the success of the method it will be possible to predict phase diagrams of (bio)macromolecule solutions based on model parameters obtained from adjusting to SLS data.

Contact:
matthias.voges@bci.tu-dortmund.de
christoph.held@bci.tu-dortmund.de
christoph.brandenbusch@bci.tu-dortmund.de

Overcoming Yield Limitations of Enzymatic Reactions by Ionic Liquids

Experimental and Theoretical Study on the Influence of Additives on the Maximum Yield of Enzymatic Reactions

Matthias Voges, Gabriele Sadowski, Christoph Held

The maximum yield of enzymatic reactions is limited by thermodynamic equilibrium. Reaction conditions (T, pH, concentrations) usually influence the position of reaction equilibrium. The use of additives such as ionic liquids can boost the maximum yield of enzymatic reactions. In this work, the influence of reaction conditions as well as of additives on two enzymatic reactions was measured. The results showed that the maximum yield of these enzymatic reactions could be shifted remarkably to the product side by adding ionic liquids as inert additives to the reaction mixtures. This could be predicted accurately with electrolyte PC-SAFT.

The efficiency of enzymatic reactions can be limited by the stability (and thus by catalytic activity) of the enzymes, by the low solubility of substrates in the (mostly aqueous) reaction media, and by the reaction equilibrium that limits product yield. The latter is characterized by the thermodynamic equilibrium constant K_{th} that only depends on temperature and is defined by

$$K_{th} = \prod m_i^{\nu_i} \cdot \prod \gamma_i^{\nu_i} \qquad (1)$$

In Eq. (1) m is the molality in mol/(kg$_{water}$), γ is the activity coefficient and ν is the stoichiometric coefficient of reacting agent i at equilibrium. Addition of inert substances (additives) to the reaction mixture will impact the activity coefficients of the reacting agents, while K_{th} remains constant. This causes a change of the equilibrium molalities of the reacting agents and thus influences the maximum yield of the reaction (Figure 1).
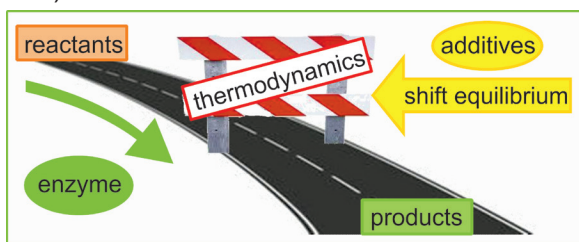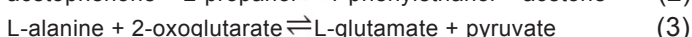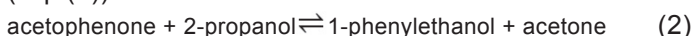

Figure 1: The maximum yield of enzymatic reactions is limited by the thermodynamic reaction equilibrium, which can be shifted by adding inert substances to the reaction mixture.

This work investigated the influence of inert additives on the yield of an alcohol dehydrogenase (ADH) reaction (Eq. (2)) and of an aminotransferase (ALAT) reaction (Eq. (3)).

acetophenone + 2-propanol $\rightleftharpoons$ 1-phenylethanol + acetone   (2)
L-alanine + 2-oxoglutarate $\rightleftharpoons$ L-glutamate + pyruvate   (3)

The additives under investigation were the ionic liquids 1-butyl-3-methylimidazolium trifluoromethanesulfonate ([bmim]Otf), 1-butyl-3-methylimidazolium chloride ([bmim]Cl), 1-ethyl-3-methylimidazolium chloride ([emim]Cl), choline chloride ([choline]Cl), ([choline]H$_2$PO$_4$) and ammoeng110, as well as the osmolyte trimethylamine N-oxide (TMAO) and urea.

Contact:
matthias.voges@bci.tu-dortmund.de
christoph.held@bci.tu-dortmund.de
gabriele.sadowski@bci.tu-dortmund.de

In a first step, the stability of the enzymes in the reaction mixtures containing these additives was ensured by UV-tests and FTIR-spectroscopy. Secondly, the molalities of the reacting agents were measured over the reaction time until constant molalities were observed. The catalytic activity of the enzymes was ensured at these stationary conditions. Thus, the stationary molalities equaled reaction-equilibrium molalities, therewith defining the maximum yield at equilibrium.

The tremendous influence of the considered additives is illustrated in Figure 2. For both reactions, the addition of 0.25 molal ammoeng110 improved the yield most strongly. In the final step, the activity coefficients of the reacting agents were predicted by electrolyte PC-SAFT. Using these and the K_{th} values for the neat reactions allowed predicting the maximum yield of both reactions in very good agreement with the experiments (Figure 2).
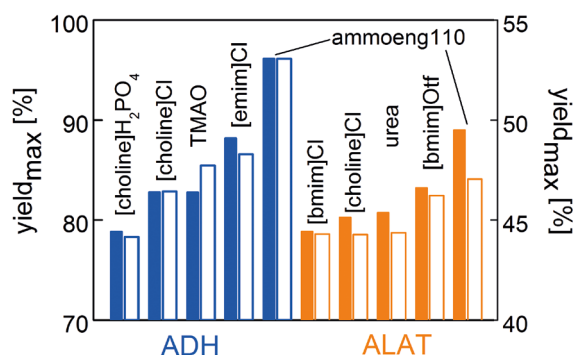
Figure 2: The maximum yield of the ADH reaction (30 °C, pH 7) and ALAT reaction (37 °C, pH 7) in the presence of different additives in the aqueous reaction media. Filled bars represent experimental values and open bars represent electrolyte PC-SAFT predictions.

In sum, the significant influence of additives on the yield of enzymatic reactions that was observed experimentally could be explained by activity coefficients. This opens the door for process design and electrolyte PC-SAFT is proposed as tool to screen additives in order to boost yield of enzymatic reactions.

Publications:
M. Voges, F. Schmidt, D. Wolff, G. Sadowski, C. Held,
Fluid Phase Equilib. 2016, 422, 87-98.
M. Voges, I.V. Prikhodko, S. Prill, M. Hübner, G. Sadowski, C. Held,
J. Chem. Eng. Data 2017, 1, 52-61.

Phase Separation in Biphasic Whole-Cell Biocatalysis

Development of a Prototype for Continuous Phase Separation of Stable Emulsions

Lisa Vahle, Gabriele Sadowski, Christoph Brandenbusch

The main bottleneck for an industrial implementation of high-potential biphasic whole-cell bio-processes is the formation of stable Pickering type emulsions (mechanical stabilization) due to the presence of whole cells acting like particles. Common processes for phase separation e.g. centrifugation or the use of de-emulsifiers often fail for these biphasic emulsions leading to inefficient and cost-intensive processes. In contrast, using the catastrophic phase inversion (CPI) phenomenon applied within this work, phase separation is easily achieved by a sudden switch of emulsion type caused by addition of dispersed phase showing minimal effort in both time and costs.

Based on a patent filed at TU Dortmund University, a continuous process concept for the phase separation in biphasic whole-cell biocatalysis (termed: Applied Catastrophic Phase Inversion; ACPI) was developed. The fully automated prototype was planned and constructed, demonstrating the efficiency and applicability for phase separation of stable Pickering type emulsions. Figure 1 illustrates the process concept of the ACPI prototype.
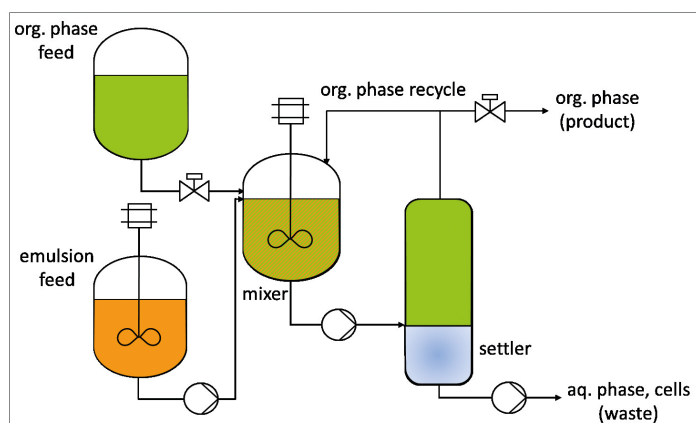

Figure 1: Schematic illustration of ACPI concept.

In the first step dispersed (organic) phase is added to the stable emulsion (Figure 2 a) until the amount exceeds the value needed for phase inversion. Constant stirring ensures homogeneity and a persistent CPI in the mixer. In order to achieve phase separation, the destabilized emulsion is transferred to a settler, where separation is achieved by gravimetric settling. After the desired phase separation (Figure 2 b) has taken place both phases are separated at either the bottom (aqueous phase, cells) or the top of the settler (organic phase). The organic phase is then separated into two streams: (1) for further processing (2) for recycle.

The organic phase recycled to the mixer ensures a constant excess of organic phase and thus guarantees persistent phase inversion. As the product concentration in the recycle is equal to the product concentration in the organic phase of the feed (initial) emulsion, product dilution is prevented.

The major befit of the concept is, that as CPI is a physical phenomenon and does not depend on the course of biotransformation, the ACPI-concept can be applied to all emulsions from biphasic whole-cell biotransformations stabilized by a Pickering-type mechanism. Only the amount of dispersed phase required for CPI has to be adjusted.
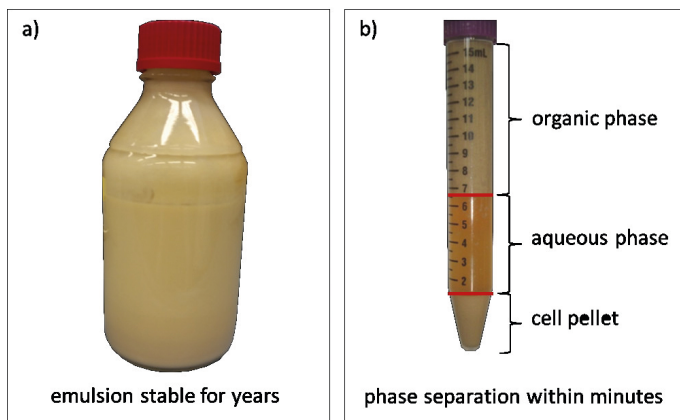
Figure 2: Emulsion sample before (a) and after (b) CPI took place.

In summary, ACPI benefits from its simple setup as well as low operating costs and broad applicability irrespective of product concentration and success of the initial biotransformation. This fact qualifies ACPI as first separation step in the DSP of biphasic whole-cell biotransformations.

Publications:
G. Sadowski, C. Brandenbusch, J. Collins, B. Bühler, Patent EP 2 870 988 A1 (2015).

S. Glonke, G. Sadowski, C. Brandenbusch, Journal of Industrial Microbiology & Biotechnology (2016), 43, 1527-1535.

Contact:
lisa.vahle@bci.tu-dortmund.de
gabriele.sadowski@bci.tu-dortmund.de
christoph.brandenbusch@bci.tu-dortmund.de

Publications 2016 - 2014

2016

- I. Domínguez, B. Gonzalez, B. Orge, C. Held, M. Voges, A. Macedo E.
  Activity coefficients at infinite dilution for different alcohols and ketones in [EMpy][ESO4]: Experimental data and modeling with PC-SAFT
  Fluid Phase Equilibria, 424, 32-40 (2016)

- J. Gorden, T. Zeiner, G. Sadowski, C. Brandenbusch
  Recovery of cis,cis-Muconic Acid from Organic Phase after Reactive Extraction
  Separation and Purification Technology, 169, 1-8 (2016)

- J. Pfeiffer, H.-D. Kühl
  New Analytical Model for Appendix Gap Losses in Stirling Cycle Machines
  Journal of Thermophysics and Heat Transfer, 30, 288-300 (2016)

- J. Pfeiffer, H.-D. Kühl
  Optimization of the Appendix Gap Design in Stirling Engines
  Journal of Thermophysics and Heat Transfer, 30, 831-842 (2016)

- L. Lange, S. Heisel, G. Sadowski
  Predicting the Solubility of Pharmaceutical Cocrystals in Solvent/ Anti-Solvent Mixtures
  Molecules, 21, 593 (2016)

- M. Herhut, C. Brandenbusch, G. Sadowski
  Modeling and prediction of protein solubility using the second osmotic virial coefficient
  Fluid Phase Equilibria, 422, 32-42 (2016)

- M. Voges, F. Schmidt, D. Wolff, G. Sadowski, C. Held
  Thermo-dynamics of the alanine aminotransferase reaction
  Fluid Phase Equilibria, 422, 87-98 (2016)

- N. Emelyanenko V., V. Yermalayeu A., M. Voges, C. Held, G. Sadowski, P. Verevkin S.
  Thermodynamics of a model biological reaction: A comprehensive combined experimental and theoretical study
  Fluid Phase Equilibria, 422, 99-110 (2016)

- S. Glonke, G. Sadowski, C. Brandenbusch
  Applied catastrophic phase inversion: a continuous non-centrifugal phase separation step in biphasic whole-cell biocatalysis
  Journal of Industrial Microbiology & Biotechnology, 43, 1527-1535 (2016)

- S. Mohammad, C. Held, E. Altuntepe, T. Köse, T. Gerlach, I. Smirnova, G. Sadowski
  Salt influence on MIBK/water liquid–liquid equilibrium: Measuring and modeling with ePC-SAFT and   COSMO-RS
  Fluid Phase Equilibria, 416, 83-93 (2016)

- S. Mohammad, G. Grundl, R. Müller, W. Kunz, G. Sadowski, C. Held
  Influence of electrolytes on liquid-liquid equilibria of water/1-butanol and on the partitioning of 5-hydroxymethylfurfural in water/1-butanol
  Fluid Phase Equilibria, 428, 102-111 (2016)

- T. Färber, O. Riechert, T. Zeiner, G. Sadowski, A. Behr, J. Vorholt A.
  Homogeneously catalyzed hydroamination in a Taylor–Couette reactor using a thermormorphic multicomponent solvent system
  Chemical Engineering Research and Design, 112, 263-273 (2016)

- T. Reschke, V. Zherikova K., P. Verevkin S., C. Held
  Benzoic Acid and Chlorobenzoic Acids: Thermodynamic Study of the Pure Compounds and Binary Mixtures With Water, J
  Pharm Sci-Us, 105, 1050-1058 (2016)

- V. Zherikova K., A. Svetlov, M. Varfolomeev, P. Verevkin S., C. Held
  Thermochemistry of halogenobenzoic acids as an access to PC-SAFT solubility modeling
  Fluid Phase Equilibria, 409, 399-407 (2016)

- X. Ji, C. Held
  Modeling the density of ionic liquids with ePC-SAFT
  Fluid Phase Equilibria 410, 9-22 (2016)

- Y. Ji, K. Lesniak A., A. Prudic, R. Paus, G. Sadowski
  Drug Release Kinetics and Mechanism from PLGA Formulations
  AIChE Journal, 62, 4055-4065 (2016)

- C. Held, G. Sadowski
  Thermodynamics of Bioreactions
  Annual Review of Chemical and Biomolecular Engineering, 7, 395-414 (2016)

- C. Kress, G. Sadowski, C. Brandenbusch
  Protein partition coefficients can be estimated efficiently by hybrid shortcut calculations
  Journal of Biotechnology, 233, 151-159 (2016)

- C. Kress, G. Sadowski, C. Brandenbusch
  Novel Displacement Agents for Aqueous 2-Phase Extraction Can Be Estimated Based on Hybrid Shortcut Calculations, J
  Pharm Sci-Us, 105, 3030-3038 (2016)

- C. Held, G. Sadowski: Compatible solutes
  Thermodynamic properties relevant for effective protection against osmotic stress
  Fluid Phase Equilibria, 407, 224-235 (2016)

- F. Zubeir L., C. Held, G. Sadowski, C. Kroon M.
  PC-SAFT Modeling of CO_2 Solubilities in Deep Eutectic Solvents
  The Journal of Physical Chemistry B, 120, 2300-2310 (2016)

- S. Mohammad, C. Held, E. Altuntepe, T. Köse, G. Sadowski
  Influence of Salts on the Partitioning of 5-Hydroxymethylfurfural in Water/MIBK
  The Journal of Physical Chemistry B, 120, 3797-3808 (2016)

- L. Lange, K. Lehmkemper, G. Sadowski
  Predicting the Aqueous Solubility of Pharmaceutical Cocrystals As a Function of pH and Temperature
  Crystal Growth & Design, 16, 2726-2740 (2016)

- L. Lange, M. Schleinitz, G. Sadowski
  Predicting the Effect of pH on Stability and Solubility of Polymorphs, Hydrates, and Cocrystals
  Crystal Growth & Design, 16, 4136-4147 (2016)

- N. Gushterov, F. Doghieri, D. Quitmann, E. Niesing, F. Katzenberg, C. Tiller J., G. Sadowski
  VOC Sorption in Stretched Cross-Linked Natural Rubber
  Industrial & Engineering Chemistry Research, 55, 7191-7200 (2016)

- C. Held, N. Tsurko E., R. Neueder, G. Sadowski, W. Kunz
  Cation Effect on the Water Activity of Ternary (S)-Aminobutanedioic Acid Magnesium Salt Solutions at 298.15 and 310.15 K
  Journal of Chemical & Engineering Data, 61, 3190-3199 (2016)

- L. Lange, G. Sadowski
  Polymorphs, Hydrates, Cocrystals, and Cocrystal Hydrates: Thermodynamic Modeling of Theophylline Systems
  Crystal Growth & Design, 16, 4439-4449 (2016)

- F. Meurer, M. Bobrownik, G. Sadowski, C. Held
  Standard Gibbs Energy of Metabolic Reactions: I. Hexokinase Reaction
  Biochemistry, 55, 5665-5674 (2016)

- M. Herhut, C. Brandenbusch, G. Sadowski
  Non-monotonic course of protein solubility in aqueous polymer-salt solutions can be modeled using the sol-mxDLVO model
  Biotechnology journal11, 282-9 (2016)

- M. Herhut, C. Brandenbusch, G. Sadowski
  Inclusion of mPRISM potential for polymer-induced protein interactions enables modeling of second osmotic virial coefficients in aqueous polymer-salt solutions
  Biotechnology journal, 11, 146-54 (2016)

2015

- M. Uyan, G. Sieder, T. Ingram, C. Held
  Predicting CO2 solubility in aqueous N-methyldiethanolamine solutions with ePC-SAFT
  Fluid Phase Equilibria, 393, 91-100 (2015)

- I. Rodriguez-Palmeiro, O. Rodriguez, A. Soto, C. Held
  Measurement and PC-SAFT modelling of three-phase behaviour
  Physical Chemistry Chemical Physics, 17, 1800-1810 (2015)

- R. Paus, A. Prudic, Y. Ji
  Influence of excipients on solubility and dissolution of pharmaceuticals
  International Journal of Pharmaceutics, 485, 277-287 (2015)

- T. Färber, R. Schulz, O. Riechert, T. Zeiner, A. Górak, G. Sadowski, A. Behr
  Different recycling concepts in the homogeneously catalysed synthesis of terpenyl amines
  Chemical Engineering and Processing: Process Intensification, 98, 22-31 (2015)

- S. Neves C. M. S., C. Held, S. Mohammad, M. Schleinitz, P. Coutinho J. A., G. Freire M.
  Effect of salts on the solubility of ionic liquids in water: experimental and electrolyte Perturbed-Chain Statistical Associating Fluid Theory
  Physical Chemistry Chemical Physics, 17, 32044-32052 (2015)

- R. Paus, Y. Ji, F. Braak, G. Sadowski
  Dissolution of Crystalline Pharmaceuticals: Experimental Investigation and Thermodynamic Modeling
  Industrial & Engineering Chemistry Research, 54, 731-742 (2015)

- J. Gorden, T. Zeiner, C. Brandenbusch
  Reactive extraction of cis,cis-muconic acid
  Fluid Phase Equilibria, 393, 78-84 (2015)

- N. Emel'yanenko V., H. Zaitsau D., E. Shoifet, F. Meurer, P. Verevkin S., C. Schick, C. Held
  Benchmark Thermochemistry for Biologically Relevant Adenine and Cytosine. A Combined Experimental and Theoretical Study
  The Journal of Physical Chemistry A, 119, 9680-9691 (2015)

- P. Verevkin S., Y. Sazonova A., K. Frolkova A., H. Zaitsau D., V. Prikhodko I., C. Held
  Separation Performance of BioRenewable Deep Eutectic Solvents
  Industrial & Engineering Chemistry Research, 54, 3498-3504 (2015)

- F. Laube, T. Klein, G. Sadowski
  Partition Coefficients of Pharmaceuticals as Functions of Temperature and pH
  Industrial & Engineering Chemistry Research, 54, 3968-3975 (2015)

- H. Ji Y., R. Paus, A. Prudic, C. Lubbert, G. Sadowski
  A Novel Approach for Analyzing the Dissolution Mechanism of Solid Dispersions
  Pharm Res, 32, 2559-2578 (2015)

- R. Paus, E. Hart, H. Ji Y., G. Sadowski
  Solubility and Caloric Properties of Cinnarizine
  J Chem Eng Data, 60, 2256-2261 (2015)

- Y. Ji, R. Paus, A. Prudic, C. Lubbert, G. Sadowski
  A Novel Approach for Analyzing the Dissolution Mechanism of Solid Dispersions
  Pharm Res, 32, 2559-78 (2015)

- R. Paus, Y. Ji, L. Vahle, G. Sadowski
  Predicting the Solubility Advantage of Amorphous Pharmaceuticals: A Novel Thermodynamic Approach
  Molecular Pharmaceutics, 12, 2823-2833 (2015)

- T. Reschke, C. Brandenbusch, G. Sadowski
  Modeling aqueous two-phase systems: III. Polymers and organic salts as ATPS former
  Fluid Phase Equilibria, 387, 178-189 (2015)

- O. Riechert, T. Zeiner, G. Sadowski
  Measurement and Modeling of Phase Equilibria in Systems of Acetonitrile, n-Alkanes and beta-Myrcene
  I*ndustrial & Engineering Chemistry Research, 54, 1153-1160 (2015)*

- O. Riechert, T. Zeiner, G. Sadowski
  Phase Equilibria in Systems of Morpholine, Acetonitrile and n-Alkanes
  J Chem Eng Data, 60, 2098-2103 (2015)

- J. Collins, M. Grund, C. Brandenbusch, G. Sadowski, A. Schmid, B. Buehler
  The dynamic influence of cells on the formation of stable emulsions in organic-aqueous biotransformations
  Journal of Industrial Microbiology & Biotechnology, 42, 1011-1026 (2015)

- A. Prudic, K. Lesniak A., Y. Ji, G. Sadowski
  Thermodynamic phase behaviour of indomethacin/PLGA formulations
  European Journal of Pharmaceutics and Biopharmaceutics, 93, 88-94 (2015).

- C. Kress, C. Brandenbusch
  Osmotic Virial Coefficients as Access to the Protein Partitioning in Aqueous Two-Phase Systems
  J Pharm Sci-Us, 104, 3703-3709 (2015)

- C. Brandenbusch, S. Glonke, J. Collins, R. Hoffrogge, K. Grunwald, B. Buehler, A. Schmid, G. Sadowski
  Process boundaries of irreversible scCO(2)-assisted phase separation in biphasic whole-cell biocatalysis
  Biotechnology and Bioengineering, 112, 2316-2323 (2015)

- L. Shen G., C. Held, H. Lu X.,Y. Ji X.
  Modeling thermodynamic derivative properties of ionic liquids with ePC-SAFT
  Fluid Phase Equilibria, 405, 73-82 (2015)

- L. Lange, G. Sadowski
  Thermodynamic Modeling for Efficient Cocrystal Formation
  Crystal Growth & Design, 15, 4406-4416 (2015)

- O. Riechert, M. Husham, G. Sadowski, T. Zeiner
  Solvent effects on esterification equilibria
  AIChE Journal, 61, 3000-3011 (2015)

2014

- C. Held, T. Reschke, S. Mohammad, A. Luza, G. Sadowski
  ePC-SAFT revised
  Chemical Engineering Research and Design, 92, 2884-2897 (2014)

- C. Vogelpohl, C. Brandenbusch, G. Sadowski
  High-pressure gas solubility in multicomponent solvent systems for hydroformylation. Part II: Syngas solubility
  The Journal of Supercritical Fluids, 88, 74-84 (2014)

- E. Schäfer, G. Sadowski, S. Enders
  Interfacial tension of binary mixtures exhibiting azeotropic behavior: Measurement and modeling with PCP-SAFT combined with Density Gradient Theory
  Fluid Phase Equilibria, 362, 151-162 (2014)

- E. Schäfer, G. Sadowski, S. Enders
  Calculation of complex phase equilibria of DMF/alkane systems using the PCP-SAFT equation of state
  Chemical Engineering Science, 115, 49-57 (2014)

- X. Ji, C. Held, G. Sadowski
  Modeling imidazolium-based ionic liquids with ePC-SAFT. Part II. Application to H2S and synthesis-gas components
  Fluid Phase Equilibria, 363, 59-65 (2014)

- J. Pfeiffer, H.-D. Kühl
  Review of Models for Appendix Gap Losses in Stirling Cycle Machines
  Journal of Propulsion and Power, 30, 1419-1432 (2014)

- M. Umer, K. Albers, G. Sadowski, K. Leonhard
  PC-SAFT parameters from ab initio calculations
  Fluid Phase Equilibria, 362, 41-50 (2014)

- P. Carneiro A., O. Rodríguez, C. Held, G. Sadowski, A. Macedo E.
  Density of Mixtures Containing Sugars and Ionic Liquids: Experimental Data and PC-SAFT Modeling
  Journal of Chemical & Engineering Data, 59, 2942-2954 (2014)

- H. Passos, I. Khan, F. Mutelet, B. Oliveira M., J. Carvalho P., F. Santos L. M. N. B., C. Held, G. Sadowski, G. Freire M., P. Coutinho J. A.
  Vapor–Liquid Equilibria of Water + Alkylimidazolium-Based Ionic Liquids: Measurements and Perturbed-Chain Statistical Associating Fluid Theory Modeling
  Industrial & Engineering Chemistry Research, 53, 3737-3748 (2014)

- P. Hoffmann, C. Held, T. Maskow, G. Sadowski
  A thermodynamic investigation of the glucose-6-phosphate isomerization
  Biophysical Chemistry, 195, 22-31 (2014)

- T. Reschke, C. Brandenbusch, G. Sadowski
  Modeling aqueous two-phase systems: I. Polyethylene glycol and inorganic salts as ATPS former
  Fluid Phase Equilibria, 368, 91-103 (2014)

- C. Held, T. Reschke, R. Müller, W. Kunz, G. Sadowski
  Measuring and modeling aqueous electrolyte/amino-acid solutions with ePC-SAFT
  The Journal of Chemical Thermodynamics, 68, 1-12 (2014)

- M. Sadeghi, C. Held, C. Ghotbi, M. Abdekhodaie, G. Sadowski
  Thermodynamic Properties of Aqueous Glucose–Urea–Salt Systems
  J Solution Chem, 43, 1110-1131 (2014)

- A. Prudic, Y. Ji, G. Sadowski
  Thermodynamic Phase Behavior of API/Polymer Solid Dispersions
  Molecular Pharmaceutics, 11, 2294-2304 (2014)

- A. Prudic, T. Kleetz, M. Korf, Y. Ji, G. Sadowski
  Influence of Copolymer Composition on the Phase Behavior of Solid Dispersions
  Molecular Pharmaceutics, 11, 4189-4198 (2014)

- G. Shen, C. Held, J.-P. Mikkola, X. Lu, X. Ji
  Modeling the Viscosity of Ionic Liquids with the Electrolyte Perturbed-Chain Statistical Association Fluid Theory
  Industrial & Engineering Chemistry Research, 53, 20258-20268 (2014)

- B. Hentschel, A. Peschel, Q. Xie M., C. Vogelpohl, G. Sadowski, H. Freund, K. Sundmacher
  Model-based prediction of optimal conditions for 1-octene hydroformylation
  Chemical Engineering Science, 115, 58-68 (2014)

- T. Reschke, C. Brandenbusch, G. Sadowski
  Modeling aqueous two-phase systems: II. Inorganic salts and polyether homo- and copolymers as ATPS former
  Fluid Phase Equilibria, 375, 306-315 (2014)

Proceedings

- H.-D. Kühl, J. Pfeiffer, J. Sauer
  Operating Characteristics of a Laboratory-Scale, Convertible Stirling-Vuilleumier-Hybrid CHP System Including a Reversed-Rotation Stirling Mode
  Proc. 16th International Stirling Engine Conference, 294-304, Bilbao, Spain, Sep 24-26, 2014. ISSN 2409-0387

- J. Pfeiffer, H-D. Kühl
  Analytical Modeling of Appendix Gap Losses in Stirling Cycle Machines
  Proc. 16th International Stirling Engine Conference, 451-463, Bilbao, Spain, Sep 24-26, 2014. ISSN 2409-0387

- J. Pfeiffer, H.-D. Kühl
  New Analytical Model for Appendix Gap Losses in Stirling Cycle Machines
  Proc. 12th International Energy Conversion Engineering Conference, AIAA 2014-3856, Cleveland, OH, Jul 28-30, 2014. http://dx.doi.org/10.2514/6.2014-3856

- J. Pfeiffer, H.-D. Kühl
  Optimization of the Appendix Gap Design in Stirling Engines
  Proc. 13th International Energy Conversion Engineering Conference, AIAA 2015-3902, Orlando, FL, Jul 27-29, 2015. http://dx.doi.org/10.2514/6.2015-3902

SCIENTIFIC HIGHLIGHTS 2016